



EDUCACIÓN
SECRETARÍA DE EDUCACIÓN PÚBLICA



TECNOLÓGICO
NACIONAL DE MÉXICO

Instituto Tecnológico de La Laguna
División de Estudios de Posgrado e Investigación

DIVISIÓN DE ESTUDIOS DE POSGRADO E INVESTIGACIÓN

**“Nuevas Estrategias de Control Robusto para Sistemas Dinámicos
con Saturación en la Entrada y Restricción en los Estados”**

POR

M.C. Ariana Gutiérrez Ortega

T E S I S

PRESENTADO COMO REQUISITO PARCIAL PARA OBTENER EL GRADO DE
DOCTOR EN CIENCIAS EN INGENIERÍA ELÉCTRICA

DIRECTOR DE TESIS

Dr. Héctor Ríos Barajas

CODIRECTOR DE TESIS

Dr. Manuel Leonardo Mera Hernández

ISSN: 0188-9060



RIITEC: (03)-TDCIE - 2024

Torreón, Coahuila. México

Agosto 2024



DEPENDENCIA: Div. Est. Posg. E Invest.
NO. OFICIO: DEP/351
ASUNTO: Autorización de Impresión
Torreón Coah., 12/AGO/2024

**C. ARIANA GUTIÉRREZ ORTEGA
CANDIDATO(A) AL GRADO DE DOCTOR(A)
EN CIENCIAS EN INGENIERÍA ELÉCTRICA
PRESENTE.-**

Después de haber sometido a revisión su trabajo de tesis titulado:

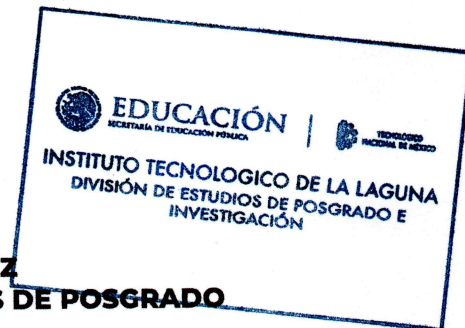
**“Nuevas Estrategias de Control Robusto para Sistemas Dinámicos con Saturación
en la Entrada y Restricción en los Estados”**

Habiendo cumplido con todas las indicaciones que el jurado revisor de tesis hizo, se le comunica que se le concede la autorización con número de registro RiITEC: (03)-TDCIE-2024, para que proceda a la impresión del mismo.

ATENTAMENTE

*Excelencia en Educación Tecnológica®
Educación Tecnológica Fuente de Innovación*

**JOSÉ IRVING HERNÁNDEZ JÁQUEZ
JEFE DE LA DIVISIÓN DE ESTUDIOS DE POSGRADO
DE INVESTIGACIÓN**



JIHJ/*mjsl



ASUNTO: Se autoriza Impresión
Torreón, Coahuila, 12/AGO/2024

C. JOSÉ IRVING HERNÁNDEZ JÁQUEZ
JEFE DE LA DIVISIÓN DE ESTUDIOS DE POSGRADO E INVESTIGACIÓN
PRESENTE.-

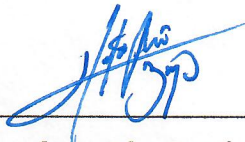
Por medio de la presente, hacemos de su conocimiento que después de haber sometido a revisión el trabajo de tesis titulado:

“Nuevas Estrategias de Control Robusto para Sistemas Dinámicos con Saturación en la Entrada y Restricción en los Estados”

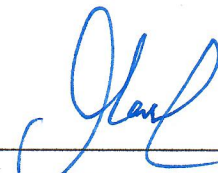
Desarrollado por el C. **ARIANA GUTIÉRREZ ORTEGA**, con número de control D2013004, y habiendo cumplido con todas las correcciones que se le indicaron, estamos de acuerdo que se le conceda la autorización de la fecha de examen de grado para que proceda a la impresión de la misma.

ATENTAMENTE

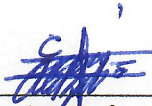
*Excelencia en Educación Tecnológica®
Educación Tecnológica Fuente de Innovación*



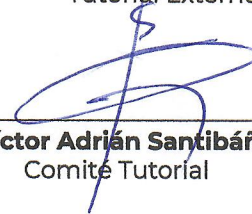
Dr. Héctor Ríos Barajas
Director(a) de Tesis



Dr. Manuel Mera Hernández
Co-Director de Tesis y comité
Tutorial Externo



Dr. Alejandro Enrique Dzul López
Comité Tutorial



Dr. Víctor Adrián Santibáñez Dávila
Comité Tutorial



Dr. Miguel Ángel Llana Leal
Comité Tutorial



The realization of this project has been possible thanks to the following tutorial committee:

Advisor: Dr. Héctor Ríos Barajas

Co–advisor: Dr. Manuel Leonardo Mera Hernández

Tutorial Committee: Dr. Alejandro Enrique Dzul López

Tutorial Committee: Dr. Víctor Adrian Santibáñez Dávila

Tutorial Committee: Dr. Miguel Ángel Llama Leal

*I cry a lot but I am so productive,
it's an art.*

– Taylor Swift

Dedicate to all those who have been part of my journey and provided
unwavering support.

ACKNOWLEDGEMENTS

To my parents *María Eugenia Ortega* and *Francisco Gutiérrez*, for providing me with their love and understanding throughout my life.

To my beloved sister *Graciela*, for motivating me to take on this great challenge and demonstrating that everything is achievable when you fight for it.

To my best friend, *Abril Meza*, who always trusted in me, offered support, and provided words of encouragement when I needed them most.

To my laboratory colleagues, *Dr. Romeo Falcón*, *M.C. Julio Rodríguez*, *Ing. Servando Encina*, *Ing. Fernanda Govea*, and *Ing. Daniel Jiménez*, with whom I shared special moments and who became great friends.

To my friends, *M.C. Emanuel Márquez*, *M.C. Gibran López*, *M.C. Aldo Osuna*, *M.C. Diana Triana*, *Ing. Arely Montelongo*, and *Ing. Emil Velázquez*, who taught me to always see the best in life and enjoy every moment.

To my advisor, *Dr. Héctor Ríos Barajas*, for showing me that any goal can be achieved through effort, patience, and dedication. Also, to my co-advisor, *Dr. Manuel Mera Hernandez*, for all his assistance and patience during the completion of this work.

To the thesis committee, *Dr. Alejandro Dzul López*, *Dr. Víctor Santibáñez Dávila*, and *Dr. Miguel Ángel Llama Leal*, for their contributions to this research.

To *Prof. Denis Efimov* and *Dr. Rosane Ushirobira* for providing me with the opportunity to expand my knowledge and experiences.

To CONAHCYT for the financial support provided during my doctoral studies, with CVU number 932774, which culminated in the presentation of this thesis.

ABSTRACT

This thesis presents the design of novel robust control strategies for dynamics systems with input saturation and state constraints affected by disturbances. The problem considers both linear and nonlinear systems taking into account some systems constraints, *i.e.*, state, input, and communications constraints. To develop the new robust control algorithms for both linear and nonlinear systems, several tools are used. These tools include the model predictive control, the attractive ellipsoid method, and the barrier Lyapunov function, which effectively handle input and state constraints. Additionally, integral sliding-mode control can counteract the effects of some class of external perturbations, while event-triggered control theory addresses communication constraints. Numerical simulations, over some academic examples, and experimental results, using the unicycle mobile robot, validate the effectiveness of the proposed robust control strategies.

ACRONYMS

AEM	Attractive Ellipsoid Method
BLF	Barrier Lyapunov Function
IP	Interval Predictor
ISMC	Integral Sliding-Mode Control
ISS	Input-to-State Stability
ISpS	Input-to-State practically Stability
LPV	Linear Parameter Varying
LMI	Linear Matrix Inequality
MPC	Model Predictive Control
OMR	Omnidirectional Mobile Robot
RMS	Root Mean Square
SMC	Sliding-Mode Control
UMR	Unicycle Mobile Robot

CONTENTS

I	INTRODUCTION AND PRELIMINARIES	1
1	INTRODUCTION	3
1.1	Motivation	3
1.2	Problem Statement	4
1.3	Contribution	4
1.4	Thesis Structure	6
2	PRELIMINARIES	7
2.1	Notation	7
2.2	Definitions and Supporting Lemmas	8
2.3	Barrier Lyapunov Function	9
II	CONTROL STRATEGIES FOR CONSTRAINED SYSTEMS	11
3	AN ISM-BASED ROBUST CONTROL FOR UNCERTAIN LINEAR SYSTEMS	13
3.1	Introduction	13
3.2	Problem Statement	15
3.3	Robust Control Design	15
3.3.1	Integral Sliding-Mode Control Design	17
3.3.2	Linear Control Design	18
3.4	Simulation Results	21
3.5	Remarks	28
3.6	Proof of the Results	28
4	AN IP-BASED ROBUST CONTROL FOR UNCERTAIN NONLINEAR SYSTEMS	31
4.1	Introduction	31
4.2	Problem Statement	33
4.3	Control Design	34
4.3.1	Interval Predictor	34
4.3.2	State-Feedback Control	36
4.3.3	Design of the Model Predictive Control	38
4.4	Simulations Results	39
4.5	Remarks	41
4.6	Proof of the Results	42
5	A SAMPLED ROBUST CONTROL FOR UNCERTAIN NONLINEAR SYSTEMS	49
5.1	Introduction	49
5.2	Problem Statement	50
5.3	Robust Control Design	51
5.3.1	Linear Control Design	52
5.3.2	Event-Triggered Controller	52
5.3.3	Constant Sampled Controller	54
5.4	Simulation Results	55

5.5	Remarks	57
5.6	Proof of the Results	58
III	APPLICATIONS	63
6	REGULATION PROBLEM IN A CONSTRAINED OMR	65
6.1	Introduction	65
6.2	Problem Statement	65
6.3	Robust Control Design	66
6.4	Simulation Results	68
6.5	Remarks	73
7	TRAJECTORY TRACKING PROBLEM IN A CONSTRAINED UMR	75
7.1	Introduction	75
7.2	Problem Statement	75
7.3	Tracking Error Dynamics	76
7.4	Robust Control Design	78
7.4.1	Integral Sliding–Mode Control Design	78
7.4.2	Linear Control Design	79
7.5	Experimental Results	80
7.5.1	Lemniscate Curve Tracking	81
7.5.2	Sine Curve Tracking	84
7.6	Remarks	87
8	TRAJECTORY TRACKING PROBLEM IN A UMR WITH COMMU- NICATION CONSTRAINTS	89
8.1	Introduction	89
8.2	Problem Statement	89
8.3	Robust Control Design	90
8.4	Experimental Results	91
8.5	Remarks	92
9	CONCLUSIONS	95
	BIBLIOGRAPHY	99

Part I

INTRODUCTION AND PRELIMINARIES

INTRODUCTION

This chapter contains the motivation of this work, which serves as the foundation for the main problem formulation. The contribution section outlines the novel aspects of this work in addressing the stated problem. Finally, the structure of the document is also presented.

1.1 MOTIVATION

In control theory, the mathematical models are normally used to represent physical systems and design controllers. However, if the controller is applied to a real dynamical system, there exist some restrictions due to structural limitations such as saturation in the control input and state constraints, (see, *e.g.*, [1], [2], and [3]). Nevertheless, this class of restrictions is rarely included in most of the mathematical models. On the other hand, the behavior and the stability of the systems can be affected by parameter uncertainties and external perturbations. Moreover, in most cases, the dynamical systems are managed through a digital platform, and then, there is limited bandwidth and it is necessary to restrict the frequency of control input updates to save communication resources.

Therefore, the control strategies must consider these challenges during their design. In this sense, it is essential to ensure that the designed controller does not violate the system constraints. To achieve this, control techniques need to take into account these constraints and be capable of compensating the effects of external perturbations.

Fig. 1, illustrates some examples of dynamical systems for which it is required to take into account possible state, input, and communication constraints as well as external perturbations. For instance, the wheeled mobile robots operate in a confined workspace, *i.e.*, they are restricted by obstacles, terrain, and workspace boundaries. On the other hand, aerial robots, also have workspace limitations and limited flight time due to the battery capacity, *i.e.*, they have input and state constraints.



Figure 1: Constrained dynamic systems

With this in mind, the main problem statement is presented below.

1.2 PROBLEM STATEMENT

Consider a general class of nonlinear system

$$\dot{x}(t) = f(t, x(t), u(t), w(t)), \quad t \geq 0, \quad (1)$$

where $x(t) \in \mathbb{R}^n$ is the state, $f : \mathbb{R}_+ \times \mathbb{R}^n \times \mathbb{R}^p \times \mathbb{R}^q \rightarrow \mathbb{R}^n$ is a locally Lipschitz function in x and u , and piecewise continuous in t , $u(t) \in \mathbb{R}^p$ is the control input, and $w : \mathbb{R}_+ \rightarrow \mathbb{R}^q$ is the disturbance term.

Then, it is considered that the control signals are constrained, *i.e.*,

$$u(t) \in \mathcal{U} := \{u \in \mathbb{R}^p \mid -u_{\max_j} \leq u_j \leq u_{\max_j}, \forall j = \overline{1, p}\}, \quad (2)$$

where $0 < u_{\max_j}$ is the maximum amplitude value that u_j can take. Moreover, the control signal could possess sampling communication constraints, *i.e.*, $u(t) = u(t_k)$, for all $t \in [t_k, t_{k+1})$ and $k \in \mathbb{N}$, where the sampling instants t_k monotonously increase, so that $\lim_{k \rightarrow \infty} t_k = +\infty$. Additionally, the solutions of the system (1) must be constrained inside the polytope

$$\mathcal{X} := \{x \in \mathbb{R}^n \mid \mathbf{b}x \leq \mathbf{1}_{k_x}\}, \quad (3)$$

where $\mathbf{b} = (b_1, \dots, b_{k_x})^\top \in \mathbb{R}^{k_x \times n}$, with $b_i \in \mathbb{R}^n$ being some given vectors that characterize the state constraints, $k_x \in \mathbb{Z}$ is the number of the polytope faces, and $\mathbf{1}_{k_x} = (1, \dots, 1)^\top \in \mathbb{R}^{k_x}$.

Thus, the general objective is to develop new robust control strategies for stabilizing some classes of perturbed dynamical systems taking into account state, input, and/or communication constraints. Specifically, the particular goals of this work are listed below:

- 1) To design a robust control strategy to regulate the output of a class of uncertain linear systems, with state and input constraints, affected by external perturbations.
- 2) To design a robust control strategy to stabilize a particular class of uncertain nonlinear systems, taking into account state and input constraints, and external perturbations.
- 3) To design a sampled robust control strategy to stabilize a particular class of uncertain nonlinear systems, taking into account state, input, and communication constraints, and external perturbations.

1.3 CONTRIBUTION

Motivated by the aforementioned challenges, *i.e.*, external perturbations, state, input, and communications constraints, this document presents a solution to the controller design problem for some classes of uncertain linear and nonlinear systems with state, input, and/or communication constraints. Specifically, this thesis contributes with

- 1) The design of a robust output–regulation control for a class of uncertain linear systems. The proposed algorithm is composed of a linear and nonlinear part, with the following features:
 - The linear control part is designed based on the BLF and the AEM approach.
 - The nonlinear control part is based on an ISMC approach.
 - Characterization of safe set where the system trajectories do not transgress the system constraints.

This contribution is reflected in the works given in [4], [5], [6], [7], [8], and [9].

- 2) The design of a robust sampled controller to stabilize a particular class of uncertain nonlinear systems, taking into account state and input constraints, affected by external perturbations. The proposed controller possesses the following features:
 - The controller is based on a discrete–time IP–based state–feedback controller and a MPC approach.
 - The measurements of the system states are not required.
 - Characterization of safe set where the system trajectories do not transgress the state constraints.
 - Low computational cost.

This contribution is reflected in the works given in [10], [11], [12], and [13].

- 3) The design of a sampled control strategy to stabilize a particular class of uncertain nonlinear system, taking into account communication, state and input constraints, affected by external perturbations. The proposed control scheme is composed of an aperiodic and a periodic sampled controller, with the following features:
 - The aperiodic sampled controller is based on a state–feedback event–triggered controller designed through the AEM and the BLF.
 - The periodic sampled control part is based on a state–feedback controller designed using a Lyapunov–Krasovskii function approach.
 - Characterization of a safe set, where the state constraints are not transgressed.

This contribution is reflected in the works given in [14], [15], and [16].

A schematic diagram of the academic contribution is presented in Fig.

2.

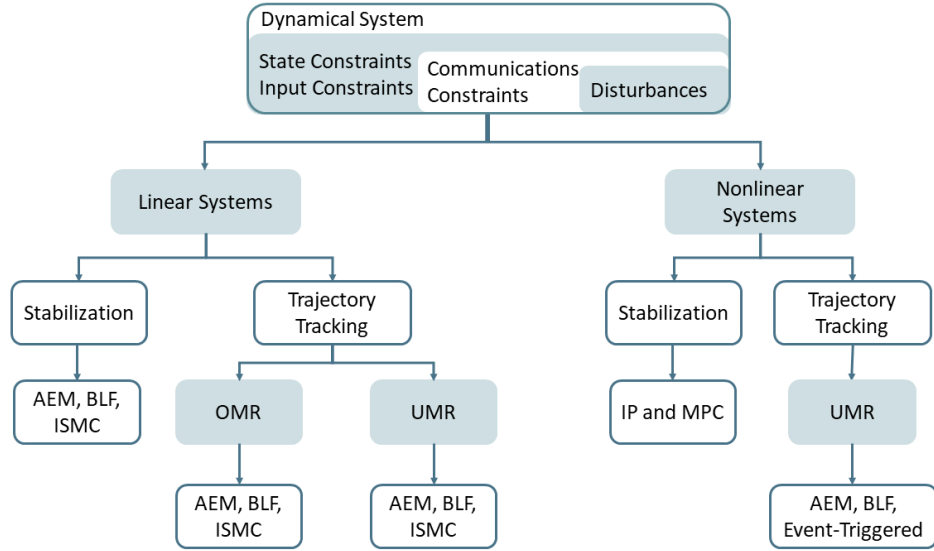


Figure 2: Schematic diagram of the academic contribution

1.4 THESIS STRUCTURE

The rest of the document is organized as follows. In Chapter 2, the mathematical preliminaries along with some useful results are given. The second part of the thesis focuses on designing control strategies for constrained systems. Chapter 3 introduces the design of an ISM-based control. Chapter 4 presents the design of an interval predictor-based robust control. Chapter 5 presents the development of a sampled robust control. In the third part of the thesis, the applications of the algorithms presented in the second part are shown. Chapter 6 contains the application of ISM-based robust control to solve the trajectory tracking in an omnidirectional mobile robot. Chapter 7 shows the application of the ISM-based robust control algorithm to solve the trajectory tracking problem in an unicycle mobile robot. Chapter 8 presents the application of sampled robust control in an unicycle mobile robot. Finally, Chapter 9 provides the concluding remarks.

PRELIMINARIES

In this chapter, it is described the notation that will be used throughout the rest of the document, as well as fundamental definitions and concepts necessary for the development of the control algorithms.

2.1 NOTATION

The sets of real and integer numbers are defined by \mathbb{R} and \mathbb{Z} , respectively; $\mathbb{R}_+ := \{s \in \mathbb{R} : s \geq 0\}$ and $\mathbb{Z}_+ := \{s \in \mathbb{Z} : s \geq 0\}$. The matrix $A^\dagger = (A^\top A)^{-1} A^\top \in \mathbb{R}^{m \times n}$ denotes the left pseudoinverse of a matrix $A \in \mathbb{R}^{n \times m}$. The term $\text{He}\{A\}$ denotes $A + A^\top$, for a matrix $A \in \mathbb{R}^{n \times n}$. For a matrix A , it is defined that $A^+ = \max\{0, A\}$ and $A^- = A^+ - A$ (similarly for vectors), where the operation \max is understood in an element-wise sense. For two vectors $x_1, x_2 \in \mathbb{R}^n$ or matrices $A_1, A_2 \in \mathbb{R}^{n \times n}$, the relations $x_1 \leq x_2$ and $A_1 \leq A_2$ are understood in an element-wise sense. The relation $P \prec 0$ ($P \succeq 0$) means that a symmetric matrix $P \in \mathbb{R}^{n \times n}$ is negative (positive semi-) definite. For a matrix $A \in \mathbb{R}^{m \times n}$, the induced norm is the spectral norm, *i.e.*, $\|A\| = \sqrt{\lambda_{\max}(A^\top A)}$.

The set $\mathcal{E}(\mathbf{R}) := \{x \in \mathbb{R}^n | x^\top \mathbf{R} x \leq 1\}$ is an ellipsoid characterized by a matrix $0 < \mathbf{R}^\top = \mathbf{R} \in \mathbb{R}^{n \times n}$ centered at the origin. The set $\mathcal{E}(\mathbf{P}, x_c) := \{x \in \mathbb{R}^n | (x - x_c)^\top \mathbf{P} (x - x_c) \leq 1\}$ is an ellipsoid characterized by a matrix $0 < \mathbf{P}^\top = \mathbf{P} \in \mathbb{R}^{n \times n}$ and centered at $x_c \in \mathbb{R}^n$. For any $\theta \in \mathbb{R}^n$, $\|\theta\|_{\mathcal{E}} := \inf_{\eta \in \mathcal{E}} \|\theta - \eta\|$, is the distance from θ to the set \mathcal{E} . The Minkowski addition of two subsets $A, B \in \mathbb{R}$ is defined by $A + B = \{a + b | a \in A, b \in B\}$. The set $\mathcal{P} := \{x \in \mathbb{R}^n | \mathbf{b}x \leq \mathbf{1}_{k_x}\}$ is a polytope, where $\mathbf{b} = (b_1, \dots, b_{k_x})^\top \in \mathbb{R}^{k_x \times n}$, with $b_i \in \mathbb{R}^n$ being some given vectors that characterize the state constraints, $k_x \in \mathbb{Z}$ is the number of the polytope faces, and $\mathbf{1}_{k_x} = (1, \dots, 1)^\top \in \mathbb{R}^{k_x}$.

For a Lebesgue measurable function $w : \mathbb{R}_+ \rightarrow \mathbb{R}^q$, define $\|w\|_{(t_0, t_1)} := \text{ess sup}_{t \in (t_0, t_1)} \|w(t)\|$; then, $\|w\|_\infty = \|w\|_{(0, +\infty)}$ and the set of all the functions w with the property $\|w\|_\infty < +\infty$ is denoted as \mathcal{L}_∞^q . A continuous function $\alpha : \mathbb{R}_+ \rightarrow \mathbb{R}_+$ belong to class \mathcal{K} if it is strictly increasing and $\alpha(0) = 0$. A continuous function $\beta : \mathbb{R}_+ \rightarrow \mathbb{R}_+$ belongs to class \mathcal{KL} if, for each fixed s , $\beta(r, s) \in \mathcal{K}$ with respect to r , and for each fixed r , $\beta(r, s)$ is decreasing to zero with respect to s . A matrix is called Metzler when all its non-diagonal coefficients are non-negative. Let us denote a sequence of integers $1, \dots, n$ as $\overline{1, n}$, for any $n \in \mathbb{N}$.

Denote the trigonometric functions $\sin(\theta)$, $\cos(\theta)$, and $\text{sinc}(\theta)$ as $s(\theta)$, $c(\theta)$, and $sc(\theta)$, respectively. The OR operation is denoted by the symbol \wedge .

2.2 DEFINITIONS AND SUPPORTING LEMMAS

Consider the following nonlinear system

$$\dot{x}(t) = f(x(t), w(t)), \quad (4)$$

where $x(t) \in \mathbb{R}^n$ is the state vector, $w : \mathbb{R}_+ \rightarrow \mathbb{R}^q$ is the external input; $f : \mathbb{R}^n \times \mathbb{R}^q \rightarrow \mathbb{R}^n$ is a locally Lipschitz function. The solution of system (4) for an initial condition $x_0 \in \mathbb{R}^n$ and $w \in \mathcal{L}_\infty^q$ is denoted as $x(t, x_0, w)$, for any $t \geq 0$ for which the solution exists.

Definition 1 [17]. *The system (4) is said to be Input-to-State practically Stable (ISpS) if there exist some functions $\beta \in \mathcal{KL}$ and $\gamma \in \mathcal{K}$, and a constant $\kappa \in \mathbb{R}_+$, such that for any $w \in \mathcal{L}_\infty^q$, and any $x_0 \in \mathbb{R}^n$*

$$\|x(t, x_0, w)\| \leq \beta(\|x_0\|, t) + \gamma(\|w\|_\infty) + \kappa, \forall t \geq 0. \quad (5)$$

If $\kappa = 0$, the system (4) is said to be Input-to-State Stable (ISS).

The next lemma gives the interval upper and lower bounds for product of matrix and vector variables.

Lemma 1 [18]. *Let $x \in \mathbb{R}^n$ be a vector variable, $\underline{x} \leq x \leq \bar{x}$ for some $\underline{x}, \bar{x} \in \mathbb{R}^n$, then*

- If $A \in \mathbb{R}^{m \times n}$ is a constant matrix then

$$A^+ \underline{x} - A^- \bar{x} \leq Ax \leq A^+ \bar{x} - A^- \underline{x}. \quad (6)$$

- If $A \in \mathbb{R}^{m \times n}$ is a variable matrix and $\underline{A} \leq A \leq \bar{A}$ for some $\underline{A}, \bar{A} \in \mathbb{R}^{m \times n}$, then

$$A_m \leq Ax \leq A_M, \quad (7)$$

with $A_m = \underline{A}^+ \underline{x}^+ - \bar{A}^+ \underline{x}^- - \underline{A}^- \bar{x}^+ + \bar{A}^- \bar{x}^-$ and $A_M = \bar{A}^+ \bar{x}^+ - \underline{A}^+ \bar{x}^- - \bar{A}^- \underline{x}^+ + \underline{A}^- \underline{x}^-$.

A variant of Grönwall–Bellman inequality is formulated in the next lemma:

Lemma 2 [19]. *Let $\lambda : [a, b] \rightarrow \mathbb{R}$ be a continuous function and $\mu : [a, b] \rightarrow \mathbb{R}$ be a continuous and non-negative function. If a continuous function $y : [a, b] \rightarrow \mathbb{R}$ satisfies*

$$y(t) \leq \lambda(t) + \int_a^t \mu(s)y(s)ds,$$

for $a \leq t \leq b$, then, on the same interval, it holds that

$$y(t) \leq \lambda(t) + \int_a^t \lambda(s)\mu(s)e^{\int_s^t \mu(r)dr} ds.$$

2.3 BARRIER LYAPUNOV FUNCTION

Consider the following system

$$\dot{x}(t) = f(x(t)), \quad x(0) = x_0, \quad (8)$$

where $x(t) \in \mathbb{R}^n$ is the state and $f : \mathbb{R}^n \rightarrow \mathbb{R}^n$ is a continuous function with respect to $x(t)$. The solution of system (8) for an initial condition $x_0 \in \mathbb{R}^n$ is denoted as $x(t, x_0)$, for any $t \geq 0$ for which the solution exists.

Definition 2 [20]. A barrier Lyapunov function is a scalar function $V(x)$, defined with respect to the system (8) on an open region \mathcal{D} containing the origin, that is continuous, positive definite, has continuous first-order partial derivatives at every point of \mathcal{D} , has the property $V(x) \rightarrow \infty$ as x approaches the boundary of \mathcal{D} , and satisfies $V(x(t)) \leq b$, for all $t \geq 0$, along the solution of system (8), for $x_0 \in \mathcal{D}$ and some positive constant b .

Note that if $\dot{V} \leq 0$ and $x_0 \in \mathcal{D}$, then $b = V(x_0)$, and any trajectory will be bounded inside \mathcal{D} .

A graphical representation of a Lyapunov barrier function is depicted in Fig. 3.

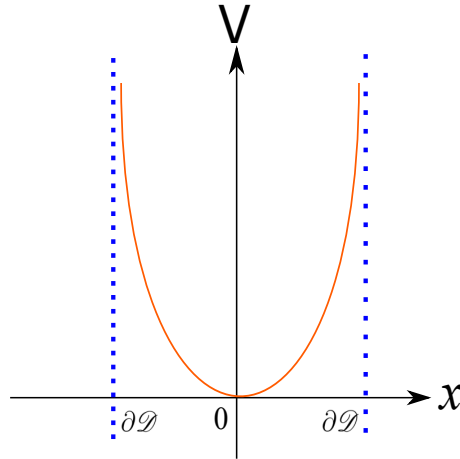


Figure 3: Barrier Lyapunov Function

Let us consider the input vector $u = (u_1, \dots, u_p)^\top \in \mathbb{R}^p$, then it is possible to apply the saturation function to each element of $u \in \mathbb{R}^p$, i.e.,

$$\sigma_j(u_j) = \begin{cases} u_{\max_j}, & \text{if } u_{\max_j} \leq u_j, \\ u_j, & \text{if } -u_{\max_j} < u_j < u_{\max_j}, \\ -u_{\max_j}, & \text{if } u_j \leq -u_{\max_j}. \end{cases} \quad (9)$$

where $u_{\max_j} > 0$, for $j = \overline{1, p}$, is the maximum amplitude value that u_j can take. Due to the structure of this function there exists a linear control region, where $\sigma(u_j) = u_j$, is characterized by the set $\mathcal{U} := \{u \in \mathbb{R}^p \mid -u_{\max_j} \leq u_j \leq u_{\max_j}, \forall j = \overline{1, p}\}$. Define the function $\phi_j : \mathbb{R} \rightarrow \mathbb{R}$ as $\phi_j(u_j) := \sigma_j(u_j) - u_j$ and $\phi(u) := (\phi_1(u_1), \dots, \phi_p(u_p))^\top$. For the multiple input case, let us introduce the following lemma.

Lemma 3 [21]. *If $\bar{\alpha} - \bar{\beta}$ is an element of \mathcal{U} , then the function $\phi_j(\alpha)$ satisfies $\phi^\top(\bar{\alpha})\Delta[\phi(\bar{\alpha}) + \bar{\beta}] \leq 0$, with $\Delta = \text{diag}(\delta_1, \dots, \delta_p)$, for any $\delta_j > 0$, $j = \overline{1, p}$.*

The conditions to get an asymptotic attractive ellipsoid are given by the following definition.

Definition 3 [22]. *The set $\mathcal{E}(\tilde{P}) = \{x \in \mathbb{R}^n | x^\top \tilde{P}x \leq 1\}$ is an asymptotically attractive ellipsoid for the system (8), if $\|x(t, x_0)\|_{\mathcal{E}} \rightarrow 0$, when $t \rightarrow \infty$, for any $x_0 \in \mathbb{R}^n$.*

Part II

CONTROL STRATEGIES FOR CONSTRAINED
SYSTEMS

AN ISM-BASED ROBUST CONTROL FOR UNCERTAIN LINEAR SYSTEMS

This chapter presents a robust control for uncertain linear systems with input saturation, state constraints, and external perturbations. The control design consists of a nominal and a robust part, both independently designed using an ISMC approach. The proposed scheme guarantees asymptotic convergence to zero of the output regulation error coping with the system constraints and perturbations.

3.1 INTRODUCTION

The mathematical models are normally used to represent physical systems and design controllers. However, if the controller is applied to a real dynamical system, there exist some restrictions due to structural limitations such as saturation in the control input and state constraints. Nevertheless, this class of restrictions is rarely included in most of the mathematical models. On the other hand, the behavior and the stability of the systems can be affected by parameter uncertainties and external perturbations. Therefore, robust control techniques, *e.g.*, SMC, are necessary to design a controller that counteracts the effect of external perturbations. In particular, the ISMC technique is capable of compensating the effect of these perturbations without the presence of a reaching phase [23]. Moreover, the ISMC allows to independently design the control law in two parts, *i.e.*, a nominal and a robust part. Each part of the control could deal with different constraints and perturbations.

Regarding the control design for systems with state constraints, the BLF appears as a possible solution [20]. For instance, based on the BLF technique, in [24], a feedback control is proposed for nonlinear switched systems with state constraints. The proposed scheme ensures that the output tracking error converges to zero asymptotically. The BLF can be combined with other different techniques, *e.g.*, the AEM, adaptive control techniques, and backstepping, to solve the problem of the control design for systems with state constraints. The BLF combined with the AEM allows an ellipsoid to characterize a region where none of the system constraints are transgressed. For instance, in [25], considering that the state constraints are described by a polytope, a robust state feedback controller is proposed for uncertain linear systems. The proposed scheme ensures asymptotic convergence of the system trajectories to a region around the origin. In the context of the adaptive control, in [26], a robust adaptive control based on an asymmetric BLF is proposed for a class of strict-feedback nonlinear systems in presence of state constraints. However, in some of the previ-

ously mentioned works, the external perturbations are not contemplated and only state constraints are considered.

On the other hand, in the control design for systems with input saturation, in [27], an output feedback control is proposed for a chain of integrators with input saturation. The proposed approach guarantees asymptotic convergence to zero of the closed-loop dynamics. However, parameter uncertainties and external perturbations are not taken into account. In [4], a robust output-based control, based on the AEM and the BLF, is proposed for uncertain linear systems with input saturation and external perturbations. The proposed algorithm guarantees asymptotic convergence to a certain set. However, in the above-mentioned works only input saturation is considered.

Concerning the control design for constrained systems, *i.e.*, systems with input saturation and state constraints, different techniques have been used to solve this problem. For instance, in [28], an output feedback control is proposed for linear systems with external perturbations. The proposed controller ensures that the regulation error converges to a neighborhood around the origin. On the other hand, in [29], a controller based on a high-order BLF and the Nussbaum gain technique is proposed for high-order nonlinear systems. In absence of external perturbations, the closed-loop signals are bounded. Also, in [30], a constrained adaptive robust control is proposed for MIMO systems with parameter uncertainties and perturbations. The proposed algorithm guarantees finite-time convergence of the tracking error to a region around the origin. Notwithstanding, in most of the above-mentioned works, external perturbations are not contemplated, and when they are considered, only convergence to a region around of the origin is guaranteed.

Motivated by the above-mentioned issues, this chapter aims to design a robust controller to regulate the output of a class of uncertain linear systems, with input saturation and state constraints, affected by external perturbations. The proposed robust control is composed of a linear and a nonlinear part. Each part of the control can be designed independently due to the use of an ISMC approach. Then, the proposed control approach contributes with the following features:

- 1) The linear control, whose design is based on the BLF and the AEM approach, considers the input saturation, the state constraints, and the parameter uncertainties.
- 2) The nonlinear part is based on an ISMC approach and it can compensate the effect of some matched perturbations.
- 3) A safe set where the system trajectories do not transgress the state constraints and input saturation, is provided.
- 4) The proposed scheme guarantees asymptotic convergence to zero of the output regulation error coping with the system constraints and perturbations.

- 5) A constructive and simple method, based on LMIs, is proposed to compute the controller gains.

3.2 PROBLEM STATEMENT

Consider the following class of uncertain linear systems with input saturation

$$\dot{x}(t) = (A + \Delta)x(t) + B(u(t) + w(t)), \quad t \geq 0, \quad (10a)$$

$$y_r(t) = Cx(t), \quad (10b)$$

where $x(t) \in \mathbb{R}^n$ is the state, $u(t) \in \mathbb{R}$ is the control input, $y_r(t) \in \mathbb{R}$ is the output to be regulated, $w : \mathbb{R} \rightarrow \mathbb{R}^q$ is the external perturbation, and $\Delta \in \mathbb{R}^{n \times n}$ represents some parameter uncertainties. The matrices A, B , and C are known and they have suitable dimensions. It is assumed that the controllability of the system is not affected by the presence of the parameter uncertainties, *i.e.*, the pair $(A + \Delta, B)$ is controllable.

It is considered that $u \in [-u_{\max}, u_{\max}]$, where $u_{\max} > 0$ is the maximum value that the control signal can take. The solutions of the system (10) must be constrained inside the polytope

$$\mathcal{P}_x := \{x \in \mathbb{R}^n \mid \mathbf{b}x \leq \mathbf{1}_{k_x}\}. \quad (11)$$

Let us define a desired constant reference as $r \in \mathbb{R}$. Thus, the problem is to design the control input u , for the system (10), such that

$$\lim_{t \rightarrow \infty} r - y_r(t) = 0 \quad \text{subject to} \quad u \in [-u_{\max}, u_{\max}],$$

where $r \in \mathbb{R}$ is the desired constant reference, despite some class of external perturbations $w(t)$ and parameter uncertainties Δx .

3.3 ROBUST CONTROL DESIGN

The following assumption is imposed on system (10).

Assumption 1 *The unknown input w is bounded, *i.e.*, $w \in \mathcal{W} := \{w \in \mathcal{L}_\infty : \|w\|_\infty \leq \bar{w}\}$, with \bar{w} a positive known constant; and the unknown matrix Δ is norm bounded, *i.e.*, $\|\Delta\| \leq \bar{\delta}$, with $\bar{\delta}$ a positive known constant.*

Since the external perturbation w is bounded, and due to the fact that the system (10) is linear; then, the solutions of the system exist and they do not escape to infinity in finite time, *i.e.*, $\|x\|_{(0,t_1)} < \infty$, for any $t_1 < \infty$.

Define the regulation error $e_y := r - y_r$ and the following variable

$$x_r := \int_0^t (r - y_r(\tau)) d\tau = \int_0^t e_y(\tau) d\tau.$$

Then, the following extended system is introduced

$$\dot{z}(t) = (\bar{A} + \bar{\Delta})z(t) + \bar{B}(u(t) + w(t)) + Fr, \quad (12)$$

where $z := (x^\top, x_r)^\top \in \mathbb{R}^{n+1}$ is the extended state and the system matrices have the following structure

$$\bar{A} = \begin{pmatrix} A & 0 \\ -C & 0 \end{pmatrix}, \bar{B} = \begin{pmatrix} B \\ 0 \end{pmatrix}, F = \begin{pmatrix} 0 \\ 1 \end{pmatrix}, \bar{\Delta} = \begin{pmatrix} \Delta & 0 \\ 0 & 0 \end{pmatrix}.$$

The following assumption is imposed on the extended system (12).

Assumption 2 *The pair $(\bar{A} + \bar{\Delta}, \bar{B})$ is stabilizable.*

The Assumption 2 characterizes the type of outputs that can be regulated. Note that, due to (11), the solutions of the system (12) are constrained inside the polytope

$$\mathcal{P} := \{z \in \mathbb{R}^{n+1} | \mathbf{b}z \leq \mathbf{1}_k\}, \quad (13)$$

with $k = k_x + 1$ and $\mathbf{b} = (b_1^\top, \dots, b_k^\top)^\top \in \mathbb{R}^{n+1}$, where b_k is an arbitrary vector. For simplicity, b_k can be considered as 0 since the variable x_r has no constraints. It is possible to approximate the state-constrained set (13) by an ellipsoidal set completely contained in it [31]. Thus, there exists a family of ellipsoids $\mathcal{E}(R)$, parameterized by $0 \prec R = R^\top \in \mathbb{R}^{(n+1) \times (n+1)}$, contained in \mathcal{P} , if $\bar{b}_i^\top R^{-1} \bar{b}_i \leq 1$, for $i = \bar{1}, \bar{k}$, where the ellipsoid $\mathcal{E}(R)$ is the safe set in which the state constraints and the input saturation are not violated.

Note that it is possible to compute the projection of the ellipsoid $\mathcal{E}(R) \in \mathbb{R}^{(n+1) \times (n+1)}$ into the plane $\mathbb{R}^{n \times n}$, i.e., a new ellipsoid $\mathcal{E}(R_p)$, parameterized by $0 \prec R_p = R_p^\top \in \mathbb{R}^{n \times n}$, in the coordinates of the original state x . Then, it is possible to obtain a matrix R_p by partitioning R into the following matrices

$$R = \begin{pmatrix} R_{11} & R_{21}^\top \\ R_{21} & R_{22} \end{pmatrix},$$

where $R_{11} \in \mathbb{R}^{n \times n}$, $R_{21} \in \mathbb{R}^{1 \times (n-1)}$ and $R_{22} \in \mathbb{R}$. Therefore, the matrix R_p is computed as $R_p = R_{11} - R_{21}^\top R_{22}^{-1} R_{21}$. Then, the ellipsoid $\mathcal{E}(R_p)$ fulfills the condition $b_i^\top R_p^{-1} b_i \leq 1$, and it is completely contained in (11).

The proposed controller is given as follows

$$\mathbf{u}(t) = \sigma(\mathbf{u}_0(t)) + \mathbf{u}_I(t). \quad (14)$$

The controller (14) is divided into two parts. The nonlinear element \mathbf{u}_I is the ISMC that can compensate the effect of the matched perturbations; whereas \mathbf{u}_0 is the linear control part that takes into account the system constraints, i.e., the input saturation and the state constraints, and parameter uncertainties. Due to the fact that $|\mathbf{u}| \leq \mathbf{u}_{\max}$, each part of the controller can be upper bounded as $|\mathbf{u}_I| \leq \mathbf{u}_{I_{\max}}$ and $|\sigma(\mathbf{u}_0)| \leq \mathbf{u}_{0_{\max}}$, with constants $\mathbf{u}_{0_{\max}}, \mathbf{u}_{I_{\max}} > 0$, such that $\mathbf{u}_{0_{\max}} + \mathbf{u}_{I_{\max}} \leq \mathbf{u}_{\max}$.

Remark 1 *The value of \mathbf{u}_{\max} is fixed due to the physical properties of the actuators. In order to fulfill the condition $\mathbf{u}_{0_{\max}} + \mathbf{u}_{I_{\max}} \leq \mathbf{u}_{\max}$, it is possible to select $\mathbf{u}_{I_{\max}}$ according to the upper bound of the matched perturbations; then, $\mathbf{u}_{0_{\max}} = \mathbf{u}_{\max} - \mathbf{u}_{I_{\max}}$.*

Therefore, the closed-loop system dynamics, taking into account (14), is given as:

$$\dot{z}(t) = (\bar{A} + \bar{\Delta})z(t) + \bar{B}(\sigma(u_0(t)) + u_I(t) + w(t)) + Fr. \quad (15)$$

Now, define the sliding variable as follows

$$s(z) = G(z(t) - z(0)) - G \int_0^t (\bar{A}z(\tau) + \bar{B}\sigma(u_0(\tau)) + Fr) d\tau, \quad (16)$$

where $G \in \mathbb{R}^{1 \times n}$ is such that $\det(G\bar{B}) \neq 0$. The optimal way to design the matrix G is $G = \bar{B}^\top$ [32] or $G = \bar{B}^\dagger$ [33], these selections of G minimize the effect of the unmatched perturbations on the sliding mode dynamics [33], *i.e.*, $G = \bar{B}^\top$ or $G = \bar{B}^\dagger = \arg \min_{G \in \mathbb{R}^{1 \times n}} \|(I - \bar{B}(G\bar{B})^{-1}G)\bar{\Delta}z\|$.

Hence, the dynamics of the sliding variable is given as

$$\dot{s} = G\bar{B}(u_I(t) + w(t)) + G\bar{\Delta}z. \quad (17)$$

The methodology to design the robust controller can be described in two steps: the design of the ISMC and the design of the linear control. The ISMC is designed in order to ensure the existence of the sliding-mode, taking into account the input saturation and matched perturbations. On the other hand, once the sliding-mode existence is guaranteed, the linear control part is designed in order to guarantee the convergence to zero of the regulation error considering the input saturation, state constraints, and parameter uncertainties.

3.3.1 Integral Sliding-Mode Control Design

The ISMC u_I is proposed as

$$u_I(t) = -\rho(z(t))\text{sign}(s), \quad (18)$$

where the state-dependent gain ρ must be positive, *i.e.*, $\rho(z) > 0$, for all $z \in \mathbb{R}^{n+1}$. Consider the ellipsoid $\mathcal{E}(\mathbf{R})$, parameterized by $\mathbf{R} \in \mathbb{R}^{(n+1) \times (n+1)}$, that it is computed further on, as a safe set, which is an approximation of the region of attraction of system (12), where the state constraints are not violated. The following lemma provides the conditions to design ρ and ensures the existence of the sliding-mode.

Lemma 4 [32] *Let Assumptions 1 and 2 be satisfied, and the ISMC (18) be applied to the system (17), for a given $u_{I_{\max}} > 0$. If the gain ρ is designed as*

$$\rho(z) = \alpha + \bar{w} + \frac{\bar{\delta}\|G\|\|z\|}{\|G\bar{B}\|}, \quad (19)$$

for some $\alpha > 0$, such that

$$0 < \alpha \leq u_{I_{\max}} - \bar{w} - \frac{\bar{\delta}\|G\|}{\|G\bar{B}\|\lambda_{\max}^{\frac{1}{2}}\{\mathbf{R}\}}, \quad (20)$$

holds for some $u_{I_{\max}}$ and $0 \prec \mathbf{R}^\top = \mathbf{R} \in \mathbb{R}^{(n+1) \times (n+1)}$; then, $s = 0$ is Finite-Time Stable.

Note that the selection of the state-dependent gain ρ depends on the bound of the perturbation, the bound of the parameter uncertainties, and the convergence rate, i.e., \bar{w} , $\bar{\delta}$, and α , respectively.

In order to fulfill the saturation constraint $u_{I_{\max}} \leq u_{\max} - u_{0_{\max}}$, α must be selected such that (20) holds, which is explicitly related to the safe set $\mathcal{E}(\mathbb{R})$, where the system constraints are not violated, i.e., $u \in [u_{\max}, -u_{\max}]$ and $z \in \mathcal{P}$. Moreover, note that the design of the gain ρ ensures the existence of the integral sliding-mode guaranteeing the fulfillment of the input constraint. Once on the sliding surface, the linear control design will deal with the state and input constraints.

The following subsection presents the design of the linear controller u_0 for the dynamics on the sliding-mode.

3.3.2 Linear Control Design

Once on the sliding-mode, it follows that $s = 0$; and thus, based on the equivalent control method, the dynamics on the sliding surface is given by

$$\dot{z}(t) = (\bar{A} + \Gamma\bar{\Delta})z(t) + \bar{B}\sigma(u_0(t)) + Fr, \quad (21)$$

with $\Gamma = (I - \bar{B}(G\bar{B})^{-1}G)$. Then, the linear part of the control, i.e., u_0 , is proposed as follows

$$u_0(t) = Kz(t), \quad (22)$$

where $K \in \mathbb{R}^{n+1}$ is a feedback gain to be designed, which can be designed considering the state constraints (13) and the input saturation, by means of the AEM and the BLF approach.

The following lemma provides the safe set $\mathcal{E}(\mathbb{R})$ and a way to design K .

Lemma 5 *Let Assumptions 1 and 2 be satisfied, and the control (22) be applied to the system (21), for a given $u_{0_{\max}} > 0$. Suppose that there exist a positive-definite matrix $X_1 = X_1^T \in \mathbb{R}^{(n+1) \times (n+1)}$, some matrices $Y \in \mathbb{R}^{(n+1)}$ and $Z \in \mathbb{R}^{(n+1)}$, and some constant $\delta, \gamma > 0$, such that the following set of LMIs*

$$X_1 = \begin{pmatrix} \psi_1 & \bar{B}\delta - Y^T + Z^T & F & X_1 \\ * & -2\delta & 0 & 0 \\ * & * & -\gamma & 0 \\ * & * & * & -X_2 \end{pmatrix} \prec 0, \quad (23a)$$

$$\psi_1 = \bar{A}X_1 + X_1\bar{A} + \Gamma\bar{\delta}X_1 + X_1\bar{\delta}\Gamma^T + \bar{B}Y + Y^T\bar{B}^T,$$

$$X_2 = \begin{pmatrix} X_1 & Z \\ Z^T & u_{0_{\max}}^2 \end{pmatrix} \succeq 0, \quad (23b)$$

$$X_3 = \bar{b}_i^T X_1 \bar{b}_i \leq 1, \text{ for } i = \bar{1}, \bar{k}, \quad (23c)$$

$$r^2 X_2 \prec X_1, \quad (23d)$$

is feasible for some vectors \bar{b}_i and a fixed constant $\bar{\delta}$. If $z(0) \in \mathcal{E}(\mathbb{R})$, with $\mathbb{R} = X_1^{-1}$, and K is designed as $K = YR$; then, the trajectories of the system (21) converge asymptotically to $\mathcal{E}(\mathbb{P}_r)$, with $\mathbb{P} = X_2^{-1}$ and $\mathbb{P}_r := \frac{1}{r^2}\mathbb{P}$, and the state and input constraints are not violated.

An outline of the proof is provided in the section 3.6, and for more details please see [5].

Since $r \neq 0$ the system trajectories converge to an equilibrium point $z_c = -(\bar{A} + \Gamma\bar{A} + \bar{B}K)^{-1}\bar{F}r$; then, it is only necessary to verify that this equilibrium is contained in the ellipsoid $\mathcal{E}(P_r)$.

Remark 2 Note that (23d) guarantees that $\mathcal{E}(P_r) \subset \mathcal{E}(R)$. Since, in the set $\mathcal{E}(R) \setminus \mathcal{E}(P_r)$, $\dot{V} < 0$, with $V(z) = \ln(1/(1 - z^T R z))$ (please, refer to the proof of Lemma 5, section 3.6); then, there is no equilibrium point in such a set. Therefore, $z_c^T P z_c \leq r^2$ is always fulfilled.

Finally, considering the results of Lemma 4 and 5, the main result is presented in the following theorem.

Theorem 1 Let Assumptions 1 and 2 be satisfied, and the control (14), with $u_I(t) = -\rho(z(t))\text{sign}(s)$ and $u_0(t) = Kz(t)$, be applied to the system (12), for a given $u_{\max} > 0$. If $z(0) \in \mathcal{E}(R)$, K is computed as in Lemma 5, i.e., $K = YR$, and ρ is designed as in (19), i.e.,

$$\rho(z) = \alpha + \bar{w} + \frac{(\bar{\delta}\|G\|\|z\|)}{(\|G\bar{B}\|)},$$

for some $\alpha > 0$, such that

$$\alpha + \bar{w} + \frac{\bar{\delta}\|G\|}{\|G\bar{B}\|\lambda_{\max}^{\frac{1}{2}}\{R\}} \leq u_{I_{\max}} \leq u_{\max} - u_{0_{\max}},$$

then, the trajectories of the system (12) converge asymptotically to the equilibrium point z_c ; thus, $\lim_{t \rightarrow \infty} e_y(t) = 0$, and the state and input constraints are not violated.

Note that it is desirable that the safe set $\mathcal{E}(R)$, where the system constraints are not violated, is as large as possible. Thus, it is possible to establish an optimization problem in order to maximize its volume.

Corollary 1 Let Assumptions 1 and 2 be satisfied, and the control (14), with $u_I(t) = -\rho(z(t))\text{sign}(s)$ and $u_0(t) = Kz(t)$, be applied to the system (12), for a given $u_{\max} > 0$. If $z(0) \in \mathcal{E}(R)$, the gain $K = YX_1^{-1}$ is computed by solving the following optimization problem

$$\max_{X_1, Y, Z, \delta, \gamma} \log\{\det(X_1)\} \text{ subject to (23),} \quad (24)$$

and ρ is designed as in (19), i.e.,

$$\rho(z) = \alpha + \bar{w} + \frac{(\bar{\delta}\|G\|\|z\|)}{(\|G\bar{B}\|)},$$

for some $\alpha > 0$, such that

$$\alpha + \bar{w} + \frac{\bar{\delta}\|G\|}{\|G\bar{B}\|\lambda_{\max}^{\frac{1}{2}}\{R\}} \leq u_{I_{\max}} \leq u_{\max} - u_{0_{\max}},$$

then, the trajectories of the system (12) converge asymptotically to the equilibrium point z_c ; thus, $\lim_{t \rightarrow \infty} e_y(t) = 0$, and the state and input constraints are not violated.

Regarding the proof of Lemma 4, this is omitted due to it is a standard result in the sliding-mode control theory, for more details, please refers to [32].

Remark 3 Since u_I is selected as in (18), i.e., $u_I(t) = -\rho(z(t))\text{sign}(s)$, a discontinuous control signal is obtained. However, it is possible to approximate the sign function as [32]

$$\text{sign}(s) \approx \frac{s}{|s| + \tau},$$

where τ is a small positive constant, i.e., $\tau \ll 1$. Then, a continuous control signal is obtained as

$$u_I(t) = -\rho(z(t)) \frac{s}{|s| + \tau}. \quad (25)$$

The following algorithm gives some insight on the implementation of the robust controller (14).

Algorithm 3.1:

Input: $r, \bar{b}_i, u_{\max}, \bar{w}, \bar{\delta}, \bar{B}, G, \alpha, \varepsilon, \nu$;

Output: R, K, ρ ;

01: $\nu \in (0, 1)$;

02: $u_{I_{\max}} = u_{\max}$;

03: $u_{0_{\max}} = u_{\max} - u_{I_{\max}}$;

04: **while** $\chi_1 > 0 \wedge \chi_2 \leq 0 \wedge \chi_3 \geq 0 \wedge u_{I_{\max}} > 0$
 $\wedge \lambda_{\max}^{1/2}\{R\} > \frac{\|GB\|}{\bar{\delta}\|G\|}(u_{I_{\max}} - \bar{w} - \alpha)$

05: $u_{I_{\max}} = u_{I_{\max}} - \nu u_{I_{\max}}$;

06: $u_{0_{\max}} = u_{\max} - u_{I_{\max}}$;

07: **end**

08: $R = X_1^{-1}$;

09: $P = X_2^{-1}$;

10: $K = YR$;

11: $u_{I_{\max}} = u_{I_{\max}}$;

12: $u_{0_{\max}} = u_{0_{\max}}$;

Note that if the algorithm ends and no feasible solution is obtained; then, it is not possible to design a gain K for the desired reference r , the given parameter uncertainties Δ , and external perturbations w .

To better illustrate the algorithm presented in this chapter, a block diagram of the closed-loop dynamics, considering the system (10a) and the controller (14), is presented in Fig. 4.

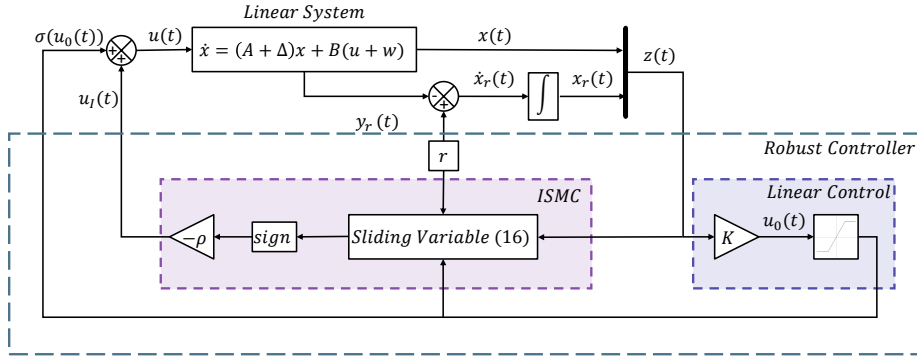


Figure 4: Closed-loop diagram

3.4 SIMULATION RESULTS

Consider the pendulum system dynamics:

$$\dot{x}_1(t) = x_2(t), \quad (26a)$$

$$\dot{x}_2(t) = \frac{1}{J}\sigma(u(t)) - \left(\frac{mgl}{2J} + \delta_p\right) \sin(x_1(t)) + w(t), \quad (26b)$$

$$y_r(t) = x_1(t), \quad (26c)$$

where x_1 is the angular position of the pendulum, x_2 is the angular velocity, and w represents some external perturbations. The system parameters are given as follows: $m = 1[\text{kg}]$ is the pendulum mass, $l = 0.707[\text{m}]$ is the pendulum longitude, $J = 0.5[\text{kg} \cdot \text{m}^2]$ is the arm inertia, $g = 9.815[\text{m}/\text{s}^2]$ is the gravitational constant, and $\delta_p = 0.1734[1/\text{s}^2]$, which represents 10% of parameter uncertainties. Then, linearizing (26) around the unstable equilibrium point $(x_1, x_2) = (0, 0)$, the system matrices, as in (10), are given as

$$A = \begin{pmatrix} 0 & 1 \\ -\frac{mgl}{2J} & 0 \end{pmatrix}, \Delta = \begin{pmatrix} 0 & 0 \\ -\delta_p & 0 \end{pmatrix}, B = \begin{pmatrix} 0 \\ \frac{1}{J} \end{pmatrix}, \\ C = \begin{pmatrix} 1 & 0 \end{pmatrix}, D = \begin{pmatrix} 0 & 1 \end{pmatrix}^\top.$$

It can be verified that system (26) satisfies Assumptions 1 and 2. The external perturbation is taken as $w(t) = 2 \sin(2t) + 2$, therefore $\bar{w} = 4$, and then, $Q_w = 0.0625$. The initial conditions are $x(0) = (-15\pi/180, 12\pi/45)^\top$ and $x_r(0) = 0$. The desired reference is selected as $r = \pi/18$ [rad]. The vectors \bar{b}_1 and \bar{b}_4 are equivalent to the maximum and minimum values for x_1 , i.e., $x_1 \in (-\bar{x}_1, \bar{x}_1)$ with $\bar{x}_1 = 10\pi/45$ [rad]. Similarly, for state x_2 , the vectors \bar{b}_2 and \bar{b}_5 are equivalent to $\bar{x}_2 = 10\pi/35$ [rad/s] and $-\bar{x}_2$, i.e., $x_2 \in (-\bar{x}_2, \bar{x}_2)$. Since $x_3 = x_r$ is the integral action no constraints are considered.

For simulation purposes, sufficiently large constraints are considered for the state x_r . Given the previous statements, the state constraints are $\bar{b}_1 = (45/10\pi, 0, 0)^\top$, $\bar{b}_2 = (0, 35/10\pi, 0)^\top$, $\bar{b}_3 = (0, 0, 10/25)^\top$, $\bar{b}_4 = -\bar{b}_1$, $\bar{b}_5 = -\bar{b}_2$ and $\bar{b}_6 = -\bar{b}_3$.

To compute the control gains, let us apply Algorithm 3.1. Consider $u_{\max} = 6$, $\alpha = 0.1$, $\nu = 0.2$, then, the following feasible solution is obtained:

$$\begin{aligned} R &= \begin{pmatrix} 41.4277 & 5.1529 & -45.8358 \\ 5.1529 & 1.9253 & -4.9642 \\ -45.8358 & -4.9642 & 63.3021 \end{pmatrix}, \\ P &= \begin{pmatrix} 3.2452 & 1.0895 & -3.2507 \\ 1.0895 & 0.5252 & -1.0206 \\ -3.2507 & -1.0206 & 3.6626 \end{pmatrix}, \\ K &= \begin{pmatrix} -20.5211 & -7.4427 & 20.2369 \end{pmatrix}, \\ u_{I_{\max}} &= 4.1761, \quad u_{0_{\max}} = 1.8239, \quad \gamma = 50, \quad \delta = 0.6809. \end{aligned}$$

Once the matrix R is obtained, it is possible to compute the matrix R_p , which is the projection of the ellipsoid in the plane $x_1 - x_2$, according to equation $R_p = R_{11} - R_{21}^\top R_{22} R_{21}$, the following matrix R_p is obtained

$$R_p = \begin{pmatrix} 8.2389 & 1.5585 \\ 1.5585 & 1.5360 \end{pmatrix}.$$

Taking into account Remark 3, it is possible to apply the ISMC (14), with the approximation (25), fixing $\tau = 0.02$ and using the same gain computed for the ISMC (14), *i.e.*, $K = (-3.2637 \quad -2.0919 \quad 1.7694)$. For comparison purposes, and in order to show the benefits of introducing the ISMC, let us consider a linear control u as the linear control u_0 , *i.e.*, $u = Kz$.

The corresponding simulations have been done in MATLAB, using the explicit Euler method with a sampling time equal to 0.001 [s]. The LMIs solutions are obtained through the SDPT3 solver. In order to simplify the nomenclature in the simulation results the sub-indexes ISM, ISM_c and u_0 are introduced for the results obtained through the proposed control law (14), the continuous ISMC with the approximation (25), and u as the linear control, respectively.

The system trajectories are depicted by Figs. 5–7. Fig. 5 illustrates the trajectories of the state x_1 and its constraints. For the case when the ISM-based controllers are applied, the output system follows the desired reference even in the presence of external perturbations. Whereas for the case when only the linear controller is applied, *i.e.*, when $u = Kz$, the output system converges to a certain neighborhood of the desired reference. However, in both cases, the state constraints are not transgressed. Fig. 6 depicts the trajectories for the state x_2 and its constraints. It is shown that for the linear case, *i.e.*, when $u = Kz$, the state trajectory transgresses the upper state constraint due to the presence of the external perturbations, while the ISM-based controllers ensure that the state trajectory does not

transgress the restricted zone. Fig. 7 depicts the trajectories of the variable x_r , it can be seen that only when the ISM-based controllers are applied, the trajectory converges to the equilibrium point \bar{z}_c . The output regulation errors are depicted by Fig. 8. It is shown that, for the case when the ISM-based controllers are applied, the regulation error converges to zero, while for the linear case, the regulation error converges to a neighborhood close to the origin. For the case with the ISM-based controller, the linear control u_0 , the nonlinear control u_1 , the control signal, and the saturation constraints are depicted by Fig. 9. The linear control signal, *i.e.*, u_0 , remains in the non-saturated region all the time, while the nonlinear control signal is bounded, *i.e.*, $u_1 < u_{I_{\max}}$; thus, the control signal u remains in the non-saturated region. Similarly, in Fig. 10 the control signals are presented for the case in which the approximation (25) is applied to the ISM-based controller (14), it can be seen that the nonlinear control part is continuous. However, with both ISM-based controllers, the tracking task is achieved. Fig. 11 illustrates the linear case, *i.e.*, $u = Kz$. It is observed that the control signal is not saturated. Nevertheless, the tracking task is not achieved due to the control is not able to compensate the external perturbations.

The states trajectories and the corresponding ellipsoid are depicted by Fig. 12, for the three cases, *i.e.*, the ISM-based controllers and the linear case. It is shown that the system trajectories, when the ISM-based controllers are applied, remain in the ellipsoid $\mathcal{E}(R)$, and converge asymptotically to ellipsoid $\mathcal{E}(P_r)$. The projection of the ellipsoids $\mathcal{E}(R)$ and $\mathcal{E}(P_r)$ in the x_1 - x_2 plane and the polytope \mathcal{P}_x are depicted by Fig. 13. It is clear that, for the case when the ISM-based controllers are applied, the trajectories of the system are always inside $\mathcal{E}(R_p)$, which is completely contained in the polytope (11). Nevertheless, for the linear case it is noticed that the states trajectories leave the ellipsoid $\mathcal{E}(R_p)$, violating the state constraints.

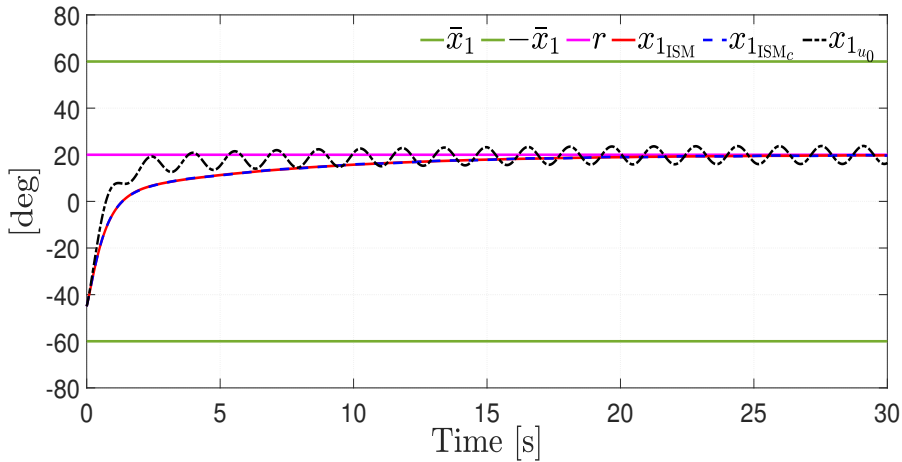


Figure 5: State x_1 and its constraints

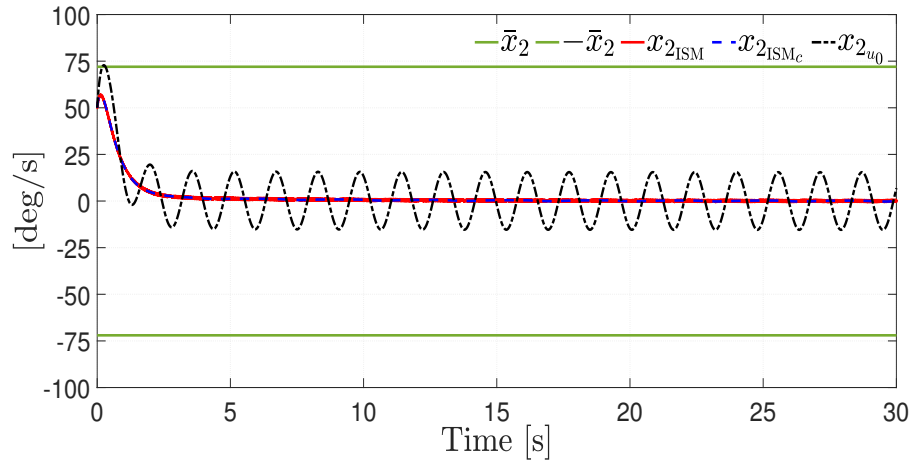
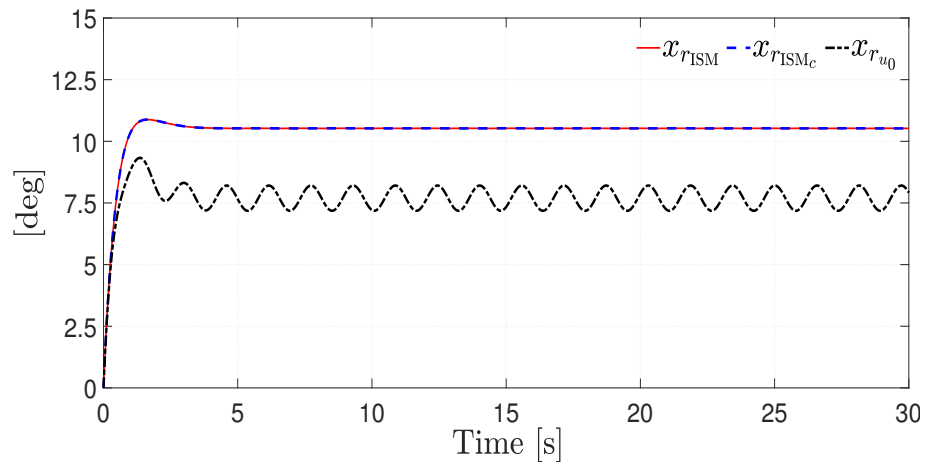
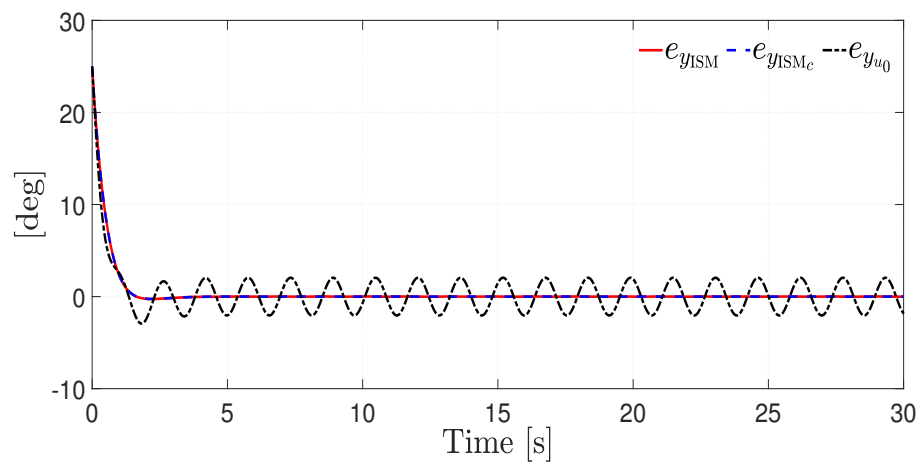
Figure 6: State x_2 and its constraintsFigure 7: State x_r 

Figure 8: Regulation errors

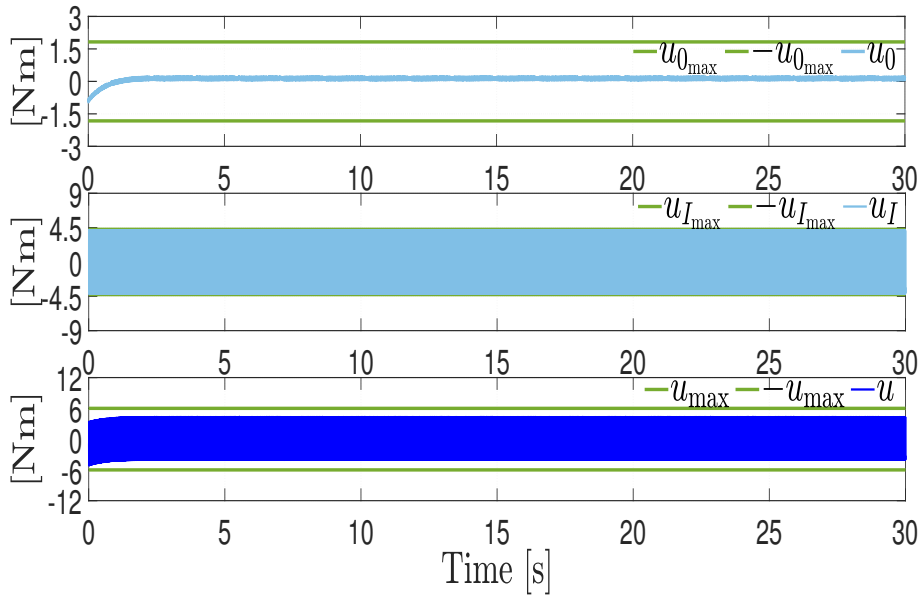


Figure 9: Control signals u_0 , u_I and u for the discontinuous ISMC

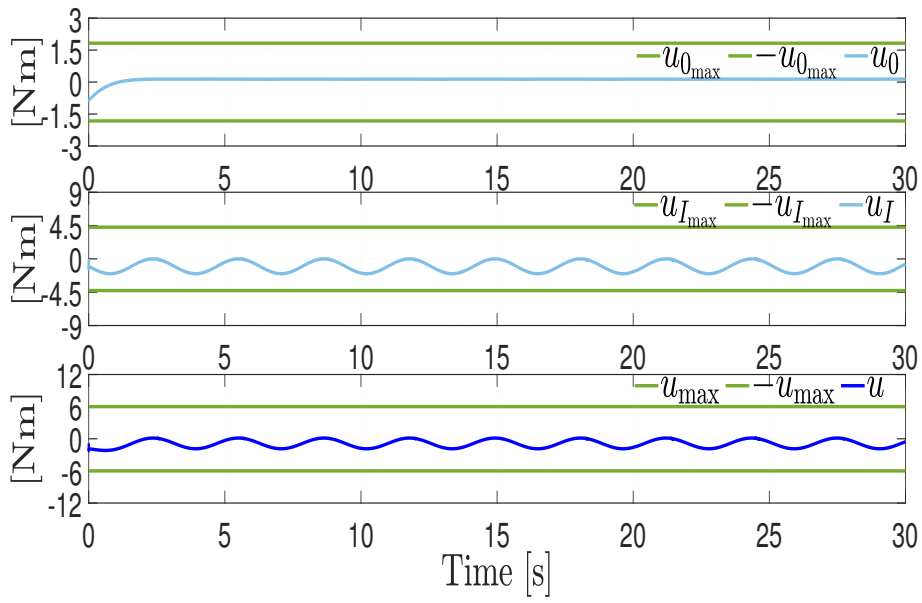
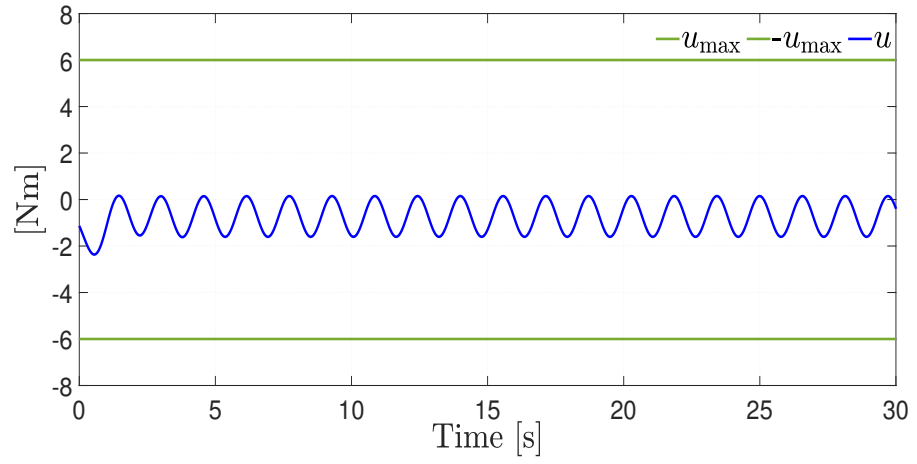
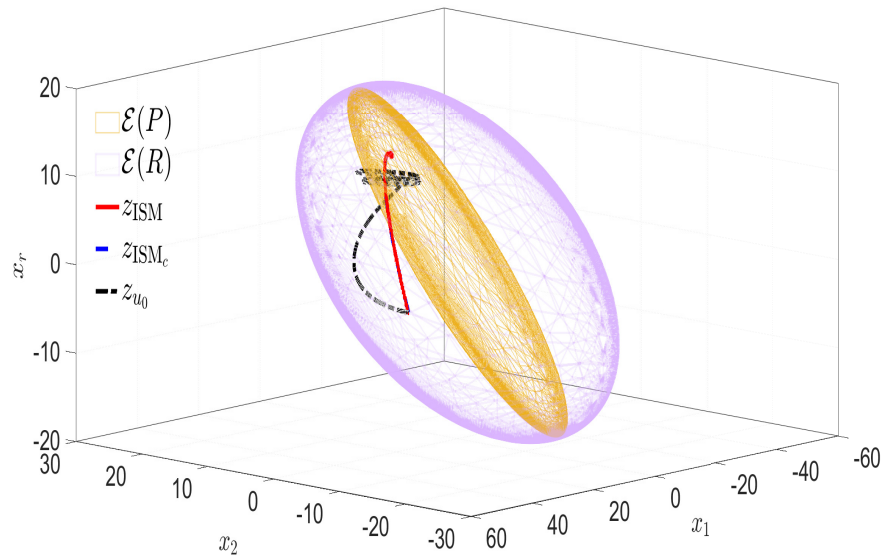


Figure 10: Control signals u_0 , u_I and u for the continuous ISMC

Figure 11: Control signal u_0 for the linear controlFigure 12: State trajectories and ellipsoid $\mathcal{E}(R)$

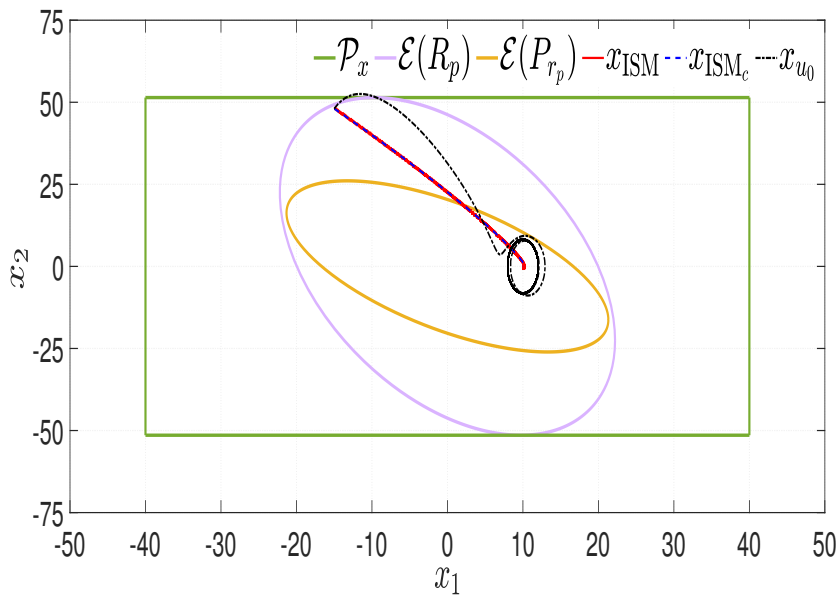


Figure 13: States trajectories, state constraints projection, ellipsoids $\mathcal{E}(R_p)$, $\mathcal{E}(P_{r_p})$, and polytope \mathcal{P}_x

3.5 REMARKS

This chapter contributes with a solution to the output regulation problem for uncertain linear systems with input saturation, state constraints, and external perturbations. The controller is split in two parts, the linear and nonlinear part. Due to the ISMC approach, both parts of the controller can be designed independently. Based on the BLF and AEM approach, the linear control considers the input saturation, state constraints, and parameter uncertainties, whereas the nonlinear control compensates the effect of matched perturbations through the ISMC technique. A safe set is provided where the state constraints and the input saturation are satisfied. The proposed scheme guarantees asymptotic convergence to zero of the output regulation error coping with the system constraints. The synthesis of the controller gains is given in terms of LMIs providing a constructive method for the design.

3.6 PROOF OF THE RESULTS

Proof of Lemma 5: Consider the function $\phi(u_0) = \sigma(u_0) - u_0$; thus, the dynamics on the sliding-mode (21) can be rewritten as

$$\dot{z}(t) = (\bar{A} + \Gamma\bar{\Delta} + \bar{B}K)z(t) + \bar{B}\phi(u_0(t)) + Fr. \quad (27)$$

Let us take into account the following BLF candidate

$$V(z) = \ln \left(\frac{1}{1 - z^\top(t)Rz(t)} \right),$$

where $0 < R = R^\top \in \mathbb{R}^{(n+1) \times (n+1)}$ is a matrix that parametrizes the ellipsoid $\mathcal{E}(R)$. Then, introducing the extended vector $\eta^\top := (z^\top(t), \phi^\top(u_0(t)), r)^\top$, the time derivative of V along the trajectories of system (27) is given by

$$\dot{V}(z) = S_z(t)\eta^\top \begin{pmatrix} \text{He}\{A_k\} & R\bar{B} & RF \\ \star & 0 & 0 \\ \star & \star & 0 \end{pmatrix} \eta,$$

where $S_z(t) = 1/(1 - z^\top(t)Rz(t))$ and $A_k = R(\bar{A} + \Gamma\bar{\Delta} + \bar{B}K)$. Then, adding and subtracting the terms $\gamma r^2 S_z$ and $\gamma S_z z^\top(t)Pz(t)$, with $\gamma > 0$, and taking into account Assumption 1, where $\bar{A}_k = R(\bar{A} + \Gamma\bar{\delta} + \bar{B}K)$, and according to Lemma 3, with $\bar{\alpha} = Kz$, $\bar{\beta} = Kz - G_0z$, and $G_0 \in \mathbb{R}^{1 \times (n+1)}$, the inequality $\delta^{-1}\phi^\top[\phi + (K - G_0)z] \leq 0$ is satisfied. In order to ensure that G_0z belongs to the set \mathcal{U} , it is sufficient that $\|G_0z\|^2 \leq u_{0,\max}^2 z^\top R z$ holds. Using the Schur's complement, the previous inequality can be written as in LMI (23b) with $Z = R^{-1}G_0$. Therefore, the LMI (23b) guarantees the fulfillment of the input constraint.

Then, \dot{V} can be rewritten as

$$\dot{V}(z) \leq \gamma S_z(t)(r^2 - z^\top(t)Pz(t)) + S_z(t)\eta^\top \Omega_1 \eta,$$

where

$$\Omega_1 = \begin{pmatrix} \text{He}\{\bar{A}_k\} + \gamma P & R\bar{B} - \delta^{-1}[K - G_0]^\top & RF \\ * & -2\delta^{-1} & 0 \\ * & * & -\gamma \end{pmatrix}.$$

Pre and post-multiplying Ω_1 by $T = \text{diag}(R^{-1}, \bar{\delta}, I)$, it follows that $\Omega_1 \prec 0$ is equivalent to χ_1 in (23a), with the change of variables $X_1 = R^{-1}$, $Y = KR^{-1}$ and $Z = R^{-1}G_0$.

Hence, if $\chi_1 \prec 0$, then

$$\dot{V}(z) \leq \gamma S_z(t)(r^2 - z^\top(t)Pz(t)).$$

Note that, for all $z^\top(t)Pz(t) > r^2$ and $z^\top(t)Rz(t) < 1$, $\dot{V} < 0$; and thus, any solution of the system starting in $\mathcal{E}(R)$, remains in $\mathcal{E}(R)$ and converges asymptotically to $\mathcal{E}(P_r)$; and hence, it follows that $\lim_{t \rightarrow \infty} e_y(t) = 0$. Finally, if the LMI (23c) holds; then, $\mathcal{E}(R)$ is also the safe set in which the state constraints and the input saturation are not violated. Moreover, LMI (23d) ensures that $\mathcal{E}(P_r) \subset \mathcal{E}(R)$. This concludes the proof. ■

AN IP-BASED ROBUST CONTROL FOR UNCERTAIN NONLINEAR SYSTEMS

This chapter presents a robust sampled-time controller for stabilizing a class of uncertain nonlinear systems. The proposed strategy consists of two key components: an IP-based state-feedback controller and an MPC approach. The switched control strategy guarantees ISpS of the nonlinear systems with respect to external perturbations.

4.1 INTRODUCTION

Real dynamical systems are restrained due to the structural limitations of the system, *i.e.*, the system dynamics have state and input constraints (see, *e.g.* [34], [35], and [36]). These kinds of systems can generally be represented by nonlinear models. Furthermore, the systems may be subject to external perturbations and/or parameter uncertainties that may have an impact on their behavior. To design a controller, which is able to counteract the effects of external perturbations while considering state and input constraint, robust control techniques are required. For instance, the MPC is a technique that obtains the current control action through the on-line solution of a finite horizon open-loop optimal control problem, at each sampling instant, using the current state of the plant as the initial state. The first control signal, obtained in the optimal control sequence, is applied to the system [37].

Concerning the control design for constrained systems affected by external perturbations, in [38], an MPC for constrained uncertain linear systems is proposed, which guarantees the robustness of the system constraints and ISS of the closed-loop system. Also, the MPC approach is widely used for LPV systems. For instance, output feedback robust MPC for uncertain LPV systems with external perturbations is proposed in [39] and [40]. In [39] the algorithm single-step dynamic output feedback robust MPC, where the infinite-horizon control moves, is parameterized as a dynamic output feedback law. However, to accomplish the control task, this method requires a heavy computational burden. While, in [40] the estimated state and estimation error converges to the corresponding invariant sets. In both works, recursive feasibility and robust stability are ensured. For discrete time systems, the MPC can also be applied, for instance, in [41], an output feedback MPC for discrete-time linear systems affected by bounded state and output perturbations is considered. The controller is composed by a stable state estimator and an MPC. Meanwhile, an on-line solution of a standard quadratic optimization program is required. The closed-loop system renders a specified invariant set robustly exponentially stable. In [42], an output-feedback MPC algorithm for discrete-time

constrained linear systems affected by additive noise is presented. The algorithm ensures convergence of the state to a suitable neighborhood of the origin. Note that most MPC results in the literature are devoted to linear systems, and this could be restrictive.

Regarding the application of the MPC approach to nonlinear systems, in [43], a robust learning-based MPC is proposed for nonlinear systems subject to input and output constraints. The prediction model is estimated by a nonparametric machine learning technique; thus, an MPC, without terminal constraint, is obtained, then the closed-loop is asymptotically stable. The MPC can also be applied to nonlinear discrete-time systems. For instance, in [44], an MPC with a composite self-triggered mechanism is proposed to reduce the communication and computational burden while maintaining the desired control performance for this kind of systems. However, the algorithm has a relatively low perturbation tolerance. Meanwhile, in the previous works, a heavy computational burden is required because the MPC is active during the control task.

It is also possible to combine the MPC with other techniques, *e.g.*, adaptive control, SMC and interval observer techniques, to improve its performance. For instance, in [45], an adaptive MPC for linear systems with external perturbations is proposed. In [46], an MPC algorithm is developed for discrete-time constrained linear-time invariant systems with parameter uncertainties. An adaptive controller is used to handle the parameter uncertainties, and it is combined with an MPC algorithm guaranteeing the constraints satisfaction. On the other hand, an MPC is proposed in [47] for nonlinear systems based on a terminal cost function characterized by an implicit SMC law. However, a linearized model is required to guarantee the asymptotic stability of the closed-loop system. In [48], an interval observer and predictor are incorporated into the classic MPC scheme for discrete-time constrained linear systems with bounded state perturbations. Nevertheless, most of the above-mentioned works do not consider sampled control.

Motivated by these issues, this chapter proposes the design of a robust sampled controller to stabilize continuous-time nonlinear systems, taking into account state and input constraints, and external perturbations. The robust controller is based on a discrete-time IP-based state-feedback controller and an MPC approach. The proposed control method possesses the following features:

- 1) Due to the use of an IP, the measurements of the system states are not required for the proposed scheme.
- 2) Characterization of a safe set where the state constraints are not transgressed using the IP-based state-feedback controller.
- 3) Low computational cost since the MPC is only activated out of the safe set, and it can be pre-computed in advance.
- 4) Local Input-to-State practical Stability of the constrained nonlinear systems with respect to external perturbations.

- 5) The synthesis of the controller is constructive since it is based on LMIs.

The fact that the proposed scheme does not require the measurement of the system state represents an advantage in real-world applications (e.g., the blood glucose regulation and the anesthesia regulation in delivery machines, and some trajectory-tracking problems in mobile robots) that could be solved by using the proposed framework. Therefore, the proposed method can be interpreted as a tool to design robust feedforward inputs.

4.2 PROBLEM STATEMENT

Consider the following class of nonlinear system

$$\dot{x}(t) = f(x(t)) + Bu(t) + Dw(t), \quad t \geq 0, \quad (28)$$

where $x(t) \in \mathbb{R}^n$ is the state, $f: \mathbb{R}^n \rightarrow \mathbb{R}^n$ is a locally Lipschitz function, $u(t) \in \mathbb{R}^p$ is the control input, and $w: \mathbb{R}_+ \rightarrow \mathbb{R}^q$ is the perturbation term. The matrices B and D are known of suitable dimensions. It is considered that $u \in \mathcal{U} := \{u \in \mathbb{R}^p \mid -u_{\max_j} \leq u_j \leq u_{\max_j}, j = \overline{1, p}\}$, where $0 < u_{\max_j}$ is the maximum value for each control signal. In this chapter, the control signal must be sampled, i.e., $u(t) = u(t_k)$, for $t \in [t_k, t_{k+1})$ and $k \in \mathbb{Z}_+$, where $t_k = kh$ form a strictly growing sequence of time instants for some $h > 0$.

Moreover, the solutions of the system (28) must be constrained inside the polytope

$$\mathcal{X} := \{x \in \mathbb{R}^n \mid \mathbf{b}x \leq \mathbf{1}_{k_x}\}, \quad (29)$$

where $\mathbf{b} = (b_1, \dots, b_{k_x})^\top \in \mathbb{R}^{k_x \times n}$. It is assumed that the origin belongs to the interior of the set \mathcal{X} . Before proceeding, the following assumptions are imposed on the system (28).

Assumption 3 *There exist a known Metzler matrix $A_0 \in \mathbb{R}^{n \times n}$ and known matrices $A_j \in \mathbb{R}^{n \times n}$, $j = \overline{1, N}$ for some $N \in \mathbb{Z}_+$, such that the following relations are satisfied*

$$f(x) = \left(A_0 + \sum_{j=1}^N \alpha_j(x) A_j \right) x,$$

$$\sum_{j=1}^N \alpha_j(x) = 1, \quad \alpha_j(x) \in (0, 1), \quad j = \overline{1, N}.$$

Assumption 4 *There exist known signals $\underline{w}, \bar{w} \in \mathcal{L}_\infty^q$, $w_{\max} > 0$, and known vectors $\underline{x}_0, \bar{x}_0 \in \mathbb{R}^n$, such that $\underline{w}(t) \leq w(t) \leq \bar{w}(t)$, $\|w\|_\infty \leq w_{\max}$, and $\underline{x}_0 \leq x(0) \leq \bar{x}_0$, respectively.*

Assumption 3 characterizes the class of nonlinearities of the system (28), i.e., those that can be expressed by a sum of a linear term, $A_0 x$, and a convex nonlinear function, $\sum_{j=1}^N \alpha_j(x) A_j x$. On the other hand, Assumption 4

and the condition that A_0 must be Metzler are required to design an MPC and an IP for the system (28).

The aim of this chapter is to design a sampled control law to ensure the stabilization of the system (28), taking into account the input and state constraints, *i.e.*, $x \in \mathcal{X}$ and $u \in \mathcal{U}$, under Assumptions 3 and 4.

4.3 CONTROL DESIGN

The proposed controller comprises the design of a robust control law, composed of an IP-based state-feedback controller and the MPC, which deals with state and input constraints. It will be demonstrated that there exists a safe set for the IP based state-feedback controller, where the state constraints are not transgressed, that characterizes the regions where each controller is activated: the MPC is activated outside the safe set while the state-feedback controller is applied inside of it. Since the control is sampled, a sampled-time IP is designed for the continuous-time system (28), which considers the error of discretization and guarantees a careful treatment of the constraints.

The following section addresses the design of the IP for the nonlinear system (30), satisfying Assumptions 3 and 4.

4.3.1 Interval Predictor

According to Assumption 3, the system (28) has the following representation

$$\dot{x}(t) = \left(A_0 + \sum_{j=1}^N \alpha_j(x) A_j \right) x(t) + Bu(t) + Dw(t). \quad (30)$$

Based on [49], assuming that $\underline{x} \leq x \leq \bar{x}$ and applying (7) to $\alpha_j(x)x$, the relation $-\underline{x}^- \leq \alpha_j(x)x \leq \bar{x}^+$ holds. Thus, according to (6), the following inequalities can be obtained

$$-\Delta A^+ \underline{x}^- - \Delta A^- \bar{x}^+ \leq \sum_{j=1}^N \alpha_j(x) A_j x \leq \Delta A^+ \bar{x}^+ + \Delta A^- \underline{x}^-,$$

where $\Delta A^+ = \sum_{i=1}^N A_i^+$ and $\Delta A^- = \sum_{i=1}^N A_i^-$. Then, a continuous-time IP for (30) can be stated as follows [50]:

$$\dot{z}(t) = \mathcal{A}_0 z(t) + \mathcal{A}_1 z^+(t) + \mathcal{A}_2 z^-(t) + \mathcal{B}u(t) + \delta(t), \quad (31)$$

where $z = [\underline{x}^\top, \bar{x}^\top]^\top \in \mathbb{R}^{2n}$ is the extended state vector of the predictor, the extended system matrices $\mathcal{A}_0 \in \mathbb{R}^{2n \times 2n}$, $\mathcal{A}_1 \in \mathbb{R}^{2n \times 2n}$, $\mathcal{A}_2 \in \mathbb{R}^{2n \times 2n}$, and $\mathcal{B} \in \mathbb{R}^{2n \times p}$ are given as

$$\mathcal{A}_0 = \begin{pmatrix} A_0 & 0 \\ 0 & A_0 \end{pmatrix}, \quad \mathcal{A}_1 = \begin{pmatrix} 0 & -\Delta A^- \\ 0 & \Delta A^+ \end{pmatrix}, \\ \mathcal{A}_2 = \begin{pmatrix} -\Delta A^+ & 0 \\ \Delta A^- & 0 \end{pmatrix}, \quad \mathcal{B} = \begin{pmatrix} B \\ B \end{pmatrix},$$

and the term $\delta \in \mathbb{R}^{2n}$ is defined as follows

$$\delta(t) = \mathcal{D} \begin{pmatrix} \underline{w}(t) \\ \overline{w}(t) \end{pmatrix} = \begin{pmatrix} D^+ & -D^- \\ -D^- & D^+ \end{pmatrix} \begin{pmatrix} \underline{w}(t) \\ \overline{w}(t) \end{pmatrix}.$$

Being properly initialized by $\underline{x}(0) = \underline{x}_0$ and $\overline{x}(0) = \overline{x}_0$, this IP ensures the desired interval inclusion property $\underline{x}(t) \leq x(t) \leq \overline{x}(t)$, $\forall t \geq 0$ [50]. Note that, based on Assumption 4, δ is known. Then, for any $t \geq t_0 \geq 0$, the solution of system (31) is given by

$$\begin{aligned} z(t) = e^{A_0(t-t_0)}z(t_0) &+ \int_{t_0}^t e^{A_0(t-\tau)}\mathcal{B}u(\tau)d\tau \\ &+ \int_{t_0}^t e^{A_0(t-\tau)}\delta(\tau)d\tau + \int_{t_0}^t e^{A_0(t-\tau)}g(z(\tau))d\tau, \end{aligned} \quad (32)$$

where $g(z(t)) = \mathcal{A}_1 z^+(t) + \mathcal{A}_2 z^-(t)$. The expression (32), with a sampled control $u(t) = u(t_k)$, for $t \in [t_k, t_{k+1})$, and $k \in \mathbb{Z}$, generates a discrete-time sequence:

$$\begin{aligned} z(t_{k+1}) = e^{A_0 h}z(t_k) &+ \int_0^h e^{A_0(h-s)}\mathcal{B}ds \cdot u(t_k) + \delta_k \\ &+ \int_{t_k}^{t_{k+1}} e^{A_0(t_k-s)}g(z(s))ds, \end{aligned}$$

where $h = t_{k+1} - t_k$ is the sampling interval, t_k is the sampling time instant, and $\delta_k = \int_{t_k}^{t_{k+1}} e^{A_0(t_{k+1}-s)}\delta(s)ds$. Adding and subtracting the term $\int_0^h e^{A_0(h-s)}ds \cdot g(z(t_k))$, it follows that

$$\begin{aligned} z(t_{k+1}) = e^{A_0 h}z(t_k) &+ \int_0^h e^{A_0(h-s)}\mathcal{B}ds \cdot u(t_k) + \delta_k \\ &+ \int_0^h e^{A_0(h-s)}ds \cdot g(z(t_k)) + \varphi_k, \end{aligned} \quad (33)$$

with $\varphi_k = \int_{t_k}^{t_{k+1}} e^{A_0(t_{k+1}-s)}[g(z(s)) - g(z(t_k))]ds$. Let us consider the notation $z(t_k) = z_k$, $u(t_k) = u_k$, and $\mathcal{G} = \int_0^h e^{A_0(h-s)}ds \in \mathbb{R}^{2n \times 2n}$. Thus, (33) can be rewritten as

$$z_{k+1} = \overline{\mathcal{A}}_0 z_k + \overline{\mathcal{B}}u_k + \delta_k + \mathcal{G}g(z_k) + \varphi_k, \quad (34)$$

with $\overline{\mathcal{A}}_0 = e^{A_0 h} \in \mathbb{R}^{2n \times 2n}$ and $\overline{\mathcal{B}} = \mathcal{G}\mathcal{B} \in \mathbb{R}^{2n \times p}$. Note that the IP (34) cannot be implemented since φ_k , which characterizes the discretization accuracy and depends on $z(t)$ with $t \in [t_k, t_{k+1}]$, cannot be computed. Thus, consider the following predictor

$$\hat{z}_{k+1} = \overline{\mathcal{A}}_0 \hat{z}_k + \overline{\mathcal{B}}u_k + d_k + \mathcal{G}g(\hat{z}_k), \quad (35)$$

with $d_k = \delta_k + \overline{\varphi}$, where $\overline{\varphi}^\top = (-\varphi_{\max}\mathbf{1}_n^\top, \varphi_{\max}\mathbf{1}_n^\top)$ and $\varphi_k \leq \varphi_{\max}$, the bound φ_{\max} is obtained later during the proof. This parameter evaluates the error of discretization of (31), and taking it into account allows us to

guarantee that the constraints will not be violated due to numeric errors. To stabilize the nonlinear dynamics (28), it is necessary to design u_k to take the trajectories of the system (35) to a vicinity of zero dealing with the state and input constraints. Let us propose the following control law for the system (34)

$$u_k = \begin{cases} \bar{u}_k & \text{if } \hat{z}_k \notin \mathcal{R}, \\ \hat{u}_k & \text{if } \hat{z}_k \in \mathcal{R}, \end{cases} \quad (36)$$

where $\mathcal{R} \subset \mathbb{R}^{2n}$ is the safe set, \bar{u}_k is the control signal computed by the MPC algorithm and \hat{u}_k is the state–feedback control law. Notice that \hat{u}_k is applied only inside the safe set \mathcal{R} , defined further on, where the state constraints are not transgressed.

4.3.2 State–Feedback Control

Let us propose the following nonlinear state–feedback control

$$\hat{u}_k = K_0 \hat{z}_k + K_1 \hat{z}_k^+ + K_2 \hat{z}_k^- + S_1 d_k. \quad (37)$$

The next theorem provides a way to compute the controller gains $K_0, K_1, K_2, S_1 \in \mathbb{R}^{p \times 2n}$.

Lemma 6 *Let Assumptions 3 and 4 be satisfied, and the control law (37) be applied to the system (34). Suppose that there exist diagonal matrices $0 \prec X_1 \in \mathbb{R}^{2n \times 2n}$, $0 \prec \tilde{Q}_0 \in \mathbb{R}^{2n \times 2n}$, $0 \succ \tilde{Q}_1 \in \mathbb{R}^{2n \times 2n}$, $0 \succ \tilde{Q}_2 \in \mathbb{R}^{2n \times 2n}$, $0 \prec \tilde{R}_0, \tilde{R}_1, \tilde{R}_2 \in \mathbb{R}^{2n \times 2n}$, $\tilde{R}_3 \in \mathbb{R}^{2n \times 2n}$, and matrices $Y_0, Y_1, Y_2, Y_3 \in \mathbb{R}^{2n \times p}$, such that the following set of LMIs*

$$\begin{pmatrix} -X_1 + \tilde{Q}_0 & \tilde{R}_1 & \tilde{R}_2 & 0 & 0 & 0 & X_1 \bar{A}_0^T + Y_0 \bar{B}^T \\ * & \tilde{Q}_1 & \tilde{R}_3 & 0 & 0 & 0 & X_1 A_1^T \mathcal{G}^T + Y_1 \bar{B}^T \\ * & * & \tilde{Q}_2 & 0 & 0 & 0 & X_1 A_2^T \mathcal{G}^T + Y_2 \bar{B}^T \\ * & * & * & -\tilde{R}_0 & 0 & 0 & X_1 + Y_3 \bar{B}^T \\ * & * & * & * & -\gamma I & 0 & X_1 \\ * & * & * & * & * & -\gamma I & Y_3 \bar{B}^T \\ * & * & * & * & * & * & -X_1 \end{pmatrix} \preceq 0, \quad (38a)$$

$$\tilde{Q}_0 + \min\{\tilde{Q}_1, \tilde{Q}_2\} + 2 \min\{\tilde{R}_1, \tilde{R}_2\} \succeq \alpha X_1, \quad (38b)$$

holds, with fixed $\alpha, \gamma > 0$. Additionally, suppose that the inequality

$$\bar{q} \bar{b} X_1 \bar{b}^T \leq \mathbf{1}_{2k_x}, \quad (39)$$

holds with $\bar{\mathbf{b}} = (\mathbf{b}^\top, \mathbf{b}^\top)$, $\bar{q} = \alpha \varepsilon^{-1}$, $\varepsilon = \lambda_{\max}\{\mathbf{R}_0\} \bar{\delta}_k^2 + q_1 \bar{\delta}_k + q_2$, $\bar{\delta}_k = 2\|\mathcal{D}\|w_{\max}$, and

$$q_1 = 2c_3 \bar{e}, \quad (40a)$$

$$q_2 = 2(c_1 \zeta + c_2 \bar{e} + (c_4 + \sqrt{2n}c_5) \varphi_{\max}) \bar{e} + c_3^2 \lambda_{\max}\{\mathbf{R}_0\} + 4\gamma(1 + 2n)(c_6^2 + c_7^2) \zeta + k_{e_2} \|\mathcal{B}\|^2 \bar{u}_{\max}^2 \quad (40b)$$

$$\zeta = \sqrt{2k_x \lambda_{\max}^{-1}\{\mathbf{b}^\top \mathbf{b}\}}, \quad \bar{u}_{\max} = \|\mathbf{u}_{\max}\|,$$

$$\bar{e} = [k_{e_1}(\xi + 1) + k_\xi(\|\mathcal{A}_1\| + \|\mathcal{A}_2\|)] \zeta + k_\xi[\|\mathcal{B}\| \bar{u}_{\max} + \lambda_{\max}^{-1/2}\{\mathbf{R}_0\}],$$

$$\varphi_{\max} = (c_6 + c_7) \zeta + c_8(\|\mathcal{B}\| \bar{u}_{\max} + \lambda_{\max}^{-1/2}\{\mathbf{R}_0\}),$$

for given $\mathbf{R}_0 = \mathbf{X}_1 \tilde{\mathbf{R}}_0 \mathbf{X}_1$, $\mathbf{b} = (\mathbf{b}_1, \dots, \mathbf{b}_{k_x})^\top \in \mathbb{R}^{k_x \times n}$, $\xi, \mathbf{u}_{\max} > 0$, and

$$c_1 = (\|\tilde{\mathcal{A}}_0\| + \|\tilde{\mathcal{A}}_1\| + \|\tilde{\mathcal{A}}_2\|) \|\mathbf{P}\bar{\mathcal{B}}\| \|\bar{\mathbf{K}}\|, \quad (41a)$$

$$c_2 = (0.5\|\mathbf{K}_0\| + \|\mathbf{K}_1\| + \|\mathbf{K}_2\|) \|\mathbf{P}\bar{\mathcal{B}}\mathbf{K}_0\| + (\|\mathbf{K}_0\| + 0.5\|\mathbf{K}_1\| + \|\mathbf{K}_2\|) \|\mathbf{P}\bar{\mathcal{B}}\mathbf{K}_1\| + (\|\mathbf{K}_0\| + \|\mathbf{K}_1\| + 0.5\|\mathbf{K}_2\|) \|\mathbf{P}\bar{\mathcal{B}}\mathbf{K}_2\|, \quad (41b)$$

$$c_3 = \|\tilde{\mathbf{S}}_1^\top \mathbf{P}\bar{\mathcal{B}}\| \|\bar{\mathbf{K}}\|, \quad c_4 = \|\mathbf{P}\bar{\mathcal{B}}\| \|\bar{\mathbf{K}}\|, \quad (41c)$$

$$c_5 = \|\mathbf{S}_1^\top \bar{\mathcal{B}}^\top \mathbf{P}\bar{\mathcal{B}}\| \|\bar{\mathbf{K}}\|, \quad (41d)$$

$$c_6 = (1 + \sqrt{2n})^{-1} (k_{e_1} \xi - \|\bar{\mathcal{A}}_0\| - \mathbf{L}\|\mathcal{G}\| + \|\mathcal{A}_1\| + \|\mathcal{A}_2\|), \quad (41e)$$

$$c_7 = (1 + \sqrt{2n})^{-1} (k_{e_1} - \|\bar{\mathcal{A}}_0\| - \mathbf{L}\|\mathcal{G}\|), \quad (41f)$$

$$c_8 = (1 + \sqrt{2n})^{-1} k_{e_1} k_\xi, \quad (41g)$$

where $k_{e_1} = 1 + \xi v^{-1} e^{k_\xi} k_\xi$, $k_{e_2} = k_{e_1} k_\xi$, $k_\xi = (1 - e^{-v})^{-1}$, $v = |\operatorname{Re}\{\lambda_{\max}\{\mathbf{A}_0\}\}|$, $\tilde{\mathcal{A}}_0 = \bar{\mathcal{A}}_0 + \bar{\mathcal{B}}\mathbf{K}_0$, $\tilde{\mathcal{A}}_1 = \mathcal{G}\mathcal{A}_1 + \bar{\mathcal{B}}\mathbf{K}_1$, $\tilde{\mathcal{A}}_2 = \mathcal{G}\mathcal{A}_2 + \bar{\mathcal{B}}\mathbf{K}_2$, $\tilde{\mathbf{S}}_1 = \mathbf{I} + \bar{\mathcal{B}}\mathbf{S}_1$, and $\bar{\mathbf{K}} = \|\mathbf{K}_0\| + \|\mathbf{K}_1\| + \|\mathbf{K}_2\|$. If the IP (35) is initialized as $\hat{\mathbf{z}}_0 = (\hat{\mathbf{x}}_0^\top, \hat{\mathbf{x}}_0^\top)^\top$, and the controller gains are selected as $\mathbf{K}_0 = \mathbf{Y}_0^\top \mathbf{X}_1^{-1}$, $\mathbf{K}_1 = \mathbf{Y}_1^\top \mathbf{X}_1^{-1}$, $\mathbf{K}_2 = \mathbf{Y}_2^\top \mathbf{X}_1^{-1}$, and $\mathbf{S}_1 = \mathbf{Y}_3^\top \mathbf{X}_1^{-1}$, then the origin of the system dynamics (35) is ISpS, with respect to δ_k , and the system trajectories fulfill the state constraints, i.e., $\mathbf{x} \in \mathcal{X}$. Moreover, the safe set is given as

$$\mathcal{R} = \{\hat{\mathbf{z}}_k \in \mathbb{R}^{2n} : \hat{\mathbf{z}}_k^\top \mathbf{X}_1^{-1} \hat{\mathbf{z}}_k \leq \alpha^{-1} \varepsilon\}, \quad (42)$$

with some $\alpha > 0$ satisfying (38b).

Remark 4 Note that it is desirable that the safe set \mathcal{R} is as large as possible. Thus, it is possible to establish an optimization problem in order to maximize its volume. For example, let assumptions 3 and 4 be satisfied and the control law (37) be applied to the system (34). If the controller gains $\mathbf{K}_0 = \mathbf{Y}_0^\top \mathbf{X}_1^{-1}$, $\mathbf{K}_1 = \mathbf{Y}_1^\top \mathbf{X}_1^{-1}$, $\mathbf{K}_2 = \mathbf{Y}_2^\top \mathbf{X}_1^{-1}$, and $\mathbf{S}_1 = \mathbf{Y}_3^\top \mathbf{X}_1^{-1}$ are computed by solving the following optimization problem

$$\max_{\mathbf{X}_1, \mathbf{Y}_0, \mathbf{Y}_1, \mathbf{Y}_2, \mathbf{Y}_3} \log \det(\mathbf{X}_1) \text{ subject to (38a)}, \quad (43)$$

then the origin of the system dynamics (35) is ISpS with respect to δ_k with optimized perturbation attenuation.

4.3.3 Design of the Model Predictive Control

Assumption 5 implies that the invariant set \mathcal{R} , which is the safe set of system (28), is completely contained inside the polytope (29), i.e., the constrained region \mathcal{X} .

For the design of the MPC, the following assumption is considered.

Assumption 5 *There exist gains $K_0, K_1, K_2, S_1 \in \mathbb{R}^{p \times 2n}$, satisfying the conditions of Lemma 6, and $\hat{u}_k(t) = K_0 \hat{z}_k(t) + K_1 \hat{z}_k^+(t) + K_2 \hat{z}_k^-(t) + S_1 d_k \in \mathcal{U}$, for all $\hat{z}_k \in \mathcal{R}$ and $t \geq 0$.*

Let us consider that the prediction can be performed in a receding horizon fashion with a window length $N > 1$. The IP (35) has a sequence of inputs $\mathcal{S}_N = \{s_0, \dots, s_{N-1}\}$, with $s_m \in \mathcal{U}$ for all $m = \overline{0, N-1}$, the values $\hat{z}_{k,m+1}$ will be calculated for $m = \overline{0, N-1}$ under substitution $u_{k+m} = s_m$. Let us define $\hat{z}_{k+j} = \hat{z}_{k,j}$, for $j = \overline{0, N}$. Thus, the optimal control problem to be solved by the MPC is given as follows:

Problem 1 *For given matrices $0 \prec W = W^\top \in \mathbb{R}^{2n \times 2n}$, $0 \prec H = H^\top \in \mathbb{R}^{2n \times 2n}$, and $M = M^\top \in \mathbb{R}^{2p \times 2p}$, find the control signals*

$$\mathcal{S}_N^k = \operatorname{argmin} V_N(\hat{z}_{k,0}, \dots, \hat{z}_{k,N}, \mathcal{S}_N), \quad (44)$$

with the cost function $V_N(\hat{z}_{k,0}, \dots, \hat{z}_{k,N}, \mathcal{S}_N) = V_f(\hat{z}_{k,N}) + \sum_{m=0}^{N-1} \ell(\hat{z}_{k,m}, s_m)$, where $V_f(\hat{z}) = \hat{z}^\top W \hat{z}$, $\ell(\hat{z}, s) = \hat{z}^\top H \hat{z} + s^\top M s$, such that the following constraints are satisfied: i) $\hat{z}_{k+j} \in \mathcal{X}$, for $j = \overline{0, N}$ are computed by (35). ii) $u_k \in \mathcal{U}$. iii) $\hat{z}_{k,N} \in \mathcal{R}$.

Finally, considering the results of Lemma 6 and the solution of the Problem 1, the following theorem is presented.

Theorem 2 *Let Assumptions 3–5 be satisfied, the conditions of Lemma 6 be also satisfied, and Problem 1 be feasible. If the control law (36), given by (37) and (44), is applied to the system (28) and designed according to Lemma 6 and the solution of Problem 1; then, the origin of the system dynamics (34) is ISpS, with respect to δ_k , in the safe set \mathcal{R} .*

The proof of the results are postponed to section 4.6.

Remark 5 *The proposed scheme does not require the measurement of the system state, i.e., the control (37) is only based on the IP (35). This can represent an advantage in real-world applications such as many problems in biological systems, e.g., the blood glucose regulation and the anesthesia regulation in delivery machines, and some trajectory-tracking problems in mobile robots, where the state measurements are complicated or subject to significant perturbations and delays.*

Remark 6 *An LPV representation of the nonlinear function $f(x(t))$ is used, and since $x(t)$ is not measured while in general the scheduling parameters have to be dependent on the state in such a case, the values of these parameters are not used in the design. Thus, the presented approach can be applied to uncertain continuous LPV systems, without measured scheduling parameters, in the presence of perturbations and constraints.*

To better illustrate the algorithm presented in this chapter, a block diagram of the proposed control law is presented in Fig. 14.

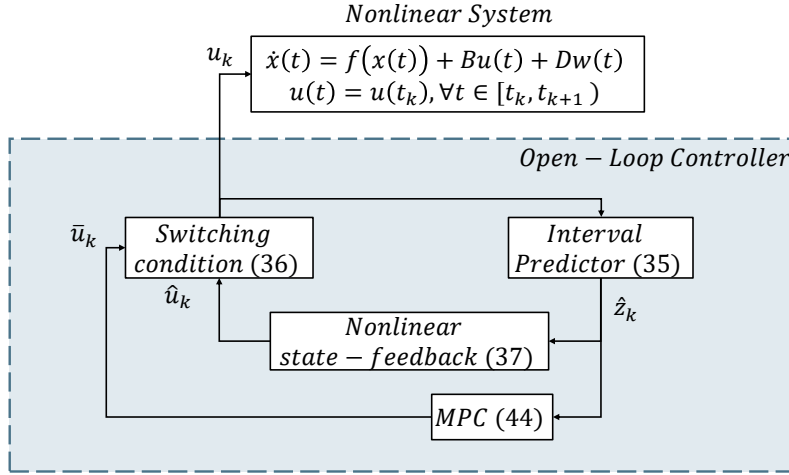


Figure 14: Closed-loop diagram

4.4 SIMULATIONS RESULTS

Consider the following nonlinear system

$$\begin{aligned} \dot{x}_1(t) &= -x_1(t) + (1 + 0.01x_1(t))x_2(t) + w(t), \\ \dot{x}_2(t) &= (0.2x_1(t) - 1)x_2(t) + u(t) + w(t), \end{aligned}$$

with $w(t) = 0.2 \sin(3t) + 0.05$, thus, $\underline{w}(t) = -0.15$, $\bar{w}(t) = 0.25$, and $w_{\max} = 0.25$. This system satisfies Assumptions 3 and 4. The matrices A_0 and A_j can be obtained by the convex polythopic method [51], as follows

$$\begin{aligned} A_0 &= \begin{pmatrix} -1 & 1 \\ 0 & -1 \end{pmatrix}, A_1 = \begin{pmatrix} 0 & 0.07 \\ 0.14 & 0 \end{pmatrix}, A_2 = \begin{pmatrix} 0 & 0.07 \\ -0.14 & 0 \end{pmatrix}, \\ A_3 &= \begin{pmatrix} 0 & -0.07 \\ 0.14 & 0 \end{pmatrix}, A_4 = \begin{pmatrix} 0 & -0.07 \\ -0.14 & 0 \end{pmatrix}, \end{aligned}$$

Let us consider that $u_{\max} = 3.5$, $x_1 \in (-7, 7)$ and $x_2 \in (-7, 7)$, and hence $b_1 = (1/7, 0)^\top$, $b_2 = -b_1$, $b_3 = (0, 1/7)^\top$, and $b_4 = -b_3$. The initial conditions for the system are $x(0) = (5, 5)^\top$. It is possible to show that this nonlinear system, for such initial conditions, is unstable (see, please Fig. 15).

All the simulations are done in MATLAB, with the Euler discretization method, and an integration step equal to 0.001 [s]. In order to show the efficiency of the algorithm, the following values for the sampled control are considered $h = 0.1$ [s], $h = 0.2$ [s], $h = 0.3$ [s], and $h = 0.5$ [s]. The solution for the LMIs is found by means of SDPT3 solver, among YALMIP, while the MPC is implemented using the nmpc MATLAB toolbox.

The controller gains are obtained looking for the solutions of the LMIs given in Lemma 6, for each value of h , with $\gamma = 1 \times 10^2$ and $\alpha = 1 \times 10^4$.

For illustrative purposes, numerical results are provided for the case $h = 0.2$ [s], which are:

$$\begin{aligned}
P &= \text{diag}(0.1778, 0.1211, 0.2446, 0.2565), \\
\tilde{Q}_0 &= \text{diag}(0.0059, 0.0019, 0.0086, 0.0074), \\
\tilde{Q}_1 &= \text{diag}(-0.0630, -0.0642, -0.0871, -0.0772), \\
\tilde{Q}_2 &= \text{diag}(-0.0862, -0.0769, -0.0602, -0.0621), \\
\tilde{R}_0 &= (4.0175, 4.1258, 3.9378, 3.8402)10^3, \\
\tilde{R}_1 &= \text{diag}(0.0894, 0.0737, 0.0431, 0.0541), \\
\tilde{R}_2 &= \text{diag}(0.2254, 0.1771, 0.1173, 0.0891), \\
K_0 &= (-0.206, -1.5403, -0.2802, -3.0885), \\
K_1 &= (0.0004, 0, -0.1880, -0.0082), \\
K_2 &= (0.0938, 0.0069, 0.0015, 0.0016), \\
S_1 &= (0.0102, 0.0678, 0.0216, 0.1717).
\end{aligned}$$

Then, it is possible to verify that the condition (38b) is fulfilled. For the MPC, it is considered $W = I$, $H = 1 \times 10^3 I$, $M = 1 \times 10^{-4}$, and $N = 10$.

The initial conditions for the IP are set in $\hat{z}_k(0) = (3.2, 3.2, 6.8, 6.9)^\top$. For comparison purposes, the simulation results for the case when the MPC is active during all the control task have been added. The system trajectories, the IP (35) trajectories, and the corresponding state constraints are depicted in Fig. 16, for $h = 0.2$. Note that both the IP and the system trajectories never transgress the system constraints despite the external perturbations. On the other hand, Fig. 17 shows that the trajectories of the system are inside of the polytope \mathcal{X} , all the time and despite to the external perturbations, for each value of h . Meanwhile, when only the MPC is applied, it can be seen that, under the same initial conditions, the system trajectories converge toward a region farther from the origin. Additionally, Fig. 18 depicts the behavior of the control signals that never transgress the input constraints. While for the case in which only the MPC is applied, the control signal remains saturated most of the time during the control task.

In order to illustrate, through simulations, that the computational burden is relaxed in our control algorithm, with respect to a classic MPC, then, it is sufficient to determine the time required to simulate the proposed switched scheme and the scheme when the MPC is active all the time. Considering that the simulations have been done in MATLAB with the Euler discretization method, sampling-time equal to 0.001 [s], simulation time equal to 10 [s], while the MPC has been implemented using the `nmpc` toolbox in MATLAB, the proposed switching scheme takes around 5 seconds to perform the simulation, while the scheme when the MPC is active all the time takes more than 14 seconds to perform the same simulation for the same initial conditions.

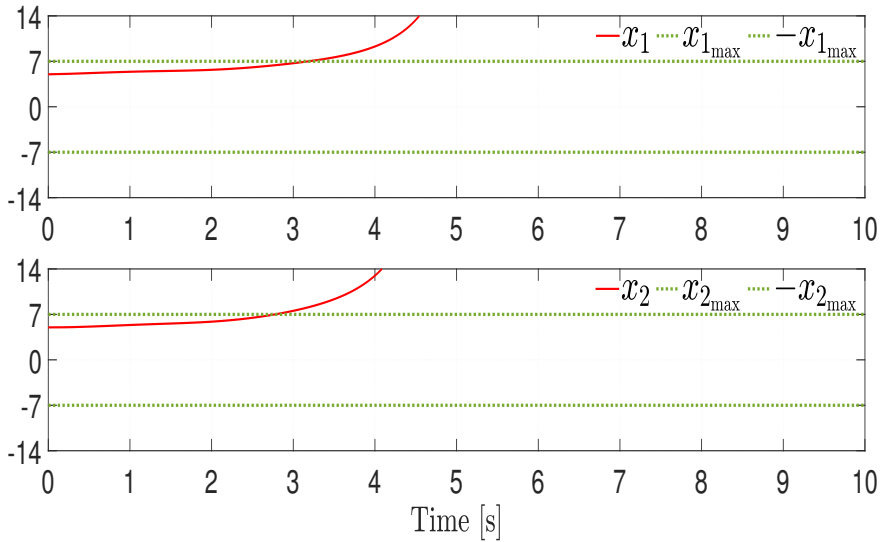


Figure 15: System trajectories in open-loop and state constraints

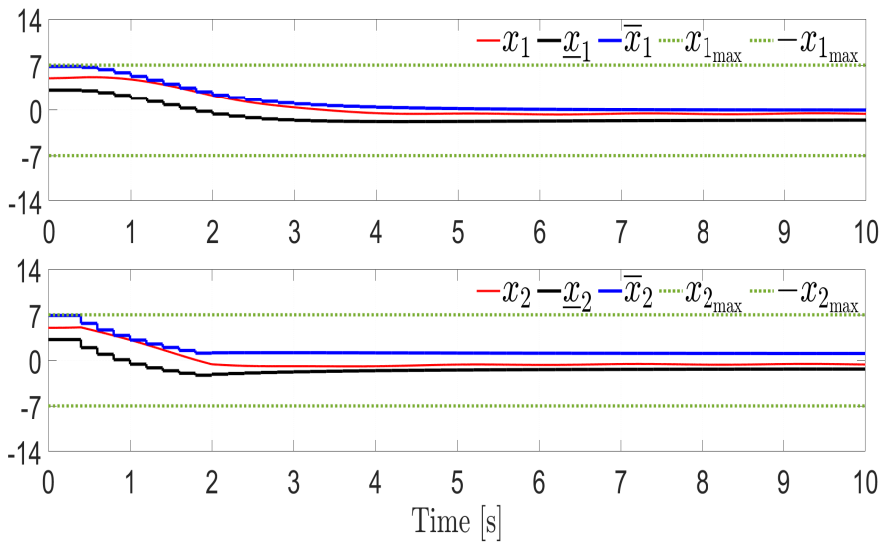


Figure 16: System trajectories and state constraints for $h = 0.2$

4.5 REMARKS

This chapter proposed the design of a robust sampled-time controller for stabilizing continuous-time nonlinear systems, considering state and input constraints, and external perturbations. The proposed strategy is based on two essential components: an IP-based state-feedback controller and an MPC approach, which deals with the state and input constraints. The IP-based state-feedback controller is designed such that a safe set was provided, where the state constraints are not violated. Such a safe set characterizes the region where the MPC is activated, guaranteeing the fulfillment of the state and input constraints. The proposed switched control strategy ensures the ISpS of the considered nonlinear systems with re-

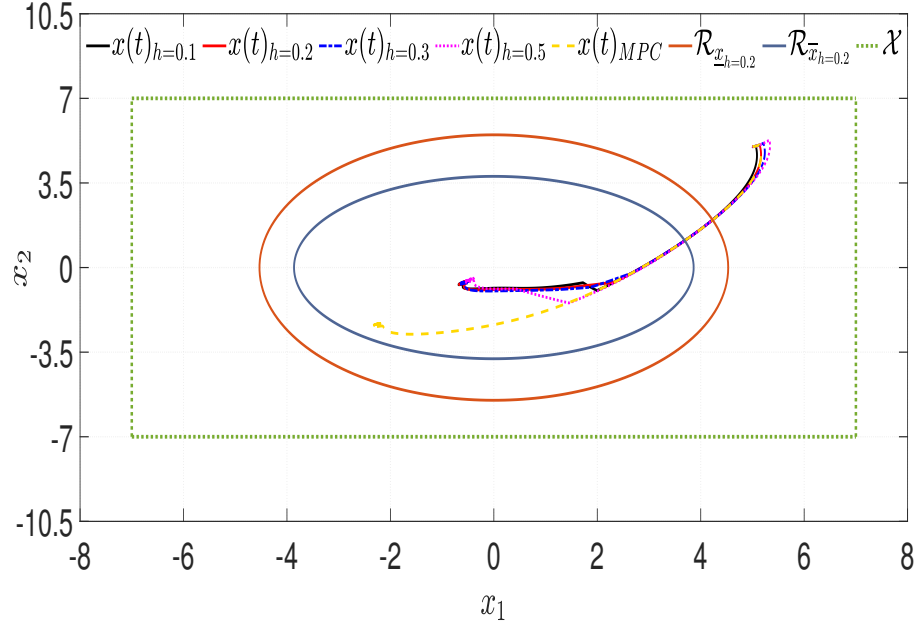


Figure 17: Phase portrait

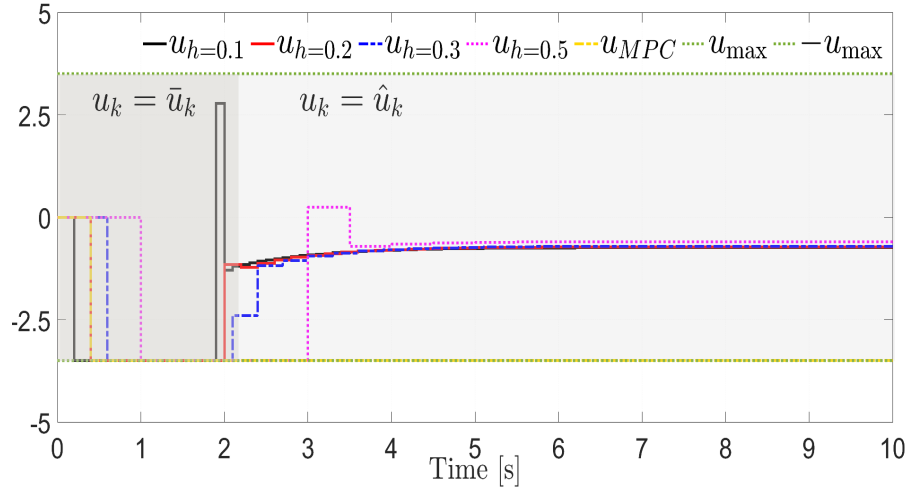


Figure 18: Control signals

spect to external perturbations, by means of a constructive method based on LMIs without using the system states.

4.6 PROOF OF THE RESULTS

Proof of Lemma 6: Define the error between the IP (34) and (35) as $e_k = z_k - \hat{z}_k$. Then, considering the state-feedback control (37), the closed-loop system dynamics is given as

$$z_{k+1} = \tilde{A}_0 z_k + \tilde{A}_1 z_k^+ + \tilde{A}_2 z_k^- + \tilde{S}_1 \delta_k + \varphi_k + \bar{B} S_1 \bar{\varphi} - \bar{B} K_0 e_k - \bar{B} K_1 e_k^+ - \bar{B} K_2 e_k^-, \quad (45)$$

where $\tilde{\mathcal{A}}_0 = \bar{\mathcal{A}}_0 + \bar{\mathcal{B}}\mathcal{K}_0$, $\tilde{\mathcal{A}}_1 = \mathcal{G}\mathcal{A}_1 + \bar{\mathcal{B}}\mathcal{K}_1$, $\tilde{\mathcal{A}}_2 = \mathcal{G}\mathcal{A}_2 + \bar{\mathcal{B}}\mathcal{K}_2$, and $\tilde{\mathcal{S}}_1 = \mathcal{I} + \bar{\mathcal{B}}\mathcal{S}_1$.

Let us propose the following candidate Lyapunov function

$$V(z_k) = z_k^\top P z_k, \quad (46)$$

with a diagonal matrix $P \succ 0 \in \mathbb{R}^{2n \times 2n}$ and the extended vectors $\eta^\top = (z_k^\top, z_k^{+\top}, z_k^{-\top}, \delta_k^\top, \varphi_k^\top, \bar{\varphi}^\top)^\top$ and $\bar{\eta}^\top = (\eta^\top, e_k^\top, e_k^{+\top}, e_k^{-\top})^\top$. Then, the increment of the candidate Lyapunov function is

$$V(z_{k+1}) - V(z_k) = \eta^\top \Sigma \eta + \bar{\eta}^\top \Gamma \bar{\eta} - z_k^\top P z_k, \quad (47)$$

with $\Sigma = \Omega^\top P \Omega$, where $\Omega = (\tilde{\mathcal{A}}_0, \tilde{\mathcal{A}}_1, \tilde{\mathcal{A}}_2, \tilde{\mathcal{S}}_1, \mathcal{I}, \bar{\mathcal{B}}\mathcal{S}_1)$, and

$$\Gamma = \begin{pmatrix} 0 & 0 & 0 & 0 & 0 & 0 & -\tilde{\mathcal{A}}_0^\top P \bar{\mathcal{B}}\mathcal{K}_0 \\ * & 0 & 0 & 0 & 0 & 0 & -\tilde{\mathcal{A}}_1^\top P \bar{\mathcal{B}}\mathcal{K}_0 \\ * & * & 0 & 0 & 0 & 0 & -\tilde{\mathcal{A}}_2^\top P \bar{\mathcal{B}}\mathcal{K}_0 \\ * & * & * & 0 & 0 & 0 & -\tilde{\mathcal{S}}_1 P \bar{\mathcal{B}}\mathcal{K}_0 \\ * & * & * & * & 0 & 0 & -P \bar{\mathcal{B}}\mathcal{K}_0 \\ * & * & * & * & * & 0 & -\mathcal{K}_0^\top \bar{\mathcal{B}}^\top P \bar{\mathcal{B}}\mathcal{S}_1 \\ * & * & * & * & * & * & \mathcal{K}_0^\top \bar{\mathcal{B}}^\top P \bar{\mathcal{B}}\mathcal{K}_0 \\ * & * & * & * & * & * & * \\ * & * & * & * & * & * & * \\ & & & & & & -\tilde{\mathcal{A}}_0^\top P \bar{\mathcal{B}}\mathcal{K}_1 & -\tilde{\mathcal{A}}_0^\top P \bar{\mathcal{B}}\mathcal{K}_2 \\ & & & & & & -\tilde{\mathcal{A}}_1^\top P \bar{\mathcal{B}}\mathcal{K}_1 & -\tilde{\mathcal{A}}_1^\top P \bar{\mathcal{B}}\mathcal{K}_2 \\ & & & & & & -\tilde{\mathcal{A}}_2^\top P \bar{\mathcal{B}}\mathcal{K}_1 & -\tilde{\mathcal{A}}_2^\top P \bar{\mathcal{B}}\mathcal{K}_2 \\ & & & & & & -\tilde{\mathcal{S}}_1 P \bar{\mathcal{B}}\mathcal{K}_1 & -\tilde{\mathcal{S}}_1 P \bar{\mathcal{B}}\mathcal{K}_2 \\ & & & & & & -P \bar{\mathcal{B}}\mathcal{K}_1 & -P \bar{\mathcal{B}}\mathcal{K}_2 \\ & & & & & & -\mathcal{K}_1^\top \bar{\mathcal{B}}^\top P \bar{\mathcal{B}}\mathcal{S}_1 & -\mathcal{K}_2^\top \bar{\mathcal{B}}^\top P \bar{\mathcal{B}}\mathcal{S}_1 \\ & & & & & & 2\mathcal{K}_0^\top \bar{\mathcal{B}}^\top P \bar{\mathcal{B}}\mathcal{K}_1 & 2\mathcal{K}_0^\top \bar{\mathcal{B}}^\top P \bar{\mathcal{B}}\mathcal{K}_2 \\ & & & & & & \mathcal{K}_1^\top \bar{\mathcal{B}}^\top P \bar{\mathcal{B}}\mathcal{K}_1 & 2\mathcal{K}_1^\top \bar{\mathcal{B}}^\top P \bar{\mathcal{B}}\mathcal{K}_2 \\ & & & & & & * & \mathcal{K}_2^\top \bar{\mathcal{B}}^\top P \bar{\mathcal{B}}\mathcal{K}_2 \end{pmatrix}. \quad (48)$$

Let us add and subtract the following terms $\gamma \varphi_k^\top \varphi_k$, $\gamma \bar{\varphi}^\top \bar{\varphi}$, $\delta_k^\top R_0 \delta_k$, $z_k^\top Q_0 z_k$, $z_k^{+\top} Q_1 z_k^+$, $z_k^{-\top} Q_2 z_k^-$, $2z_k^\top R_1 z_k^+$, $2z_k^\top R_2 z_k^-$, $2z_k^{+\top} R_3 z_k^-$, with symmetric matrices $R_0, Q_0, Q_1, Q_2 \in \mathbb{R}^{2n \times 2n}$, and diagonal matrices $R_1, R_2, R_3 \in \mathbb{R}^{2n \times 2n}$, to the right-hand side of (47), i.e.,

$$\begin{aligned} V(z_{k+1}) - V(z_k) &= \eta^\top \Sigma \eta + \bar{\eta}^\top \Gamma \bar{\eta} + \gamma \varphi_k^\top \varphi_k + \gamma \bar{\varphi}^\top \bar{\varphi} \\ &\quad - z_k^\top Q_0 z_k - z_k^{+\top} Q_1 z_k^+ - z_k^{-\top} Q_2 z_k^- + \delta_k^\top R_0 \delta_k \\ &\quad - 2z_k^\top R_1 z_k^+ - 2z_k^\top R_2 z_k^- - 2z_k^{+\top} R_3 z_k^-, \end{aligned} \quad (49)$$

with

$$\begin{aligned} \lambda(t, z(t_k), u_k) = & \|e^{A_0(t-t_k)} - I\| \|z_k\| + \int_{t_k}^t \|e^{A_0(t-\tau)} \mathcal{B}\| \|u(\tau)\| d\tau \\ & + \int_{t_k}^t \|e^{A_0(t-\tau)}\| \|\delta(\tau)\| d\tau \\ & + \int_{t_k}^t \|e^{A_0(t-\tau)}\| \|g(\hat{z}(\tau))\| d\tau. \end{aligned} \quad (54)$$

Thus, applying Lemma 2 to (53), it is obtained that

$$\begin{aligned} \|z(t) - z_k\| \leq & \lambda(t, z(t_k), u_k) \\ & + \int_{t_k}^t \lambda(s, z(t_k), u_k) \|e^{A_0(t-s)}\| \|\rho(t, s)\| ds = W(t, z_k, u_k), \end{aligned} \quad (55)$$

with $\rho(t, s) = e^{\int_s^t \|e^{A_0(t-r)}\| dr}$. It is worth mentioning that (55) represents the error between the continuous trajectory of the IP (32), and the discrete-time version (35).

Then, the step forward error between the IP (34) and (35) is given as

$$\|z_{k+1} - \hat{z}_{k+1}\| = (\|\bar{\mathcal{A}}_0\| + L\|\mathcal{G}\|) \|z_k - \hat{z}_k\| + \|\varphi_k\| + \|\bar{\varphi}\|. \quad (56)$$

Considering (55), it is possible to obtain an upper bound for (56), i.e.,

$$\begin{aligned} (\|\bar{\mathcal{A}}_0\| + L\|\mathcal{G}\|) \|z_k - \hat{z}_k\| + \|\varphi_k\| + \|\bar{\varphi}\| \leq & \lambda(t, z(t_k), u_k) \\ & + \int_{t_k}^t \lambda(s, z(t_k), u_k) \|e^{A_0(t-s)}\| \|\rho(t, s)\| ds. \end{aligned}$$

Taking into account that $\|\varphi_k\| + \|\bar{\varphi}\| \leq (1 + \sqrt{2n})\varphi_{\max}$. Hence, is possible to accomplish that

$$\varphi_{\max} \leq (1 + \sqrt{2n})^{-1} (W(t_{k+1}, z_k, u_k) - (\|\bar{\mathcal{A}}_0\| + L\|\mathcal{G}\|) \|z_k - \hat{z}_k\|). \quad (57)$$

Thus, since A_0 is Hurwitz; one can take into account that $\|e^{A_0(t-t_k)}\| \leq \xi e^{-\nu(t-t_k)}$, with $\nu = |\operatorname{Re}\{\lambda_{\max}\{A_0\}\}|$ and $\xi > 0$, for all $t \in [t_k, t_{k+1}]$; thus, (54) with $t = t_{k+1}$ can be upper bounded as

$$\begin{aligned} \lambda(t_{k+1}, z(t_k), u_k) \leq & \xi \|z_k\| + \|\hat{z}_k\| + k_\xi (\|\mathcal{B}\| \bar{u}_{\max} \\ & + \|g(z(t_k))\| + \|\delta_k\|) = \lambda_c, \end{aligned} \quad (58)$$

with $\bar{u}_{\max} = \|u_{\max}\|$ and $k_\xi = \xi \nu^{-1} (1 - e^{-\nu h})$. Then, taking into account that $\int_s^{t_{k+1}} \|e^{A_0(t_{k+1}-r)}\| dr \leq \xi \nu^{-1} (1 - e^{-\nu h})$ and considering (58), $W(t_{k+1}, z_k, u_k)$ is upper bounded as $W(t_{k+1}, z_k, u_k) \leq k_{e_1} \lambda_c = W_c$, with $k_{e_1} = 1 + e^{k_\xi} k_\xi$. Therefore, (57) can be upper bounded as follows

$$\begin{aligned} \varphi_{\max} \leq & (1 + \sqrt{2n})^{-1} [(k_{e_1} \xi - \|\bar{\mathcal{A}}_0\| - L\|\mathcal{G}\| + \|\mathcal{A}_1\| + \|\mathcal{A}_2\|) \|z_k\| \\ & + (k_{e_1} - \|\bar{\mathcal{A}}_0\| - L\|\mathcal{G}\|) \|\hat{z}_k\| + k_{e_1} k_\xi (\|\mathcal{B}\| \bar{u}_{\max} + \|\delta_k\|)]. \end{aligned} \quad (59)$$

Considering (59), the term φ_{\max}^2 can be upper bounded as follows

$$\begin{aligned} \varphi_{\max}^2 &\leq 4(1 + \sqrt{2n})^{-1} [(k_{e_1} \xi - \|\bar{\mathcal{A}}_0\| - L\|\mathcal{G}\| + \|\mathcal{A}_1\| + \|\mathcal{A}_2\|)^2 \|z_k\|^2 \\ &\quad + (k_{e_1} - \|\bar{\mathcal{A}}_0\| - L\|\mathcal{G}\|)^2 \|\hat{z}_k\|^2 + k_{e_2}^2 (\|\mathcal{B}\|^2 \bar{u}_{\max}^2 + \|\delta_k\|^2)], \end{aligned} \quad (60)$$

with $k_{e_2} = k_{e_1} k_\xi$. Note that, from (29), it can be obtained that $\|x\| \leq \|\mathbf{1}k_x\| \|\mathbf{b}\|^{-1} = \sqrt{k_x \lambda_{\max}^{-1}\{\mathbf{b}^\top \mathbf{b}\}}$. Recalling that $z_k = [\underline{x}_k^\top, \bar{x}_k^\top]^\top$, then $\|z_k\| \leq \sqrt{2k_x \lambda_{\max}^{-1}\{\mathbf{b}^\top \mathbf{b}\}} = \zeta$. Moreover, after some algebraic manipulations, it is possible to prove that $\bar{\eta}^\top \Gamma \bar{\eta}$, with $\bar{\eta} = (\eta^\top, e_k^\top, e_k^{+\top}, e_k^{-\top})^\top$ and (48) is upper bounded as

$$\bar{\eta}^\top \Gamma \bar{\eta} \leq 2[\zeta c_1 + c_2 \tilde{\epsilon} + \|\delta_k\| c_3 + \|\varphi_k\| c_4 + \|\bar{\varphi}\| c_5] \tilde{\epsilon}, \quad (61)$$

with c_1, c_2, c_3, c_4 , and c_5 given as in (41a)–(41d). where $\bar{K} = \|K_0\| + \|K_1\| + \|K_2\|$. By definition, $\|e_k\| \leq \tilde{\epsilon} = W_c$ and, $\|\varphi_k\| \leq \varphi_{\max} = \varphi_c$ with

$$W_c = [k_{e_1}(\xi + 1) + k_\xi(\|\mathcal{A}_1\| + \|\mathcal{A}_2\|)] \zeta + k_\xi [\|\mathcal{B}\| \bar{u}_{\max} + \lambda_{\max}^{-1/2}\{R_0\}],$$

$$\varphi_c = (c_6 + c_7) \zeta + c_8 (\|\mathcal{B}\| \bar{u}_{\max} + \lambda_{\max}^{-1/2}\{R_0\}),$$

with c_6, c_7 , and c_8 given as in (41e)–(41g). Then, according to (61) and taking into account that $\delta_k^\top R_0 \delta_k \leq \lambda_{\max}\{R_0\} \|\delta_k\|^2$ holds, it follows that

$$\begin{aligned} V(z_{k+1}) - V(z_k) &\leq -z_k^\top Q_0 z_k - z_k^{+\top} Q_1 z_k^+ - z_k^{-\top} Q_2 z_k^- \\ &\quad - 2z_k^\top R_1 z_k^+ - 2z_k^\top R_2 z_k^- - 2z_k^{+\top} R_3 z_k^- \\ &\quad + \lambda_{\max}\{R_0\} \|\delta_k\|^2 + q_1 \|\delta_k\| + q_2, \end{aligned} \quad (62)$$

with q_1 and q_2 given as in (40a) and (40b). Thus, if $\bar{Q} = Q_0 + \min\{Q_1, Q_2\} + 2 \min\{R_1, R_2\} \succeq \alpha P$ is satisfied, and since, by definition $z_k^{+\top} R_1 z_k \geq 0$ and $(-z_k^-)^\top R_2 z_k \geq 0$, $z_k^{+\top} R_3 z_k^- = 0$, for any diagonal matrices R_1, R_2 and R_3 ; then, it follows that $V(z_{k+1}) - V(z_k) \leq -\alpha z_k^\top P z_k + \lambda_{\max}\{R_0\} \|\delta_k\|^2 + q_1 \|\delta_k\| + q_2$. Note that pre- and post-multiplying \bar{Q} by P^{-1} , $\bar{Q} \succeq \alpha P$ is equivalent to (38b). Therefore, the system (45) is ISpS, with respect to δ_k .

Moreover, we have that $\|\delta_k\| \leq 2\|\mathcal{D}\|w_{\max} = \bar{\delta}_k$. Then, the increment of the candidate Lyapunov function is negative definite outside the invariant convergence set

$$\mathcal{R} = \{z_k \in \mathbb{R}^{2n} : z_k^\top P z_k \leq \alpha^{-1} \varepsilon\}, \quad (63)$$

with $\varepsilon = \lambda_{\max}\{R_0\} \bar{\delta}_k^2 + q_1 \bar{\delta}_k + q_2$. Remark that the error (55) is taken into account in the LMI (38a), *i.e.*, the error between the continuous trajectory of the IP (32), and its discrete-time version (34). Finally, if the matrix inequality (39) is satisfied, then the set \mathcal{R} belongs to the polytope (29). Moreover, if the IP (35) is initialized as $\hat{z}_0 = (\underline{x}_0^\top, \bar{x}_0^\top)^\top$, since Assumptions 3 and 4 hold; then, the trajectories of the system (28) will also fulfill the state constraints, *i.e.*, $x \in \mathcal{X}$. This concludes the proof. \blacksquare

Proof of Theorem 2: Note that the proof is based on a classical result for MPC [37]. Recall that the controller is composed of an IP-based state-feedback controller and the MPC law, which will deal with state and input constraints. Thus, the following can be established:

- 1) First, note that the IP (35) generates an estimation \hat{z}_k such that the relation $\bar{x}(t) \leq x(t) \leq \bar{x}(t)$ is satisfied. Then, consider the control \hat{u}_k and note that, for some $t > 0$, if the initial conditions $\hat{z}_k(0) \in \mathcal{R} \subset \mathcal{X} \times \mathcal{X}$; then, the control (36) equals to (37). According to (63) and Assumption 5, $\hat{z}(t) \in \mathcal{R}$ and $\hat{u}_k \in \mathcal{U}$, for all $t \geq 0$, and the origin of the system dynamics (35) is ISpS, with respect to δ_k due to the result of Lemma 6.
- 2) Now, let $\hat{z}_k(0) \notin \mathcal{R}$ and recall that Problem 1 is assumed to be feasible. Then, applying the control (44), for $t \in [0, T)$, one has that $\hat{z}_k(t) \in \mathcal{X} \times \mathcal{X}$, and $u(t) \in \mathcal{U}$, on this time interval. Note that \mathcal{X} is a neighborhood of the origin, and the cost function is given by V_N , with positive definite matrices W , H , and M , and it is minimized inside $\mathcal{X} \times \mathcal{X}$. Using these arguments, due to Assumption 4 and $[\underline{w}_{k+1}, \bar{w}_{k+1}] \subseteq [\underline{w}_k, \bar{w}_k]$ hold, and since $\hat{z}_k(t_i + T) \in \mathcal{X} \times \mathcal{X}$ provided that the control \bar{u}_k in (44) is applied and $[\underline{z}^\top(t_i), \bar{z}^\top(t_i)] \subset [\underline{z}^\top(t_{i-1} + T), \bar{z}^\top(t_{i-1} + T)]$, for all $i \geq 1$, there is a finite time instant $t \geq T$ such that $(\underline{z}^\top(t), \bar{z}^\top(t))^\top \in \mathcal{R}$; and then, the control law (36) switches from the control signal \bar{u}_k computed by the MPC to the state-feedback control law \hat{u}_k , which provides that the system trajectories are ISpS with respect to δ_k .
- 3) As a result of the previous statements, the system constraints are satisfied.

This concludes the proof. ■

A SAMPLED ROBUST CONTROL FOR UNCERTAIN NONLINEAR SYSTEMS

This chapter presents a sampled robust controller for a certain class of uncertain nonlinear systems with state, input, and communication constraints affected by external perturbations. The proposed controller comprises the design of an aperiodic control law based on an event-triggered controller and a periodic control law based on a constant sampled state-feedback controller. The proposed strategy ensures the ISS of the tracking error dynamics with respect to the external perturbations.

5.1 INTRODUCTION

As mentioned above real dynamical systems can be represented by nonlinear models. It is well-known that the real systems have to operate in confined spaces and have energy limitations, *i.e.*, they must deal with state and input constraints (see, *e.g.*, [52], [53] and [54]). Moreover, in most cases, the dynamical systems are managed through a digital platform, and then there is limited bandwidth, so it is necessary to restrict the frequency of control input updates to save communication resources. A well-known technique to deal with this problem is the event-triggered control (see, *e.g.*, [55], [56], and [57]). Its main characteristic is that the control actions are updated only when certain well-defined events occur, resulting in an aperiodic sampling time [58].

Regarding the control design for constrained systems, for instance, in [59], an MPC algorithm is proposed for trajectory tracking of constrained linear systems. The algorithm ensures constraint satisfaction and asymptotic convergence of the tracking error. However, this algorithm only considers linear systems and it does not take into account communication constraints or external perturbations. Concerning the control design for nonlinear systems under communications constraints (*e.g.*, when the digital platform of the system imposes limitations on the control update time); for instance, in [60], an event-triggered adaptive control algorithm is proposed for a class of uncertain nonlinear systems. This algorithm guarantees that all closed-loop signals are globally bounded, and the tracking error exponentially converges to a compact set. However, the previous work does not take into account state or input constraints, and only the unperturbed case is considered. In [61], an event-triggered MPC is proposed for nonlinear continuous-time systems with additive bounded perturbations. The trajectory of the systems converges to a given set. In [62], an event-triggered MPC is proposed for continuous-time nonlinear systems

subject to bounded perturbations. The proposed algorithm consists of the triggering mechanism and the dual-mode approach. The state trajectory converge to a robust invariant set. However, in [61] and [62] the minimum sampling time is not considered. In [63], a robust self-triggered MPC with an adaptive prediction horizon scheme is proposed for constrained nonlinear discrete-time systems with external perturbations. This algorithm ensures that the system trajectories inside a defined set are ISS with respect to the external perturbations. The proposed algorithm only considers discrete-time systems. In the previous works, high computational power was needed due to the nature of the MPC implementation, *i.e.*, solving a finite time horizon optimization problem on-line. Additionally, most of the previous works do not take into account the communication constraints, *i.e.*, the limited amount of communication resources.

In this chapter, motivated by the above-mentioned issues, *i.e.*, meaningful external perturbations, system and communications constraints, and constraint complexity, a robust sampled control strategy is proposed to solve the stabilization problem in nonlinear systems with communication, state, and input constraints. The proposed control scheme is composed of an aperiodic sampled controller and a periodic sampled controller. Then, the proposed control approach contributes with the following features:

- 1) The aperiodic sampled controller is based on a state-feedback event-triggered controller designed through the AEM and the BLF, taking into account the state and input constraints.
- 2) The characterization of a safe set, where the state constraints are not transgressed, is provided, as well as a switching set defining the region where each control part is active.
- 3) The periodic sampled control part is based on a state-feedback controller designed using a Lyapunov-Krasovskii function approach, this part of the controller takes into account the minimum sampling interval.
- 4) The proposed approach ensures the ISS properties of the system trajectory with respect to external perturbations.
- 5) The synthesis of the controller is constructive since it is based on LMIs.

5.2 PROBLEM STATEMENT

Consider the following class of nonlinear system

$$\dot{x}(t) = f(x(t)) + Bu(t) + Dw(t), \quad t \geq 0, \quad (64a)$$

$$u(t) = u(t_k), \quad \forall t \in [t_k, t_{k+1}), \quad (64b)$$

where $x(t) \in \mathbb{R}^n$ is the state, $f : \mathbb{R}^n \rightarrow \mathbb{R}^n$ is a locally Lipschitz function, $w : \mathbb{R}_+ \rightarrow \mathbb{R}^q$ is the perturbation term, $u(t) \in \mathbb{R}^p$ is the control input,

which is applied at each time t_k , for all $k \in \mathbb{N}$. The sampling instants t_k monotonously increasing, so that $\lim_{k \rightarrow \infty} t_k = +\infty$, and $h(t) := t_{k+1} - t_k > h_{\min}$, where $h_{\min} > 0$ is the minimum sampling interval, and $t_0 = 0$. Note, that h_{\min} is the minimum sampling interval allowed by the digital platform of the system and the sampling instants t_k will be determined by the proposed sampled controller. The matrices B and D are known of suitable dimensions. It is considered that $u \in \mathcal{U} := \{u \in \mathbb{R}^p \mid -u_{\max_j} \leq u_j \leq u_{\max_j}, \forall j = \overline{1, p}\}$, with $0 < u_{\max_j}$ is the maximum value for each control signal.

Moreover, the solutions of the system (64a) must be constrained inside the polytope

$$\mathcal{X} := \{x \in \mathbb{R}^n \mid \mathbf{b}x \leq \mathbf{1}_{k_x}\}, \quad (65)$$

where $\mathbf{b} = (b_1, \dots, b_{k_x})^\top \in \mathbb{R}^{k_x \times n}$. It is assumed that the origin belongs to the interior of the set \mathcal{X} .

The aim of this chapter is to design a sampled controller for a nonlinear system affected by external perturbations and taking into account some communication constraints, *i.e.*, a minimum sampling time h_{\min} in which the control signal can be sent to the system; state and input constraints, *i.e.*, $x(t) \in \mathcal{X} \subset \mathbb{R}^n$ and $u(t) \in \mathcal{U} \subset \mathbb{R}^p$, for all $t \geq t_0$, for some given sets \mathcal{X} and \mathcal{U} .

Before proceeding, the following assumption is imposed on the system (64a).

Assumption 6 *There exist a known Metzler matrix $A_0 \in \mathbb{R}^{n \times n}$ and known matrices $A_j \in \mathbb{R}^{n \times n}$, $j = \overline{1, N}$ for some $N \in \mathbb{Z}_+$ such that the following relations are satisfied*

$$f(x) = \left(A_0 + \sum_{j=1}^N \alpha_j(x) A_j \right) x, \quad (66a)$$

$$\sum_{j=1}^N \alpha_j(x) = 1, \quad \alpha_j(x) \in (0, 1), j = \overline{1, N}. \quad (66b)$$

5.3 ROBUST CONTROL DESIGN

According to Assumption 7, the system (64a) has the following representation

$$\dot{x}(t) = \left(A_0 + \sum_{j=1}^N \alpha_j(x) A_j \right) x(t) + Bu(t) + Dw(t). \quad (67)$$

The proposed controller takes the following form:

$$u(t) = \begin{cases} \tilde{u}(t), & \text{if } x(t) \notin \mathcal{E}(P), \\ \hat{u}(t), & \text{if } x(t) \in \mathcal{E}(P), \end{cases} \quad (68)$$

where \tilde{u} is an event-triggered controller, \hat{u} is a constant sampled state-feedback controller, and the ellipsoid $\mathcal{E}(P)$, which is defined further on, is the switching and invariant set for system (67).

5.3.1 Linear Control Design

The following assumption is imposed on the system (67):

Assumption 7 *The pair (A_0, B) is controllable.*

Since the event-triggered control law is based on a linear state-feedback controller, then the following non-sampled control law is proposed first

$$\tilde{u}(t) = \sigma(u_0(t)), \quad (69)$$

with $u_0(t) = Kx(t)$, where $K \in \mathbb{R}^{p \times n}$ is a feedback gain, such that the state and input constraints are not transgressed.

The following lemma provides a safe set $\mathcal{E}(R)$, the switching set $\mathcal{E}(P)$, and a way to design K .

Lemma 7 *Let Assumption 7 be satisfied and the control (69) be applied to the system (67), i.e., $u(t) = \tilde{u}(t)$. Suppose that there exist a positive-definite matrix $X_1 = X_1^T \in \mathbb{R}^{n \times n}$, matrices $Y \in \mathbb{R}^{p \times n}$, $Z = (Z_1^T, Z_2^T) \in \mathbb{R}^{p \times n}$, $M \in \mathbb{R}^{n \times n}$, $\Delta = \text{diag}(\delta_1, \delta_2)$, with $\delta_1, \delta_2 > 0$, $Q_w \in \mathbb{R}^{n \times n}$ such that $\lambda_{\max}(Q_w) = 0.5w_{\max}^2$, and a constant $\gamma > 0$, such that the following set of LMIs*

$$X_1 = \begin{pmatrix} X_{11} & B\Delta - Y^T + Z^T & X_1 D \\ * & -2\Delta & 0 \\ * & * & -\gamma Q_w \end{pmatrix} \preceq 0, \quad (70a)$$

$$X_{11} = \text{He}\{X_1 A_\psi\} + BY + Y^T B^T + M, \quad A_\psi = A_0 + A_{\max} I_3,$$

$$X_{2_i} = \begin{pmatrix} X_1 & Z_i^T \\ Z_i & \bar{u}_i^2 \end{pmatrix} \succeq 0, \quad i = 1, 2, \quad (70b)$$

$$X_3 = \begin{pmatrix} M & \gamma X_1 \\ \gamma X_1 & \gamma X_2 \end{pmatrix} \succ 0, \quad (70c)$$

$$X_2 < X_1, \quad (70d)$$

$$X_{4_j} = \bar{b}_j^T X_1 \bar{b}_j \leq 1, \quad j = \overline{1, 4}, \quad (70e)$$

is feasible for given constants $\bar{\alpha y}$, $\|w\|_\infty < w_{\max}$, and $A_{\max} = \sum_{j=1}^m \alpha^* \|A_j\|$, where $\alpha^* = \arg \max_{\alpha \in \Gamma} \sum_{j=1}^m \alpha_j \|A_j\|$, and $\Gamma \subset \mathbb{R}^m$ the set of all convex weight vectors $\alpha = (\alpha_1, \dots, \alpha_m)^T \in \mathbb{R}^m$ such that (66) holds. If $x(0) \in \mathcal{E}(R)$, with $R = X_1^{-1}$, and $K = YR$, then the ellipsoid $\mathcal{E}(P)$, with $P = X_2^{-1}$, is asymptotically attractive while $\mathcal{E}(R)$ is invariant for the system (67).

5.3.2 Event-Triggered Controller

Due to the communication restrictions, it is necessary to implement the controller (69) in a sampled way, i.e.,

$$\tilde{u}(t) = \sigma(u_0(t_k)), \quad \forall t \in [t_k, t_{k+1}), \quad k \in \mathbb{N}. \quad (71)$$

The following lemma provides a way to implement the event-triggered controller.

Lemma 8 Let the control (71) be applied to the system (67), i.e., $u(t) = \tilde{u}(t)$, with the controller parameters designed according to Lemma 7, i.e., $K = YR$. Suppose that there exist positive-definite matrices $\tilde{P}_2 = \tilde{P}_2^\top \in \mathbb{R}^{n \times n}$, $\tilde{P}_3 = \tilde{P}_3^\top \in \mathbb{R}^{n \times n}$, $\tilde{R}_1 = \tilde{R}_1^\top \in \mathbb{R}^{n \times n}$, and $\tilde{S}_1 = \tilde{S}_1^\top \in \mathbb{R}^{n \times n}$, such that the following LMI

$$\Theta = \begin{pmatrix} \Theta_{11} & \Theta_{12} & \Theta_{13} & \tilde{P}_2^\top D \\ * & \Theta_{22} & \tilde{P}_3^\top BK & \tilde{P}_3^\top D \\ * & * & \Theta_{33} & 0 \\ * & * & * & -\gamma_2 I \end{pmatrix} \preceq 0, \quad (72)$$

$$\begin{aligned} \Theta_{11} &= \text{He}\{\tilde{P}_2 A_\psi\} + \tilde{S}_1 + 2e^{-2\kappa_1 h_{\min}} \tilde{R}_1, \\ \Theta_{12} &= R - \tilde{P}_2^\top + \tilde{P}_3 A_\psi, \quad \Theta_{13} = e^{-2\kappa_1 h_{\min}} \tilde{R}_1 + \tilde{P}_2^\top BK, \\ \Theta_{22} &= -2\tilde{P}_3^\top + h_{\min}^2 \tilde{R}_1, \quad \Theta_{33} = -e^{-2\kappa_1 h_{\min}} (\tilde{R}_1 + \tilde{S}_1), \end{aligned}$$

is feasible for K and R given as in Lemma 7, some $\gamma_2 > 0$, $\kappa_1 > 0$, and $h_{\min} > 0$. Thus, if the event-triggered control law is designed as

$$\tilde{u}(t) = \begin{cases} \sigma(u_0(t)), t = t_{k+1}, & \text{if } W(t, u_0(t_k)) > \rho W(t, u_0(t)) \\ & \& h(t) \geq h_{\min}, \\ \sigma(u_0(t_k)), & \text{if } W(t, u_0(t_k)) > \rho W(t, u_0(t)) \\ & \& h(t) < h_{\min}, \\ & \text{or } W(t, u_0(t_k)) \leq \rho W(t, u_0(t)), \end{cases} \quad (73)$$

for all $t \in [t_k, t_{k+1})$, where $\rho > 0$, $W(t, u_0) = S_e(t) x^\top(t) R B \sigma(u_0)$, $S_e(t) = 1/(1 - x^\top(t) R x(t))$, and $e(0) \in \mathcal{E}(R) - \mathcal{E}(R_s)$, with $R_s = \varepsilon^{-1} I_3$ and

$$\varepsilon = \|e^{(A_0 + A_{\max} I) h_{\min}}\| \lambda_{\max}^{-\frac{1}{2}}(R) + h_{\min} \varepsilon_1 \varepsilon_2, \quad (74)$$

where

$$\varepsilon_1 = \|K\| \lambda_{\max}^{-\frac{1}{2}}(R) + \sqrt{2} \|D\| w_{\max}, \quad (75)$$

$$\varepsilon_2 = \sup_{0 \leq s \leq h_{\min}} \|e^{(A_0 + A_{\max} I)(h_{\min} - s)}\|, \quad (76)$$

then, the ellipsoid $\mathcal{E}(P)$, with P given as in Lemma 7, is asymptotically attractive while $\mathcal{E}(R)$ is invariant for the system (67) provided that

$$\gamma_2 w_{\max}^2 \leq 2\kappa_1. \quad (77)$$

The following algorithm provides a way to implement the event-triggered controller.

Algorithm 5.1:**Input:** h_{\min} ;**Output:** $\tilde{u}(t)$;o1: $h(t) = t - t_k$;o2: $k = 0$;o3: **if** $W(t, u_0(t_k)) > \rho W(t, u_0(t)) \wedge h(t) \geq h_{\min}$;o4: $\tilde{u}(t) = \sigma(u_0(t))$;o5: $k = k + 1$;o6: **else**o7: $\tilde{u}(t) = \sigma(u_0(t_k))$;o8: **end**

Note that the control (69) ensures that the tracking error converges asymptotically to $\mathcal{E}(P)$. Once in this region, the control law commutes to a constant sampled controller, which takes into account a maximum sampling time. In the following section, a way to design this controller is proposed.

5.3.3 Constant Sampled Controller

Let us consider the state–feedback control law

$$\hat{u}(t) = K_2 x(t_k), \quad \forall t \in [t_k, t_{k+1}), \quad k \in \mathbb{N}, \quad (78)$$

with $h(t) = t_{k+1} - t_k = \bar{h}$, with some $\bar{h} > h_{\min} > 0$. The following lemma provides a way to design K_2 .

Lemma 9 *Let the control (78) be applied to the system (67), i.e., $u(t) = \hat{u}(t)$. Suppose that there exist some positive–definite matrices $P_1 = P_1^\top \in \mathbb{R}^{n \times n}$, $P_2 = P_2^\top \in \mathbb{R}^{n \times n}$, $R_1 = R_1^\top \in \mathbb{R}^{n \times n}$, $S = S^\top \in \mathbb{R}^{n \times n}$, and $Y \in \mathbb{R}^{p \times n}$, such that the following LMI*

$$\Psi_1 = \begin{pmatrix} \psi_{11} & \psi_{12} & \psi_{13} & D \\ * & \psi_{22} & \epsilon BY & \epsilon D \\ * & * & \psi_{33} & 0 \\ * & * & * & -\gamma_3 I \end{pmatrix} \preceq 0, \quad (79)$$

$$\psi_{11} = P_2^\top A_\psi^\top + A_\psi P_2 + 2\kappa_2 S - e^{-2\kappa_2 \bar{h}} R_1,$$

$$\psi_{12} = P_1 - P_2 + \epsilon A_\psi P_2, \quad \psi_{13} = e^{-2\kappa_2 \bar{h}} R_1 + BY,$$

$$\psi_{22} = -2\epsilon P_2 + \bar{h}^2 R_1, \quad \psi_{33} = -e^{-2\kappa_2 \bar{h}} (R_1 + S),$$

holds for some $\epsilon, \kappa_2, \gamma_3 > 0$, $\bar{h} > h_{\min} > 0$, and K_2 is designed as $K_2 = Y P_2$, then the system (67) is ISS, with respect to d , and $x(t) \in \mathcal{E}(P_c)$, with $P_c = 2\kappa_2 \gamma_3^2 w_{\max}^2 P_2^\top P_1 P_2^{-1}$. Moreover, if

$$X_2^{-1} \preceq P_c, \quad (80)$$

holds for some $w_{\max} > 0$, and X_2 given as in Lemma 7, then $\mathcal{E}(P_c) \subset \mathcal{E}(P)$.

The following algorithm provides a way to implement the constant sampled controller and to obtain \bar{h} through the bisection method, where $h_{\max} > 0$ is an auxiliary tuning variable.

Algorithm 5.2:

Input: $\varepsilon \ll 1, h_{\min}, h_{\max} > h_{\min}, X_2;$

Output: $\bar{h}, K_2, P_1, P_2, R_1, S, P_c;$

```

01:  $h_b = (h_{\min} + h_{\max})/2;$ 
02: while  $h_b > 2\varepsilon h_{\min};$ 
03:    $h_b = (h_{\min} + h_{\max})/2;$ 
04:    $\bar{h} = h_b;$ 
05:   if  $\Psi_1 \preceq 0 \wedge X_2^{-1} \preceq P_c;$ 
06:      $h_{\max} = h_b;$ 
07:   else
08:      $h_{\min} = h_b;$ 
09:   end
10: end
11:  $\bar{h} = h_b.$ 

```

Note that (80) is used to verify that the convergence region, given when the control (78) is applied, is completely contained in $\mathcal{E}(P)$. If this condition is not fulfilled, the parameter γ_3 can be modified to recalculate K_2 such that the $\mathcal{E}(P_c)$ contained in $\mathcal{E}(P)$. Finally, considering the results of Lemmas 7 and 9, the main result is presented.

Theorem 3 *Let the control (68) be applied to the system (67), with (73) and (78), where, the controller parameters are designed according to Lemma 7, Lemma 8, and Lemma 9, respectively. If $e(0) \in \mathcal{E}(R) - \mathcal{E}(R_s)$, then the system (67) is ISS with respect to w .*

The proof of the previous results are postponed to section 5.6.

To better illustrate the algorithm presented in this chapter, a block diagram of the closed-loop dynamics, considering the system (64a) and the controller (68), is presented in Fig. 19.

5.4 SIMULATION RESULTS

Consider the following nonlinear system

$$\begin{aligned}\dot{x}_1(t) &= -x_1(t) + (1 + x_1(t))x_2(t) + w(t), \\ \dot{x}_2(t) &= (2x_1(t) - 1)x_2(t) + u(t) + w(t),\end{aligned}$$

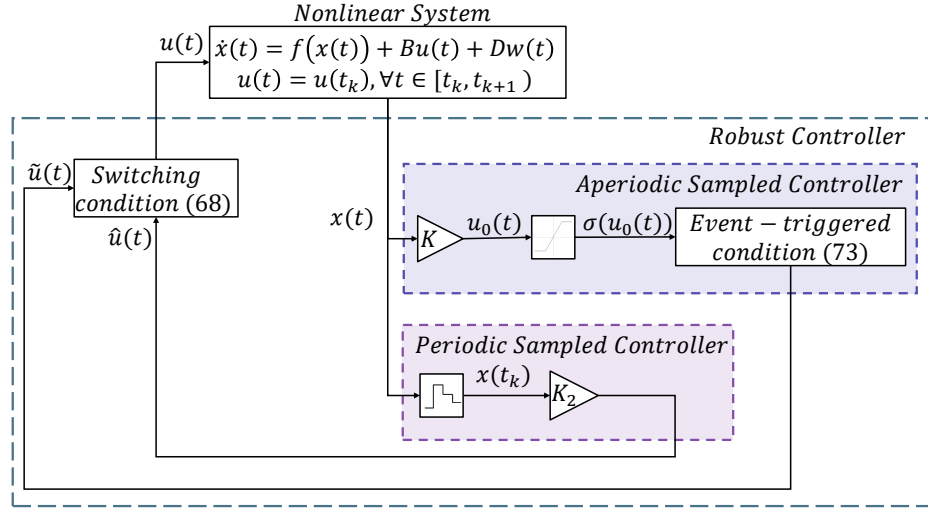


Figure 19: Closed-loop diagram

with $w(t) = 0.2 \sin(3t) + 0.2$, thus, $\underline{w}(t) = 0$, $\bar{w}(t) = 0.4$, and $w_{\max} = 0.4$. This system satisfies Assumptions 3 and 4. The matrices A_0 and A_j can be obtained by the convex polythopic method [51], as follows

$$A_0 = \begin{pmatrix} -1 & 1 \\ 0 & -1 \end{pmatrix}, A_1 = \begin{pmatrix} 0 & 2 \\ 2 & 0 \end{pmatrix}, A_2 = \begin{pmatrix} 0 & 2 \\ -2 & 0 \end{pmatrix},$$

$$A_3 = \begin{pmatrix} 0 & -2 \\ 2 & 0 \end{pmatrix}, A_4 = \begin{pmatrix} 0 & -2 \\ -2 & 0 \end{pmatrix}.$$

Let us consider that $u_{\max} = 2$, $x_1 \in (-2, 2)$ and $x_2 \in (-1, 1)$, and hence $b_1 = (1/2, 0)^\top$, $b_2 = -b_1$, $b_3 = (0, 1)^\top$, and $b_4 = -b_3$. The initial conditions for the system are $x(0) = (-1.2, 0.45)^\top$. To compute the control gains for the aperiodic control law, let us apply the statements of Lemma 7. Consider $\delta = 0.4486$ and $\gamma = 0.2$, then the following feasible solution is obtained:

$$R = \begin{pmatrix} 0.2502 & 0.0152 \\ 0.0152 & 1.2304 \end{pmatrix}, P = \begin{pmatrix} 0.5004 & 0.0304 \\ 0.0304 & 2.4607 \end{pmatrix},$$

$$K = \begin{pmatrix} -0.1394 & -1.2693 \end{pmatrix}.$$

Therefore it can be verified that that the LMI (72) is satisfied, hence, the event-triggered control can be applied.

To compute the control gains for the periodic control law, let us apply the statements of Lemma 9. Taking into account $h_{\min} = 0.1[s]$, $\gamma_2 = 0.2$, $\epsilon = 0.5$, then, the following feasible solution is obtained:

$$P_1 = \begin{pmatrix} 5.3448 & -0.0281 \\ -0.0281 & 3.8928 \end{pmatrix}, P_2 = \begin{pmatrix} 3.8978 & 0.5874 \\ 0.5874 & 3.4911 \end{pmatrix},$$

$$K_2 = \begin{pmatrix} -2.5322 & -3.8710 \end{pmatrix}, \bar{h} = 0.2.$$

Additionally, it is given that $\varepsilon = 0.0592$ and thus $R_s = 16.8910I_3$. The system trajectories are depicted in Fig. 20, which shows that they converge to a region close to the origin despite the external perturbations and never transgress the state constraints. The control signal is depicted in Fig. 21. Observe that the control signals remain inside the linear region. The ellipsoids $\mathcal{E}(R)$, $\mathcal{E}(P)$, $\mathcal{E}(P_c)$, and $(\mathcal{E}(R) - \mathcal{E}(R_s))$, are depicted in Fig. 22. It can be seen that the system trajectories in $(\mathcal{E}(R) - \mathcal{E}(R_s))$, remain inside $\mathcal{E}(R)$, then converge to $\mathcal{E}(P)$, and finally remain inside $\mathcal{E}(P_c)$.

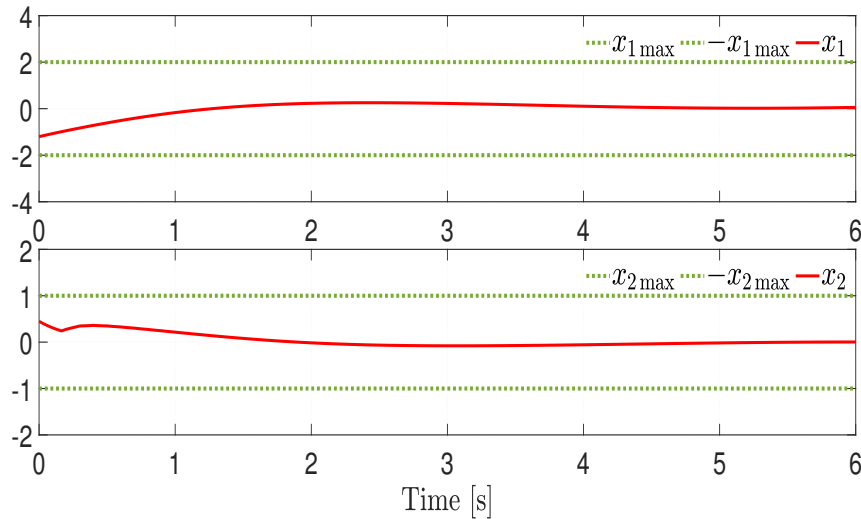


Figure 20: System trajectories

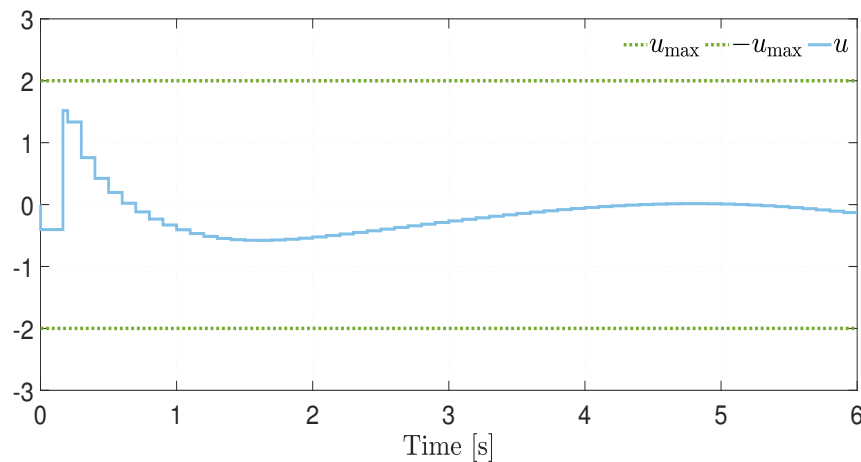


Figure 21: Control signals

5.5 REMARKS

In this chapter, a robust controller to stabilize continuous-time nonlinear system is designed. The proposed control scheme comprises an aperiodic sampled controller and a periodic sampled controller. The proposed aperiodic sampled controller is based on a state-feedback event-triggered

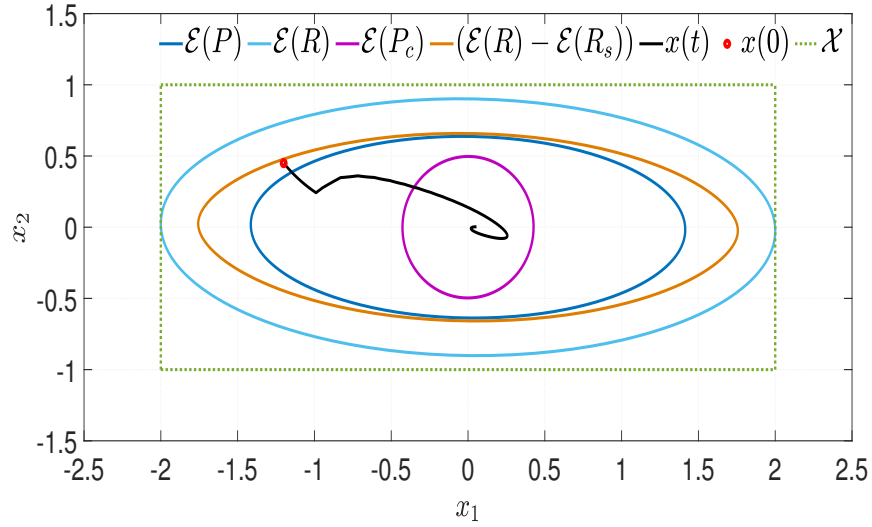


Figure 22: Phase portrait

controller designed through the AEM and the BLF, taking into account the state and input constraints. The characterization of a safe set, where the state constraints are not transgressed, is provided, as well as a switching set that defines the region where each part of the control is active. The periodic sampled control part is based on a state–feedback controller, which takes into account the minimum sampling interval. The proposed approach ensures the ISS properties of the system trajectories with respect to external perturbations.

5.6 PROOF OF THE RESULTS

Proof of Lemma 7: Consider the function $\phi(u_0(t)) = \sigma(u_0(t)) - u_0(t)$, thus the closed–loop dynamics, considering the system (67) and the controller (69), *i.e.*, $u(t) = \sigma(u_0(t))$, is given as

$$\dot{x}(t) = (A_0 + \tilde{A} + BK)x(t) + B\phi(u_0(t)) + Dw(t), \quad (81)$$

where $\tilde{A} = \sum_{j=1}^m \alpha_j(\rho_1)A_j$. Let us take into account the following BLF candidate $V(t) = \ln(1/(1 - x^\top(t)Rx(t)))$, where $0 \prec R = R^\top \in \mathbb{R}^{n \times n}$ is a matrix that parametrizes the ellipsoid $\mathcal{E}(R)$ containing the initial conditions. Then, the time–derivative of V , along the trajectories of system (81), is given by

$$\dot{V}(t) = 2S_e(t)x^\top(t)R[(A_0 + \tilde{A} + BK)x(t) + B\phi(u_0(t)) + Dw(t)], \quad (82)$$

where $S_e(t) = 1/(1 - x^\top(t)Rx(t))$. Introducing the extended vector $\eta^\top(t) := (e^\top(t), \phi^\top(t), w^\top(t))^\top$, the time–derivative of V can be rewritten as follows

$$\dot{V}(t) = S_e(t)\eta^\top(t) \begin{pmatrix} \text{He}\{A_k\} & RB & D \\ \star & 0 & 0 \\ \star & \star & 0 \end{pmatrix} \eta(t),$$

where $A_k = R(A_0 + \tilde{A} + BK)$. Considering that $\|\tilde{A}\| \leq A_{\max}$, adding and subtracting the term $\gamma S_e(t)w^\top(t)Q_w w(t)$, with Q_w such that $w^\top(t)Q_w w(t) \leq 1$, i.e., $\lambda_{\max}(Q_w) = 0.5w_{\max}^2$, then \dot{V} can be upper bounded by

$$\dot{V}(t) \leq S_e(t) \left(\gamma + \eta^\top(t) \begin{pmatrix} \text{He}\{\tilde{A}_k\} & RB & D \\ * & 0 & 0 \\ * & * & -\gamma Q_w \end{pmatrix} \eta(t) \right),$$

where $\tilde{A}_k = R(A_0 + A_{\max}I_n + BK)$. According to Lemma 3, with $\tilde{\alpha} = Kx$, $\tilde{\beta} = Kx - G_0x$, and $G_0 \in \mathbb{R}^{p \times n}$, the inequality $\phi^\top \Delta^{-1} [\phi + (K - G_0)x] \leq 0$ is satisfied, where $\Delta^{-1} = \text{diag}(\delta_1^{-1}, \delta_2^{-1})$, with $\delta_1, \delta_2 > 0$. In order to ensure that $G_0x(t)$ belongs to the set \mathcal{Z} , noting that $x^\top(t)Rx(t) < 1$, it is sufficient that $\|G_0x(t)\|^2 \leq \bar{u}_i^2 x^\top(t)Rx(t)$, for $i = 1, 2$, holds. Using the Schur's complement, the previous inequality can be written as in LMI (70b), with $Z = R^{-1}G_0$. Adding and subtracting the term $\gamma S_e(t)x^\top(t)Px(t)$, then \dot{V} can be upper bounded as follows

$$\dot{V}(t) \leq \gamma S_e(t)[1 - x^\top(t)Px(t)] + S_e(t)\eta^\top(t)\Sigma\eta(t),$$

with

$$\Sigma = \begin{pmatrix} \text{He}\{\tilde{A}_k\} + \gamma P & RB - \Delta^{-1}K_G^\top & D \\ * & -2\Delta^{-1} & 0 \\ * & * & -\gamma Q_w \end{pmatrix},$$

with $K_G = K - G_0$. Pre and post-multiplying Σ by $T = \text{diag}(R^{-1}, \Delta, I)$, it follows that $\Sigma_1 = T\Sigma T \preceq 0$ is equivalent to $\chi_1 \preceq 0$, with the change of variables $X_1 = R^{-1}$, $X_2 = P^{-1}$, $Y = KR^{-1}$, and $Z = R^{-1}G_0$, and introducing an additional variable $M \in \mathbb{R}^{n \times n}$ with constraints $M \succ \gamma R^{-1}PR^{-1}$, applying the Schur's complement, one obtains the LMI (70c).

Hence, if $\chi_1 \preceq 0$, then $\dot{V}(t) \leq \gamma S_e(t)[1 - x^\top(t)Px(t)]$. Note that, for all $x^\top(t)Px(t) > 1$ and $x^\top(t)Rx(t) < 1$, $\dot{V}(x(t)) \leq 0$; thus, any solution of system (81), starting in $\mathcal{E}(R)$, remains in $\mathcal{E}(R)$ and converges asymptotically to $\mathcal{E}(P)$, which implies that $\mathcal{E}(R)$ is invariant. Therefore, if $P \succ R$, i.e., the LMI (70d), holds then $\mathcal{E}(P)$ is completely contained into $\mathcal{E}(R)$. To ensure that $\mathcal{E}(R)$ is completely contained in the state-constrained set (65), it is sufficient that condition (70e) is satisfied. This concludes the proof. ■

Proof of Lemma 8: Based on the proof of Lemma 7, it is established that

$$\dot{V}(t) = 2S_e(t)x^\top(t)R[(A_0 + \tilde{A})x(t) + B\sigma(u_0(t)) + Dw(t)].$$

It has been shown that V is a BLEF, then it is decreasing. Therefore, the following event-triggered condition is introduced

$$\dot{V}(x(t), u_0(t_k)) \leq \rho \dot{V}(x(t), u_0(t)), \quad (83)$$

with some $\rho > 0$ whose satisfaction guarantees that $V(t, e)$ keeps its decay property. Note that (83) is equivalent to the following inequality

$$W(t, u_0(t_k)) \leq \rho W(t, u_0(t)). \quad (84)$$

Let us analyze the two scenarios provided by the condition (84), *i.e.*, when the control input needs to be updated and when it needs to remain constant. For the first scenario, *i.e.*, when the condition (84) is no longer satisfied, *i.e.*, $W(t, u_0(t_k)) > \rho W(t, u_0(t))$, this indicates that $W(t, u_0(t_k))$ decreases slower than the rate $\rho W(t, u_0(t))$. This implies that the control input needs to be updated to ensure that $W(t, u_0(t_k))$ decreases again with rate $\rho W(t, u_0(t))$.

For the second scenario, there are two cases to analyze. For the first case, if $W(x(t), u_0(t_k)) \leq \rho W(x(t), u_0(t))$, *i.e.*, $\tilde{u}(t) = \tilde{u}(t_k)$, for all $t \in [t_k, t_{k+1})$, the control signal remains constant. Since the minimum sampling time is considered, an additional condition must be imposed on the event-triggered structure to allow the control signal to be updated. Then, it is necessary to show that the trajectories will not violate the state constraints for the case when (84) does not hold and $h(t) < h_{\min}$, *i.e.*, when the control input will remain constant until $h(t) = h_{\min}$. Since Lemma 7 already provides convergence conditions when the saturated control is used, it is required to analyze the case when the control is constant out of the saturated zone, *i.e.*, in the linear zone $u_0(t_k) = Ke(t_k)$. The case when the control passes from the saturated zone to the non-saturated one, while $h(t) < h_{\min}$, can be treated similarly, and this case is omitted for brevity. Thus, let us take into account the closed-loop dynamics, considering the system (67) and the controller (71), *i.e.*, $\tilde{u}(t) = u_0(t_k)$, for all $t \in [t_k, t_{k+1})$, $k \in \mathbb{N}$:

$$\dot{x}(t) = (A_0 + \tilde{A})x(t) + BKx(t_k) + Dw(t), \quad (85)$$

where K is given as in Lemma 7 and $h(t) = h_{\min}$, *i.e.*, the worst case for which the constraints are not transgressed. The solution of system (85), taking into account that $x^\top(t_k)Rx(t_k) \leq 1$, satisfies $\|x(t)\| \leq \varepsilon$, with ε given in (74), for all $t \in [t_k, t_{k+1}]$. Then, the set $\mathcal{E}(R_s)$ is defined, with $R_s = \varepsilon^{-1}I_3$, as a threshold set. Note that the set $\mathcal{E}(R_s)$ considers a threshold region inside to $\mathcal{E}(R)$ that ensures the states do not violate the constraints, even when the control input is constant until $h(t) = h_{\min}$. Now, based on [64], let us consider the following Lyapunov–Krasovskii functional

$$\begin{aligned} V_2(t) = & x^\top(t)Rx(t) + \int_{t-h_{\min}}^t e^{2\kappa_1(s-t)} x^\top(s)\tilde{S}_1x(s)ds \\ & + h_{\min} \int_{-h_{\min}}^0 \int_{t+\theta}^t e^{2\kappa_1(s-t)} \dot{x}^\top(s)\tilde{R}_1\dot{x}(s)d\theta ds, \quad (86) \end{aligned}$$

where $\kappa_1 > 0$, $0 \prec \tilde{R}_1 = \tilde{R}_1^\top \in \mathbb{R}^{n \times n}$, $0 \prec \tilde{S}_1 = \tilde{S}_1^\top \in \mathbb{R}^{n \times n}$, and R is given as in Lemma 7. Note that for this analysis the values of K and R are fixed.

The time-derivative of V_2 , along the trajectories of system (85), and using the descriptor method, satisfies

$$\begin{aligned} \dot{V}_2(t) + 2\kappa_1 V_2(t) - \gamma_2 w^\top(t)w(t) &\leq 2x^\top(t)Rx(t) + 2\kappa_1 x^\top(t)Rx(t) \\ &\quad + h_{\min}^2 \dot{x}(t)\tilde{R}_1\dot{x}(t) + x^\top(t)\tilde{S}_1x(t) - \gamma_2 w^\top(t)w(t) \\ &\quad - x^{-2\kappa_1 h_{\min}}[x(t) - x(t - h_{\min})]^\top \tilde{R}_1[x(t) - x(t - h_{\min})] \\ &\quad - e^{-2\kappa_1 h_{\min}}[x^\top(t - h_{\min})\tilde{S}_1x(t - h_{\min})] \\ &\quad + 2[w^\top(t)\tilde{P}_2^\top + \dot{x}^\top(t)\tilde{P}_3^\top][(A_0 + \tilde{A})x(t) \\ &\quad + Dw(t) + BKx(t - h_{\min}) - \dot{x}(t)]. \end{aligned} \quad (87)$$

Then, following the same procedure as in [64], the LMI (72) is obtained to ensure that $\dot{V}_2(t) + 2\kappa_1 V_2(t) - \gamma_2 w^\top(t)w(t) < 0$. Based on Proposition 4.3 in [64], since $x^\top(t)Rx(t) \leq V_2$, the system (85) is ISS with respect to d , and this implies the asymptotic convergence of e to the ellipsoid $\mathcal{E}(\tilde{R}_c)$, with $\tilde{R}_c = 2\kappa_1\gamma_2^{-1}w_{\max}^{-2}R$. Thus, it is necessary to ensure that the convergence region $\mathcal{E}(\tilde{R}_c)$ is completely contained in $\mathcal{E}(R)$, then $R \prec \tilde{R}_c$, *i.e.*, the condition (77) must be fulfilled. Thus, if $h(t) < h_{\min}$ the control signal can remain constant until $h(t) = h_{\min}$, and the system trajectories remain in $\mathcal{E}(R)$ if $e(0) \in \mathcal{E}(R) - \mathcal{E}(R_s)$.

Therefore, it is established that $\tilde{u}(t) = \sigma(u_0(t))$, at the instant when the condition $W_1(x(t), u_0(t_k)) > \rho W_2(x(t), u_0(t))$ and $h(t) \geq h_{\min}$, *i.e.*, the control input is updated, while it remains constant if $W_1(x(t), u_0(t_k)) \leq \rho W_2(x(t), u_0(t))$, *i.e.*, $\tilde{u}(t) = \tilde{u}(t_k)$, for all $t \in [t_k, t_{k+1})$. Finally, due to the nature of the event-triggered control, the same switching behaviour occurs until the trajectories of the system (67) asymptotically converge to the ellipsoid $\mathcal{E}(P)$. This concludes the proof. ■

Proof of Lemma 9: The closed-loop system dynamics, taking into account (67) and (78), *i.e.*, $u(t) = \hat{u}(t)$, is given as

$$\dot{x}(t) = (A_0 + \tilde{A})x(t) + BK_2x(t_k) + Dw(t), \quad (88)$$

with $t \in [t_k, t_{k+1})$. Let us propose, based on [64], the following Lyapunov-Krasovskii functional

$$\begin{aligned} V_3(t) = x^\top(t)\bar{P}_1x(t) + \int_{t-\bar{h}}^t x^{2\kappa_2(s-t)}x^\top(s)\bar{S}x(s)ds \\ + \bar{h} \int_{-\bar{h}}^0 \int_{t+\theta}^t e^{2\kappa_2(s-t)}\dot{x}^\top(s)\bar{R}_1\dot{x}(s)dsd\theta, \end{aligned} \quad (89)$$

where $\kappa_2 > 0$, $0 \prec \bar{P}_1 = \bar{P}_1^\top \in \mathbb{R}^{n \times n}$, $0 \prec \bar{R}_1 = \bar{R}_1^\top \in \mathbb{R}^{n \times n}$, and $0 \prec \bar{S} = \bar{S}^\top \in \mathbb{R}^{n \times n}$. Then, the time-derivative of V_3 , along the trajectories of system (88), is given in a similar way as in (87). Following the same procedure as in [64], the LMI (79) is obtained in order to ensure that $\dot{V}_3(t) + 2\kappa_2 V_3(t) - \gamma_3 w^\top(t)w(t) < 0$. Based on Proposition 4.3 in [64], the system (88) is ISS with respect to d , and this implies the asymptotic convergence of x to the ellipsoid $\mathcal{E}(P_c)$, with $P_c = 2\kappa_2\gamma_3w_{\max}^{-2}\bar{P}_1$. Finally, since

the control (78) is only active inside the set $\mathcal{E}(P)$, it is necessary to ensure that the convergence region $\mathcal{E}(P_c)$ is completely contained in $\mathcal{E}(P)$. With this aim, $P \prec P_c$, *i.e.*, the LMI (80) must be fulfilled. This concludes the proof. ■

Part III

APPLICATIONS

This chapter proposes a solution to the regulation problem for a three-wheeled OMR with input saturation, state constraints, parameter uncertainties, and external perturbations. The proposed control algorithm, designed as in Chapter 3, consists of a nominal and a robust part, both independently designed using an ISMC approach. The proposed scheme guarantees asymptotic convergence to zero of the regulation error coping with the system constraints and perturbations.

6.1 INTRODUCTION

Mobile robots have emerged as a solution to perform a wide range of tasks in different fields due to their versatility, such as security, industrial supervision, military reconnaissance, etc. (see *e.g.*, [65] and [66]). Within mobile robots, the OMRs have the particularity of moving in any direction without changing their orientation. Motivated by this, the algorithm presented in Chapter 3 is applied to an OMR in order to demonstrate its effectiveness in real applications.

6.2 PROBLEM STATEMENT

Consider the dynamic model of a three-wheeled OMR [67]

$$M\ddot{\xi}(t) + C(\dot{\xi}(t))\dot{\xi}(t) + D\dot{\xi}(t) = \sigma(\tau(t)) + w(t), \quad (90)$$

where $\xi^\top = (x, y, \theta) \in \mathbb{R}^3$ is the configuration variable, where $x(t)$ and $y(t)$ represent the planar position of the OMR, while $\theta(t)$ represents the orientation angle, $\tau^\top = (\tau_1, \tau_2, \tau_3) \in \mathbb{R}^3$ is the vector of generalized forces, which are limited by the saturation function σ , $w^\top = (w_1, w_2, w_3) \in \mathbb{R}^3$ is the vector of external perturbations, and the matrices are given as

$$M = M_r + (I_2 + J_m r_e^2) E E^\top, \quad C(\dot{\xi}(t)) = \frac{4}{r_2} (I_2 + J_m r_e^2) \dot{\theta}(t) B,$$

$$D = r_e^2 \left(\frac{k_a k_b}{R_a} + k_v \right) E E^\top, \quad B = \begin{pmatrix} 0 & 1 & 0 \\ -1 & 0 & 0 \\ 0 & 0 & 0 \end{pmatrix},$$

$$E = -\frac{1}{r} \begin{pmatrix} \frac{\sqrt{3}}{2} & -\frac{1}{2} & -L \\ 0 & 1 & -L \\ -\frac{\sqrt{3}}{2} & -\frac{1}{2} & -L \end{pmatrix}^\top,$$

where $M_r = \text{diag}(m_1 + 3m_2, m_1 + 3m_2, 3m_2 L^2 + I_1 + 3I_3)$, m_1 is the mass of the body, m_2 is the mass of each wheel, I_1 is the inertia of the body, I_2

is the inertia of the wheels over the shaft of the motor, I_3 is the inertia of the wheels perpendicular to the shaft of the motor, L is the distance from the center of the robot to the center of the wheels, J_m is the inertia of the shaft of the motors, k_b is the back electromotive force constant, k_a is the torque constant, R_a is the armature resistance, k_v is the viscous friction of the motor, and r_e is the gear ratio.

The model (90) has the following state space representation

$$\frac{d}{dt} \begin{pmatrix} \xi(t) \\ \dot{\xi}(t) \end{pmatrix} = \begin{pmatrix} \dot{\xi}(t) \\ f(\dot{\xi}(t)) + g(\tau(t) + w(t)) \end{pmatrix}, \quad (91a)$$

$$y_c(t) = C_c(\xi^\top(t), \dot{\xi}^\top(t))^\top, \quad (91b)$$

where

$$\begin{aligned} f(\dot{\xi}(t)) &= -M^{-1}(C(\dot{\xi}(t)) + D)\dot{\xi}(t) \\ &= \begin{pmatrix} -\frac{3a_3}{2r^2}M_1^{-1} & -a_2M_1^{-1}\dot{\theta}(t) & 0 \\ a_2M_2^{-1}\dot{\theta}(t) & -\frac{3a_3}{2r^2}M_2^{-1} & 0 \\ 0 & 0 & -\frac{3L^2a_3}{r^2}M_3^{-1} \end{pmatrix} \dot{\xi}(t), \\ C_c &= \begin{pmatrix} 1 & 0 & 0 & 0 & 0 & 0 \\ 0 & 1 & 0 & 0 & 0 & 0 \\ 0 & 0 & 1 & 0 & 0 & 0 \end{pmatrix}, \end{aligned}$$

and $g = \text{diag}(M_1^{-1}, M_2^{-1}, M_3^{-1})$, with $M_1 = M_2 = m_1 + 3m_2 + 3a_1/2r^2$, $M_3 = 3m_2L^2 + I_1 + 3I_3 + (3a_1L^2)/r^2$, $a_1 = I_2 + J_m r_e^2$, $a_2 = (2/r^2)(I_2 + J_m r_e^2)$, and $a_3 = r_e^2 t[(k_a k_b / R_a) + k_v]$.

Due to the three-wheeled OMR has state constraints, it is assumed that the solutions of the system (91) are constrained inside a set of allowed values. It is possible to define this set through the following set of polytopes

$$\mathcal{P}_{\bar{z}_j} := \{\bar{z}_j \in \mathbb{R}^2 \mid \mathbf{b}_j^\top \bar{z}_j \leq \mathbf{1}_2, j = \overline{1,3}\}, \quad (92)$$

where $\bar{z}_1^\top = (x, \dot{x}) \in \mathbb{R}^2$, $\bar{z}_2^\top = (y, \dot{y}) \in \mathbb{R}^2$, and $\bar{z}_3^\top = (\theta, \dot{\theta}) \in \mathbb{R}^2$.

Then, the problem is to regulate the output of the system (91), to some desired value, despite the presence of parameter uncertainties and external perturbations, and considering state constraints and input saturation.

6.3 ROBUST CONTROL DESIGN

Note that the dynamics (90) is nonlinear due to term $C(\xi)\dot{\xi}$. Taking into account this term as external perturbation and due to the structure of the matrix g the control signals are decoupled, and hence, the system (91) can be rewritten as follows for $j = \overline{1,3}$

$$\dot{\bar{z}}_j(t) = (A_j + \Delta_j)\bar{z}_j(t) + B_j\tau_j(t) + D_z\tilde{w}(t), \quad (93a)$$

$$y_{cj}(t) = C_z\bar{z}_j(t), \quad (93b)$$

where y_{cj} is the output to be regulated and the matrices are defined as follows

$$\begin{aligned} A_i &= \begin{pmatrix} 0 & 1 \\ 0 & -\frac{3a_3}{2r^2}M_i^{-1} \end{pmatrix}, B_i = \begin{pmatrix} 0 \\ M_i^{-1} \end{pmatrix}, i = 1, 2, \\ A_3 &= \begin{pmatrix} 0 & 1 \\ 0 & -\frac{3L^2a_3}{r^2}M_3^{-1} \end{pmatrix}, B_3 = \begin{pmatrix} 0 \\ M_3^{-1} \end{pmatrix}, \\ C_z &= \begin{pmatrix} 1 & 0 \end{pmatrix}, D_z = \begin{pmatrix} 0 & 1 \end{pmatrix}^\top, \end{aligned}$$

with $\tilde{w}_1(t) = -a_2M_1^{-1}\dot{y}\dot{\theta}(t) + w_1(t)$, $\tilde{w}_2(t) = a_2M_2^{-1}\dot{x}\dot{\theta}(t) + w_2(t)$, $\tilde{w}_3(t) = w_3(t)$ as the external perturbations for each subsystem, $\Delta_j = \text{diag}(0, 1)A_j\delta_I$, with $\delta_I \in \mathbb{R}$ as a percentage of the parameter uncertainties. Despite Δ_j is an unknown matrix, it is assumed that it does not destroy the structural properties of the system.

Since the control signals are decoupled; then, it is possible to independently design a controller for each of the subsystems in the form (93).

Assumption 8 *The unknown input w is bounded, i.e., $\tilde{w} \in \mathcal{W} := \{\tilde{w} \in \mathcal{L}_\infty : \|\tilde{w}\|_\infty \leq \bar{w}\}$, with \bar{w} a positive known constant; and the unknown matrix Δ is norm bounded, i.e., $\|\Delta\| \leq \bar{\delta}$, with $\bar{\delta}$ a positive known constant.*

Considering the nature of the mechanical system and taking into account the input saturation, it can be verified that system (90) is bounded-input bounded-state. Thus, the nonlinear part of \tilde{w}_j remains bounded.

Define the regulation error $e := r - y_c$ and the following variable

$$x_r := \int_0^t (r - y_c(\tau)) d\tau = \int_0^t e(\tau) d\tau,$$

where $r \in \mathbb{R}$ is a desired reference. Then, the following extended system is introduced

$$\dot{z}(t) = (\bar{A} + \bar{\Delta})z(t) + \bar{B}(\sigma(\tau(t)) + w(t)) + Fr, \quad (94)$$

where $z := (\bar{z}^\top, x_r)^\top \in \mathbb{R}^3$ is the extended state and the system matrices have the following structure

$$\bar{A} = \begin{pmatrix} A & 0 \\ -C & 0 \end{pmatrix}, \bar{B} = \begin{pmatrix} B \\ 0 \end{pmatrix}, \bar{\Delta} = \begin{pmatrix} \Delta & 0 \\ 0 & 0 \end{pmatrix}, F = \begin{pmatrix} 0 \\ 1 \end{pmatrix}.$$

Note that due to the structure of A and B , the pair $(\bar{A} + \bar{\Delta}, \bar{B})$ is stabilizable. Due to (92), the solutions of the system (94) are constrained inside the polytope

$$\mathcal{P} := \{z \in \mathbb{R}^3 | \mathbf{b}_i^\top z \leq \mathbf{1}_3, i = \overline{1, k}\}. \quad (95)$$

It is possible to approximate the state-constrained set (95) by an ellipsoidal set completely contained in it [31], i.e., $\mathcal{E}(\mathbf{R}) := \{z \in \mathbb{R}^3 | z^\top \mathbf{R} z \leq 1\}$ is contained in \mathcal{P} , if $\bar{\mathbf{b}}_i^\top \mathbf{R}^{-1} \bar{\mathbf{b}}_i \leq 1$, for $i = \overline{1, k}$.

Now with the system in the form given in (12), it is possible to follow the methodology given in Chapter 3 subsection 3.3, to design the controller for each subsystem (93).

Note that although algorithm proposed in Chapter 3 is for regulation tasks, *i.e.*, constant references, it is possible to track sufficiently smooth time-varying references due to the ISMC, which is able to compensate for the time-varying effect of the desired trajectory.

6.4 SIMULATION RESULTS

Let us consider the dynamics (93) with the parameters given in Table 1.

Table 1: Parameters of the OMR

	Value	Units		Value	Units
m_1	1.99	kg	I_1	6.08×10^{-2}	kg m ²
m_2	0.29	kg	I_2	3.24×10^{-4}	kg m ²
r	0.05	m	I_3	4.69×10^{-4}	kg m ²
L	0.11	m	J_m	5.70×10^{-7}	kg m ²
k_a	0.0134	Nm/A	k_b	0.0133×10^{-3}	Vs/rad
k_v	0.0001	Nms/rad	R_a	1.9	Ω
r_e	64	-			

It can be verified that system (93) satisfies Assumption 8, for $j = \overline{1,3}$. The external perturbations are taken as $w_1(t) = 1 + \sin(2t)$, $w_2(t) = 1 - \cos(3t)$, $w_3(t) = 2 + \sin(t)$. The initial conditions are $\bar{z}_1(0) = (1, 0)^\top$, $\bar{z}_2(0) = (1, 0)^\top$, $\bar{z}_3(0) = (2.2, 0)^\top$, and $x_{r1}(0) = x_{r2}(0) = x_{r3}(0) = 0$. In order to show the feasibility of the proposed algorithm for a tracking task of a sufficiently smooth time-varying trajectory, the desired references are selected as

$$\begin{aligned} r_1(t) &= 0.3[1 - (1 + \tanh(\omega t - \phi)) + (1 + \tanh(\omega t - 3\phi)) \\ &\quad - (1 + \tanh(\omega t - 6\phi))], \\ r_2(t) &= r_3(t) = 0.3[1 - (1 + \tanh(\omega t - 2\phi)) + (1 + \tanh(\omega t - 4\phi))], \end{aligned}$$

with $\omega = 20$ and $\phi = 200$. For simulation purposes, let us consider that $x, y \in [-1.8, 1.8]$ [m], $\dot{x}, \dot{y} \in [-3, 3]$ [m/s], and $\dot{\theta} \in [-3\pi, 3\pi]$ [rad/s]. Note that the orientation of the OMR does not have constraints; however, it is known that $\theta \in (-\pi, \pi)$ [rad]. Given the previous statements, the state constraints are $\bar{b}_1 = (10/18, 0, 0)^\top$, $\bar{b}_2 = -\bar{b}_1$, $\bar{b}_3 = (0, 1/3, 0)^\top$, and $\bar{b}_4 = -\bar{b}_3$, for the systems \bar{z}_1 and \bar{z}_2 , while, $\bar{b}_5 = (1/\pi, 0, 0)^\top$, $\bar{b}_6 = -\bar{b}_5$, $\bar{b}_7 = (0, 1/3\pi, 0)^\top$, $\bar{b}_8 = -\bar{b}_7$ for system \bar{z}_3 .

To compute the control gains, it is possible to solve the LMIs of lemma 5 for the j systems in the form (93). Note that systems \bar{z}_1 and \bar{z}_2 are equal; thus, it is possible to design a single control gains for both systems.

Considering $\alpha_1 = 60$, $\tau_{1_{\max}} = \tau_{2_{\max}} = 314.0362$, fixing $\tau_{1I_{\max}} = \tau_{2I_{\max}} = 188.4217$, thus $\tau_{1L_{\max}} = \tau_{2L_{\max}} = 125.6145$; then, the following feasible solution is obtained:

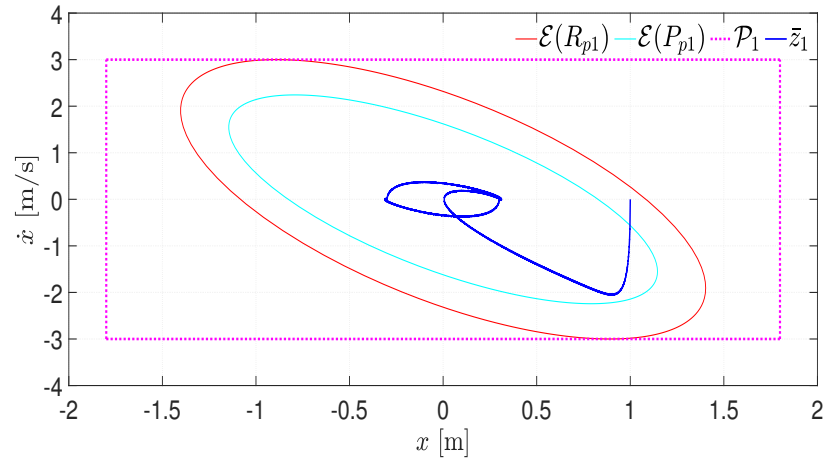
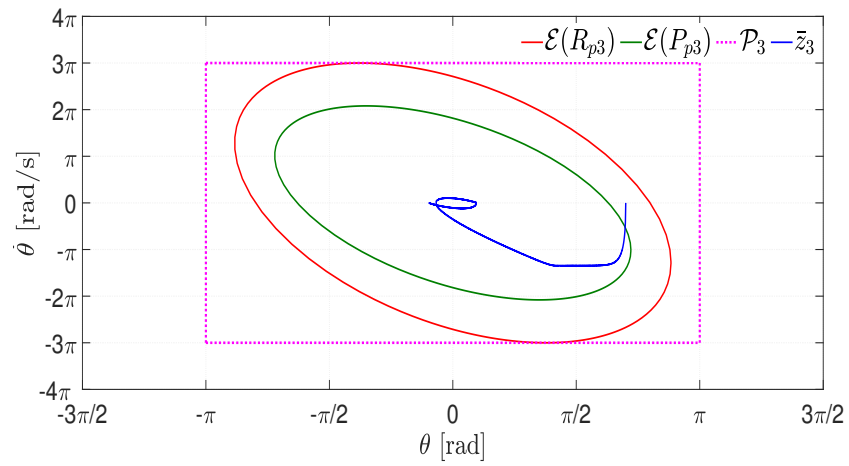
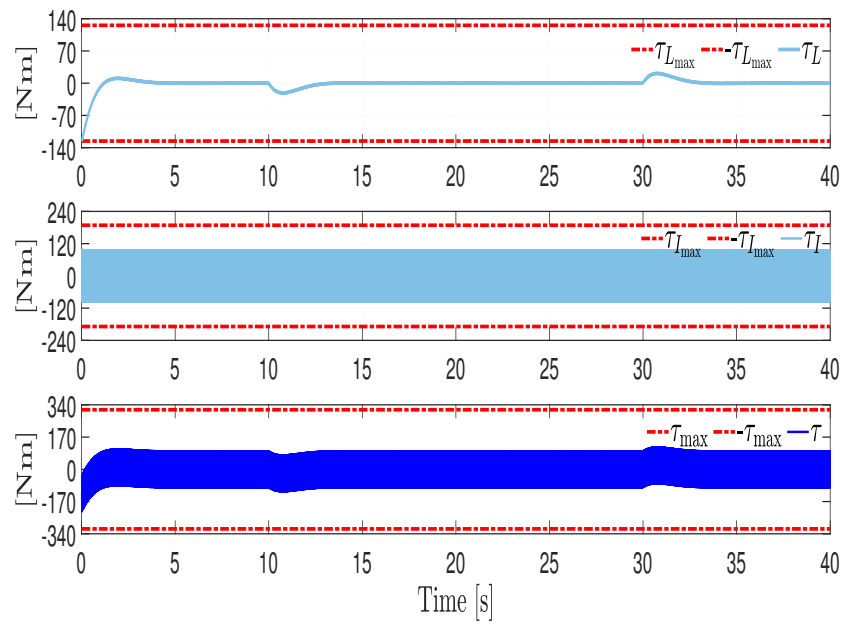
$$\begin{aligned} R_1 = R_2 &= \begin{pmatrix} 3.9072 & 0.6700 & -4.4833 \\ 0.6700 & 0.2432 & -0.6121 \\ -4.4833 & -0.6121 & 6.5782 \end{pmatrix}, \\ P_1 = P_2 &= \begin{pmatrix} 7.2234 & 1.5115 & -7.9554 \\ 1.5115 & 0.5529 & -1.3753 \\ -7.9554 & -1.3753 & 10.9782 \end{pmatrix}, \\ K_1 = K_2 &= \begin{pmatrix} -158.9036 & -1.2005 & 143.4761 \end{pmatrix}, \\ \gamma_1 = \gamma_2 &= 100, \delta_1 = \delta_2 = 0.0067. \end{aligned}$$

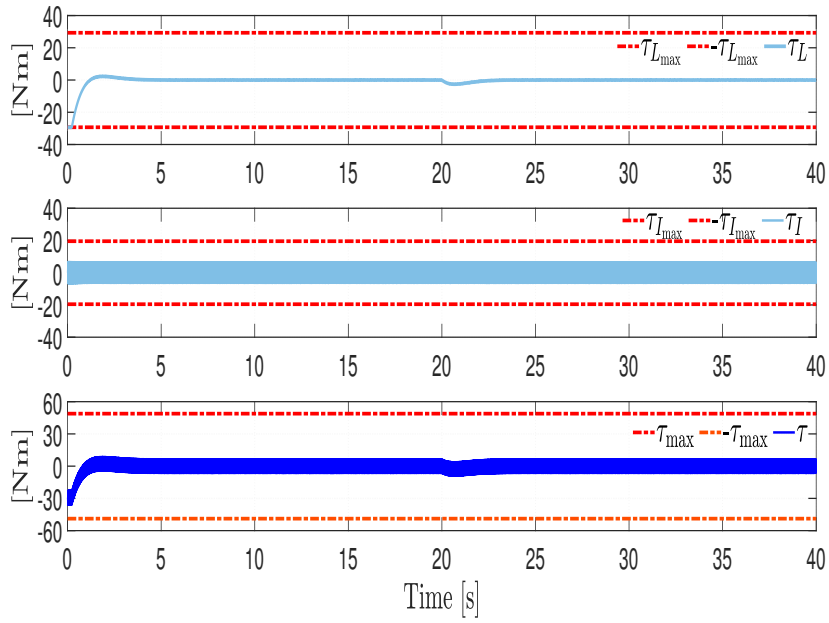
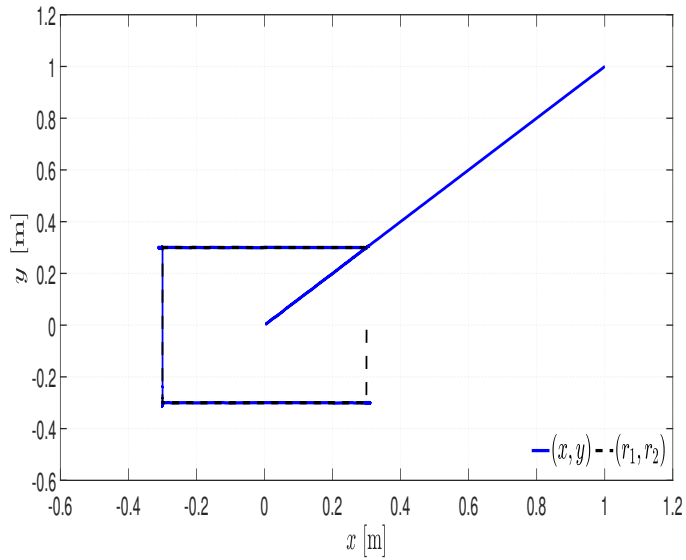
While for system \bar{z}_3 , considering $\alpha_3 = 1$, $\tau_{3_{\max}} = 48.8526$, fixing $\tau_{3I_{\max}} = 19.5410$, thus $\tau_{3L_{\max}} = 29.3115$; then, the following feasible solution is obtained:

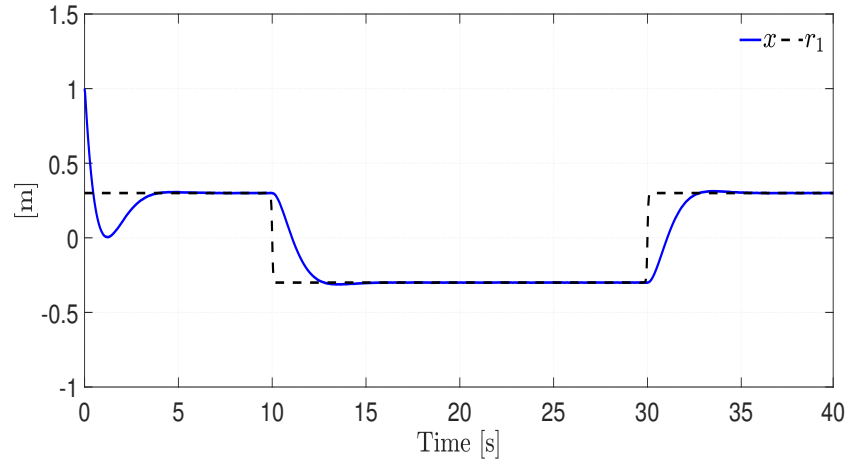
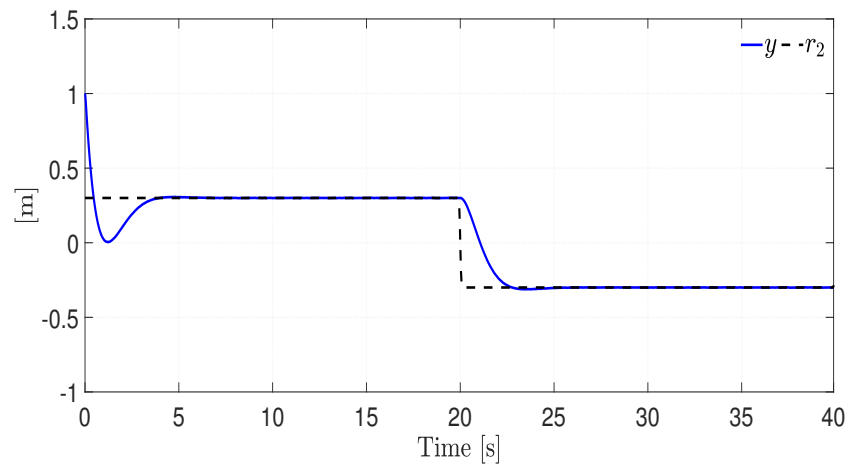
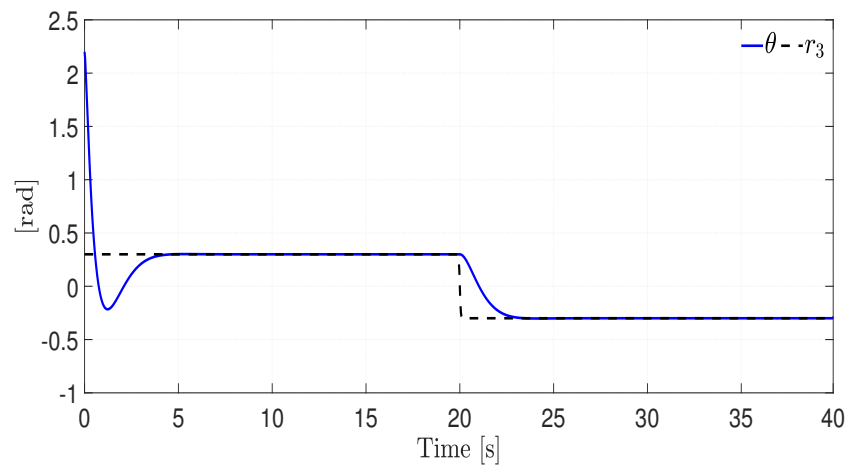
$$\begin{aligned} R_3 &= \begin{pmatrix} 0.6677 & 0.0477 & -0.8342 \\ 0.0477 & 0.0153 & -0.0455 \\ -0.8342 & -0.0455 & 1.3672 \end{pmatrix}, \\ P_3 &= \begin{pmatrix} 1.0837 & 0.1031 & -1.3235 \\ 0.1031 & 0.0350 & -0.0960 \\ -1.3235 & -0.0960 & 2.1143 \end{pmatrix}, \\ K_3 &= \begin{pmatrix} -18.9529 & -0.2783 & 16.6608 \end{pmatrix}, \\ \gamma_3 &= 100, \delta_3 = 0.0079. \end{aligned}$$

Due to the similarity between subsystems \bar{z}_1 and \bar{z}_2 , only the results for systems \bar{z}_1 and \bar{z}_3 are presented. The system trajectories and the corresponding ellipsoids are depicted by Figs. 23-24, for the system \bar{z}_1 and \bar{z}_3 , respectively. Note that for each system, the trajectories begin in ellipsoid $\mathcal{E}(R)$, remains in it, and converges to the ellipsoid $\mathcal{E}(P)$, despite the presence of external perturbations and the parameter uncertainties. The linear control τ_L , the nonlinear control τ_I , the control signal and the saturation constraints are depicted by Figs. 25-26, for system \bar{z}_1 and \bar{z}_3 , respectively. Note that for the \bar{z}_1 , both, the linear and the nonlinear control parts remains in the non-saturated zone all the time. While, in Fig. 26 it is observed that the linear control part gets saturated for an instant of time. Notice that for each system the control signal τ remains in the non-saturated zone.

The system trajectories in the plane $x - y$, and the state trajectory for x , y , and θ , with their desired reference, are depicted in Figs. 27, 28, 29, and 30, respectively, where shown that the trajectories of the system track the desired reference despite the presence of external perturbations and parameter uncertainties.

Figure 23: State trajectories, ellipsoids, and state constraints for x Figure 24: State trajectories, ellipsoids, and state constraints for θ Figure 25: Control signals τ_{1L} , τ_{1I} and τ_1 for system x

Figure 26: Control signals τ_{3L} , τ_{3I} and τ_3 for system θ Figure 27: Phase portrait $x - y$

Figure 28: State trajectory for x Figure 29: State trajectory for y Figure 30: State trajectory for θ

6.5 REMARKS

This chapter presents the results obtained from applying the algorithm presented in Chapter 3 to solve the regulation problem for a three-wheeled OMR with input saturation, state constraints, parameter uncertainties, and external perturbations. Note that the results presented are for the case in which a time-varying trajectory is considered. It can be seen in the simulation results that the asymptotic convergence to zero of the regulation error is ensured coping with the system constraints and perturbations.

TRAJECTORY TRACKING PROBLEM IN A CONSTRAINED UMR

This chapter presents a robust control strategy for the trajectory tracking problem in constrained and perturbed UMRs. The proposed control algorithm, designed as in Chapter 3, consists of a nominal and a robust part, both independently designed using an ISMC approach. The proposed scheme guarantees asymptotic convergence to zero of the tracking error coping with the system constraints and perturbations. Some experimental results, using the QBot2 unicycle mobile robot, validate the effectiveness of the proposed robust control strategy.

7.1 INTRODUCTION

The UMRs have been widely studied due to their ability to move freely from one point to another and the wide variety of possible real-world applications. In addition, it is well-known that such UMRs must deal with state and input constraints, *i.e.*, they have to move in restricted workspaces and have energy limitations (see, *e.g.*, [52], [68], and [69]). Also, the UMRs can be affected by external perturbations, *e.g.*, the skidding and slipping of wheels, and corrupt control signals, which could modify their behavior and stability. Therefore, in order to better deal with the trajectory tracking control problem, it is necessary to consider all these factors in the control design. Motivated by this, an adaptation of the algorithm presented in Chapter 3 is applied to solve the trajectory tracking problem in an UMR. Some experimental results, using the QBot2 by Quanser, validate the effectiveness of the proposed robust control strategy.

7.2 PROBLEM STATEMENT

Consider the perturbed kinematic model of an UMR (see, Fig. 31):

$$\dot{\theta}(t) = [1 + d_1(t)]\omega(t), \quad (96a)$$

$$\dot{x}(t) = [1 + d_2(t)]c(\theta(t))v(t), \quad (96b)$$

$$\dot{y}(t) = [1 + d_2(t)]s(\theta(t))v(t), \quad (96c)$$

where $x(t) \in \mathbb{R}$ and $y(t) \in \mathbb{R}$ denote the midpoint between the wheels and $\theta(t) \in \mathbb{R}$ represents the orientation angle of the UMR. The terms $v(t)$ and $\omega(t)$ contain the linear and angular velocities of the UMR, and represent the control inputs. The terms d_1 and d_2 represent some time-varying perturbations, which are multiplicative to the inputs and that may come from unmodeled kinematics phenomena proportional to the control inputs, such as slipping of the wheels. It is assumed that such time-varying

perturbations $d_i(t)$ are unknown but bounded, *i.e.*, $-1 < d_i(t) \leq d_{\max} < 1$, for all $t \geq 0$ and $i = 1, 2$, with a known positive constant d_{\max} .

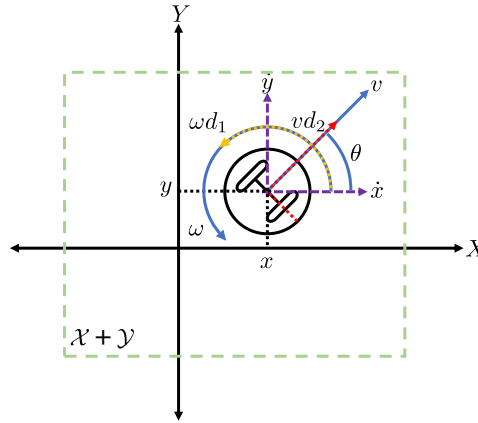


Figure 31: Schematic Diagram of the Perturbed UMR

The aim of this chapter is to solve the trajectory tracking problem for the UMR compensating some multiplicative perturbations and reaching the desired trajectory taking into account some state and input constraints, *i.e.*, $x(t) \in \mathcal{X} = [x_{\min}, x_{\max}] \subset \mathbb{R}$, $y(t) \in \mathcal{Y} = [y_{\min}, y_{\max}] \subset \mathbb{R}$, $v(t) \in \mathcal{V} = [-v_{\max}, v_{\max}] \subset \mathbb{R}$ and $\omega(t) \in \mathcal{W} = [-\omega_{\max}, \omega_{\max}] \subset \mathbb{R}$, for all $t \geq 0$, for some given sets \mathcal{X} , \mathcal{Y} , \mathcal{V} , and \mathcal{W} .

7.3 TRACKING ERROR DYNAMICS

Let us define the tracking errors as follows

$$e_1(t) = \theta_d(t) - \theta(t), \quad (97a)$$

$$e_2(t) = c(\theta(t))(x_d(t) - x(t)) + s(\theta(t))(y_d(t) - y(t)), \quad (97b)$$

$$e_3(t) = c(\theta(t))(y_d(t) - y(t)) - s(\theta(t))(x_d(t) - x(t)), \quad (97c)$$

where x_d , y_d , and θ_d come from a reference kinematic model for the UMR, *i.e.*,

$$\dot{\theta}_d(t) = \omega_d(t), \quad (98a)$$

$$\dot{x}_d(t) = c(\theta_d(t))v_d(t), \quad (98b)$$

$$\dot{y}_d(t) = s(\theta_d(t))v_d(t), \quad (98c)$$

where v_d and ω_d are the linear and angular reference velocities, respectively. These are assumed continuous and bounded by some positive constants \underline{v}_d , \bar{v}_d and $\bar{\omega}_d$, *i.e.*, $0 < \underline{v}_d < v_d(t) \leq \bar{v}_d$, and $\|\omega_d\|_\infty \leq \bar{\omega}_d$, and such that $v_d(t) \in \mathcal{V}$ and $\omega_d(t) \in \mathcal{W}$, for all $t \geq 0$. Moreover, the trajectories of the reference model also hold the state constraints, *i.e.*, $x_d(t) \in \mathcal{X}$ and $y_d(t) \in \mathcal{Y}$, for all $t \geq 0$.

Therefore, the tracking error dynamics can be calculated as

$$\dot{e}_1(t) = -\omega(t)d_1(t) + \tau_1(t), \quad (99a)$$

$$\dot{e}_2(t) = [1 + d_1(t)]\omega(t)e_3(t) - vd_2(t) + \tau_2(t), \quad (99b)$$

$$\dot{e}_3(t) = -[1 + d_1(t)]\omega(t)e_2(t) + v_d(t)s(e_1(t)), \quad (99c)$$

with the virtual control inputs τ_1 and τ_2 satisfying

$$\tau_1(t) = \omega_d(t) - \omega(t), \quad (100a)$$

$$\tau_2(t) = v_d(t)c(e_1(t)) - v(t). \quad (100b)$$

Note that the tracking error dynamics (99) can be rewritten as follows [70]:

$$\dot{e}(t) = A(\rho_1)e(t) + B[\tau(t) + F(\rho_2)d(t)], \quad (101)$$

where $e = (e_1, e_2, e_3)^\top \in \mathbb{R}^3$, $\tau = (\tau_1, \tau_2)^\top \in \mathbb{R}^2$, $d = (d_1, d_2)^\top \in \mathbb{R}^2$ and

$$A(\rho_1) = \begin{pmatrix} 0 & 0 & 0 \\ 0 & 0 & [1 + d_1(t)]\omega(t) \\ v_dsc(e_1) & -[1 + d_1(t)]\omega(t) & 0 \end{pmatrix},$$

$$B = \begin{pmatrix} 1 & 0 \\ 0 & 1 \\ 0 & 0 \end{pmatrix}, \quad F(\rho_2) = \begin{pmatrix} -\omega(t) & 0 \\ 0 & -v(t) \end{pmatrix},$$

with $\rho_1 = (v_dsc(e_1), [1 + d_1(t)]\omega)^\top \in \mathbb{R}^2$ and $\rho_2 = (v, \omega)^\top \in \mathbb{R}^2$ as the unknown and known scheduling parameters, respectively. It is clear that system (101) is in an LPV form and the input and state constraint sets are given now as follows:

$$\mathcal{E} = \{e \in \mathbb{R}^3 : (e_1, e_2, e_3) \in \mathbb{R} \times [-\bar{x}_y, \bar{x}_y] \times [-\bar{x}_y, \bar{x}_y]\}, \quad (102)$$

$$\mathcal{U} = \{\tau \in \mathbb{R}^2 : (\tau_1, \tau_2) \in [-\bar{\tau}_1, \bar{\tau}_1] \times [-\bar{\tau}_2, \bar{\tau}_2]\}, \quad (103)$$

where $\bar{x}_y = (x_{\max} - x_{\min}) + (y_{\max} - y_{\min})$, $\bar{\tau}_1 = \bar{\omega}_d + \omega_{\max}$ and $\bar{\tau}_2 = \bar{v}_d + v_{\max}$. Moreover, note that there always exist a Metzler matrix $A_0 \in \mathbb{R}^{3 \times 3}$, and some matrices $A_j \in \mathbb{R}^{3 \times 3}$, for $j = \overline{1, 4}$, such that the following equations

$$A(\rho_1) = A_0 + \sum_{j=1}^4 \alpha_j(\rho_1)A_j, \quad (104a)$$

$$\sum_{j=1}^4 \alpha_j(\rho_1) = 1, \quad \alpha_j(\rho_1) \in [0, 1], \quad (104b)$$

hold for the system (101). Thus, system (101) can be expressed as follows

$$\dot{e}(t) = \left[A_0 + \sum_{j=1}^4 \alpha_j(\rho_1)A_j \right] e(t) + B[\tau(t) + F(\rho_2)d(t)]. \quad (105)$$

Therefore, the problem now is to design a robust control law τ such that the trajectories of the system (101) converge to zero despite the perturbations d taking into account the state and input constraints (102) and (103), *i.e.*, $e(t) \in \mathcal{E}$ and $\tau(t) \in \mathcal{U}$, for all $t \geq 0$.

Thus, the idea is to design a controller as in (14), *i.e.*,

$$\tau(t) = \sigma(u_0(t)) + u_I(t). \quad (106)$$

7.4 ROBUST CONTROL DESIGN

Following a similar procedure as presented in the section 3.3, the robust control is designed as is shown in the following sections.

7.4.1 Integral Sliding-Mode Control Design

Let us define the following sliding variable

$$s(e(t)) = G[e(t) - e(0)] - G \int_0^t [A_0 e(\rho) + B u_0(\rho)] d\rho, \quad (107)$$

where $G \in \mathbb{R}^{2 \times 3}$ is such that $\det(GB) \neq 0$. The optimal way to design G is $G = B^\top$ or $G = (B^\top B)^{-1} B^\top$. Note that the dynamics of the sliding variable satisfies

$$\dot{s} = GB[u_I + F(\rho_2)d] + G \sum_{j=1}^4 \alpha_j(\rho_1) A_j e. \quad (108)$$

Then, the ISMC u_I is proposed as

$$u_I(t) = -\zeta(e(t)) \frac{(GB)^\top s}{\|(GB)^\top s\|}, \quad (109)$$

with some positive gain $\zeta(e) > 0$, for all $e \in \mathcal{E}$. The following lemma provides the conditions to ensure the finite-time convergence of the sliding variable to zero fulfilling the input constraint.

Lemma 10 *Let the ISMC (109), with $G = B^\top$, be applied to the system (108), for a given $u_{I \max} > 0$. If the gain $\zeta(e)$ is selected as*

$$\zeta(e) = \kappa + F_{\max} + A_{\max} \|e\|, \quad (110)$$

with $F_{\max} = d_{\max} \max(v_{\max}, \omega_{\max})$, $A_{\max} = \sum_{j=1}^4 \alpha_j^* \|A_j\|$, where

$$\alpha^* = \arg \max_{\alpha \in \Gamma} \sum_{j=1}^4 \alpha_j \|A_j\|,$$

with $\Gamma \subset \mathbb{R}^4$ being the set of all convex weight vectors $\alpha = (\alpha_1, \dots, \alpha_4)^\top \in \mathbb{R}^4$ such that (104) holds, and some $\kappa > 0$ such that

$$0 < \kappa \leq u_{I \max} - F_{\max} - A_{\max} e_{\max}, \quad (111)$$

with $e_{\max} \leq \sqrt{4\pi^2 + 2\bar{x}\bar{y}^2}$, is satisfied for a given $u_{I \max} > 0$; then, $s = 0$ is UFTS.

Therefore, the robust controller u_I will deal with the perturbations $F(\rho_2)d$ and part of the term $\sum_{j=1}^4 \alpha_j(\rho_1) A_j e$, satisfying the input constraint $\|u_I\| \leq u_{I \max}$. Note that the term $F(\rho_2)d$ is completely compensated from the beginning since it is matched with the control u_I . However, only the projection of the term $\sum_{j=1}^4 \alpha_j(\rho_1) A_j e$ into the matched space of B could be compensated by u_I .

Remark 7 It is possible to fix $u_{I_i \max}$, such that $|u_{I_i}| \leq u_{I_i \max}$, according to the upper bound of the perturbations, e.g., $u_{I_i \max} \leq 1.1(F_{i \max} + A_{i \max} e_{\max})$, where $F_{i \max}$ is the norm of the i -th element of $F(\rho_2)$ and $A_{i \max} = \sum_{j=1}^4 \alpha_j^* \|A_{ij}\|$, with A_{ij} as the i -th row of the matrix A_j , $i = 1, 2$. Then, to assign the rest of the control effort to u_{0_i} , i.e., $u_{0_i \max} \leq \bar{\tau}_i - 1.1(F_{i \max} + A_{i \max} e_{\max})$, with $u_{0_i \max}$ such that $|u_{0_i}| \leq u_{0_i \max}$.

7.4.2 Linear Control Design

In order to deal with the linear control design, the following assumption is imposed.

Assumption 9 The pair (A_0, B) is stabilizable.

Once in the sliding-mode, it follows that $s = 0$; and thus, based on the equivalent control method, the dynamics on the sliding surface is given by

$$\dot{e} = \left[A_0 + \Gamma \sum_{j=1}^4 \alpha_j(\rho_1) \tilde{A}_j \right] e + B u_0, \quad (112)$$

where $\Gamma = (I_3 - BG)$. Then, the linear part of the control, i.e., u_0 , is proposed as follows

$$u_0(t) = K e(t), \quad (113)$$

where $K \in \mathbb{R}^{2 \times 3}$ is a feedback gain, which can be designed considering the state constraints (102) and the input saturation, by means of the attractive ellipsoid method and the BLF approach.

The following lemma provides the safe set $\mathcal{E}(\mathbb{R})$ and a way to design K .

Lemma 11 Let Assumption 9 be satisfied, and the control (113) be applied to the system (112), for a given $u_{0 \max} > 0$. Suppose that there exist a positive-definite matrix $X_1 = X_1^T \in \mathbb{R}^{3 \times 3}$, some matrices $Y \in \mathbb{R}^{2 \times 3}$, $Z = (Z_1^T, Z_2^T)^T \in \mathbb{R}^{2 \times 3}$, $\bar{\delta} = \text{diag}(\delta_1, \delta_2)$, with $\delta_1, \delta_2 > 0$ and some constant $\gamma > 0$, such that the following set of LMIs

$$\chi_1 = \begin{pmatrix} \psi & B\bar{\delta} - Y^T + Z^T & \gamma X_1 \\ * & -2\bar{\delta} & 0 \\ * & * & -\gamma X_2 \end{pmatrix} \prec 0, \quad (114a)$$

$$\psi = (A_0 + \Gamma A_{\max}) X_1 + X_1 (A_0 + A_{\max} \Gamma^T) + \bar{B} Y + Y^T \bar{B}^T,$$

$$\chi_2 = \begin{pmatrix} X_1 & Z_i^T \\ Z_i & u_{0_i \max}^2 \end{pmatrix} \succeq 0, \quad (114b)$$

$$\chi_3 = \bar{b}_m^T X_1 \bar{b}_m \leq 1, \text{ for } m = \bar{1}, 4, \quad (114c)$$

$$\bar{b}_1 = (0, \bar{x}y^{-1}, 0)^T, \bar{b}_2 = -\bar{b}_1, \bar{b}_3 = (0, 0, \bar{x}y^{-1})^T, \bar{b}_4 = -\bar{b}_3,$$

is feasible for some constant $\bar{x}y$, $u_{0_i \max} \geq 0$, and $Z_i \in \mathbb{R}^{1 \times 3}$, with $i = 1, 2$, as the i -th row of the matrix Z . If $\|e(0)\| \in \mathcal{E}(\mathbb{R})$ and K is designed as $K = YR$, with $R = X_1^{-1}$; then, the trajectories of the system (112) converge asymptotically to zero.

The proof of Lemma 11 follows the same methodology of the proof of Lemma 5 presented in Chapter 3.

Finally, considering the results of Lemmas 10 and 11, the main result is presented in the following theorem.

Theorem 4 *Let Assumption 9 be satisfied, and the control (106), with $u_I = -\zeta(e)(GB)^T s \| (GB)^T s \|^{\tau-1}$ and $u_0 = Ke$, be applied to the system (105), for a given $u_{\max} > 0$. If $\|z(0)\| \in \mathcal{E}(\mathbb{R})$, K is computed as in Lemma 11, i.e., $K = YR$, and ζ is designed as in (110), i.e., $\zeta(e) = \kappa + F_{\max} + A_{\max}\|e\|$, for some $\kappa > 0$, such that*

$$\kappa + \bar{w} + F_{\max} + A_{\max}e_{\max} \leq u_{I_i \max} \leq \tau_{i_{\max}} - u_{0_i \max}, \quad (115)$$

for $i = 1, 2$, then, the trajectories of the system (105) converge asymptotically to zero.

Note that, due to its structure, the LMIs proposed in the previous results can be solved simultaneously through the use of a specialized toolbox, e.g, the SDPT3 solver in MATLAB®.

Remark 8 *Since u_I is selected as in (109), a discontinuous control signal is obtained. In order to avoid high-frequency control signals, it is possible to approximate (109) as*

$$u_I(t) = -\zeta(e(t)) \frac{(GB)^T s}{\| (GB)^T s \| + \varepsilon}, \quad (116)$$

where the tuning parameter $\varepsilon > 0$ is a small constant.

7.5 EXPERIMENTAL RESULTS

The proposed robust strategy is applied to the QBot2 manufactured by Quanser (see Fig. 32). The QBot2 operates with a control station with the real-time control software QUARC®. This software creates a direct interface with MATLAB®/Simulink® and provides a sampling time equal to 0.001 [s]. The QBot2 position and orientation is measured and tracked using internal sensors of the robot. Both wheels have encoders that gather information about the wheel rotation and estimate the changes in position over time. Using this information, the total displacement and orientation angle can be calculated through the UMR kinematics. Note that for the implementation of the proposed controller, the approximation presented in Remark 8 is considered.

In order to show the effectiveness of the proposed controller two different trajectories are considered in the experiments: a sine and a lemniscate curve. For both trajectories the perturbations are taken as $d_1(t) = 0.01 \cos(t) + 0.01$ and $d_2(t) = 0.02 \sin(t) + 0.01$, thus $d_{\max} = 0.8$. The perturbations are generated by means of software.



Figure 32: QBot2 by Quanser

Considering the real maximum values of the UMR for the velocities ω and v , *i.e.*, $\omega_{\max} = 3$ and $v_{\max} = 0.7$, the following matrices are obtained

$$A_0 = \begin{pmatrix} 0 & 0 & 0 \\ 0 & 0 & 0 \\ 1 & 0 & 0 \end{pmatrix}, \quad (117a)$$

$$A_1 = \begin{pmatrix} 0 & 0 & 0 \\ 0 & 0 & 5.4 \\ -5.4 & 5.4 & 0 \end{pmatrix}, \quad A_2 = \begin{pmatrix} 0 & 0 & 0 \\ 0 & 0 & 5.4 \\ 5.4 & -5.4 & 0 \end{pmatrix}, \quad (117b)$$

$$A_3 = \begin{pmatrix} 0 & 0 & 0 \\ 0 & 0 & -5.4 \\ 5.4 & 5.4 & 0 \end{pmatrix}, \quad A_4 = \begin{pmatrix} 0 & 0 & 0 \\ 0 & 0 & -5.4 \\ -5.4 & -5.4 & 0 \end{pmatrix}. \quad (117c)$$

Therefore, it is possible to compute the following: $F_{1\max} = \omega_{\max}d_{\max} = 2.4$, $F_{2\max} = v_{\max}d_{\max} = 0.56$, $A_{1\max} = \sum_{j=1}^4 \alpha_j^* \|A_{1j}\| = 0$, and $A_{2\max} = \sum_{j=1}^4 \alpha_j^* \|A_{2j}\| = 0.216$. Note that, with the above-mentioned A_0 , Assumption 9 is satisfied.

7.5.1 Lemniscate Curve Tracking

The desired trajectory is given by

$$\begin{aligned} \omega_d(t) &= \frac{\dot{x}_d \ddot{y}_d - \dot{y}_d \ddot{x}_d}{\dot{x}_d^2 + \dot{y}_d^2}, \\ v_d(t) &= \sqrt{\dot{x}_d^2 + \dot{y}_d^2}, \\ x_d(t) &= \cos(\omega_0 t), \\ y_d(t) &= \sin(2\omega_0 t), \\ \theta_d(t) &= \int_0^t \omega_d(\tau) d\tau, \end{aligned}$$

and $\omega_0 = 0.15$. The initial conditions for the kinematics are $x_0 = 1.4$ [m], $y_0 = 0$ [m] and $\theta_0 = 0$ [rad], and the state and input constraints sets are given as $\mathcal{X} = [-1.5, 1.5]$, $\mathcal{Y} = [-1.5, 1.5]$, $\mathcal{V} = [-0.7, 0.7]$, and $\mathcal{W} = [-3, 3]$.

To compute the control gains, let us apply the statements of Theorem 4. Consider $\delta_1 = 1.6374$, $\delta_2 = 1.2089$, $\gamma = 0.3$, $\bar{x}\bar{y} = 6$, $\kappa = 0.5$, $\tau_{1\max} = 4.1663$, $\tau_{2\max} = 1.1472$, and fixing $u_{I_1\max} = 2.64$, $u_{0_1\max} = 1.5263$, $u_{I_2\max} = 0.831$, and $u_{0_2\max} = 0.3162$, then, the following feasible solution is obtained:

$$R = \begin{pmatrix} 0.31 & 0.00 & 0.12 \\ 0.00 & 0.38 & 0.00 \\ 0.12 & 0.00 & 0.30 \end{pmatrix}, P = \begin{pmatrix} 0.47 & 0.00 & 0.19 \\ 0.00 & 0.45 & 0.00 \\ 0.19 & 0.00 & 0.41 \end{pmatrix},$$

$$K = \begin{pmatrix} -0.9988 & -0.0015 & -1.1312 \\ 0.0043 & -0.6173 & 0.0056 \end{pmatrix}.$$

The system trajectories are depicted in Figs. 33–34, which show that the system trajectories converge to the desired reference despite the external perturbations. Note that the state trajectories, x and y , never transgress the state constraints. On the other hand, the control signals ω and v are depicted in Fig. 35. Observe that both control signals, ω and v , remain inside the linear region. In Fig. 40, it can be seen that the trajectories of the tracking error are in the ellipsoid $\mathcal{E}(R)$, and then, converge to ellipsoid $\mathcal{E}(P)$, and to the origin. Finally, in Fig. 37, it is observed that the norm of the errors converges to a region close to the origin. Table 2 presents the RMS of the tracking errors to better illustrate the performance of the controller. It can be observed that the mean value is close to zero, thus, the controller performs well despite the presence of perturbations.

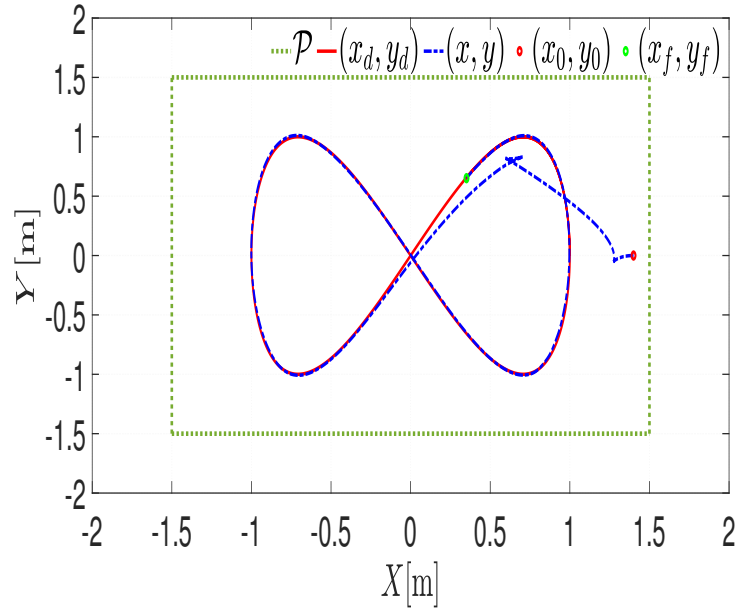


Figure 33: System Trajectories (Lemniscate Curve)

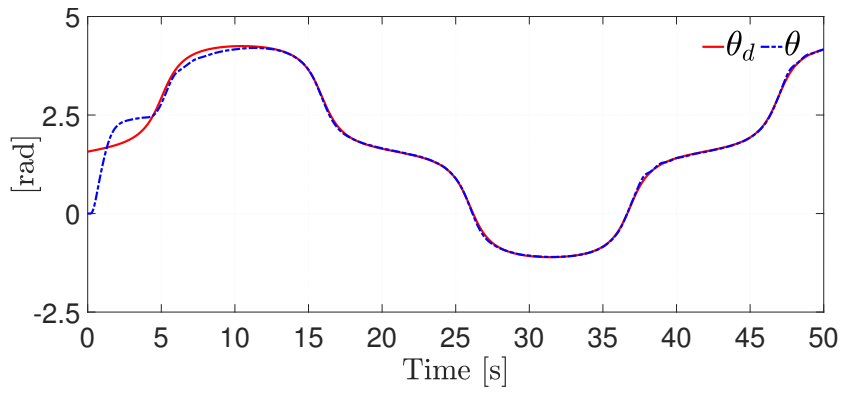


Figure 34: System Trajectories (Lemniscate Curve)

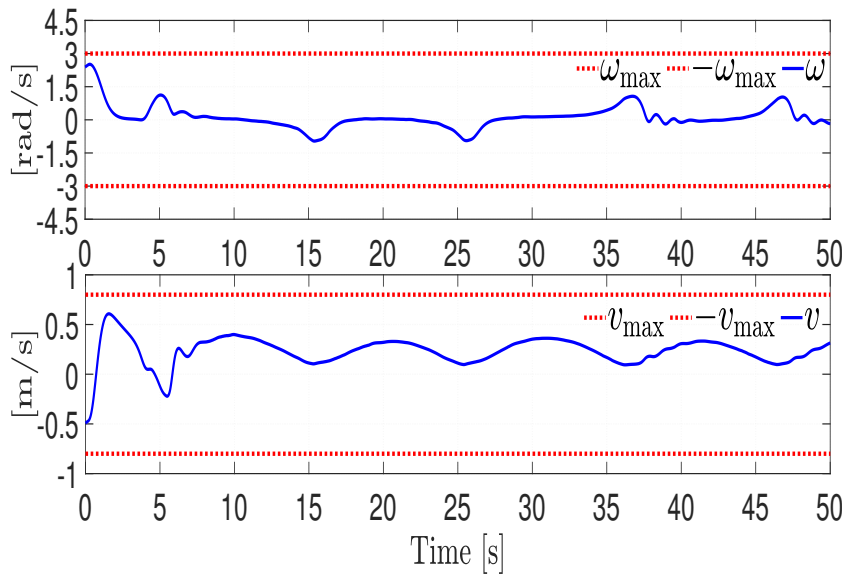


Figure 35: Control Signals (Lemniscate Curve)

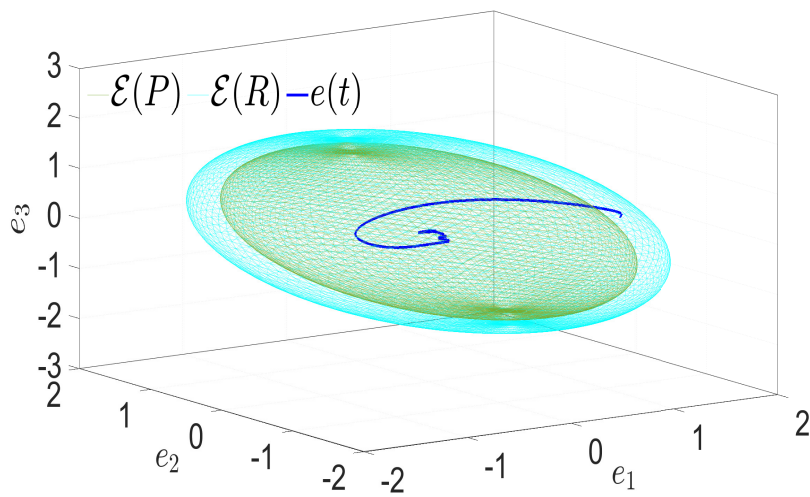


Figure 36: Tracking Error and Ellipsoids (Lemniscate Curve)

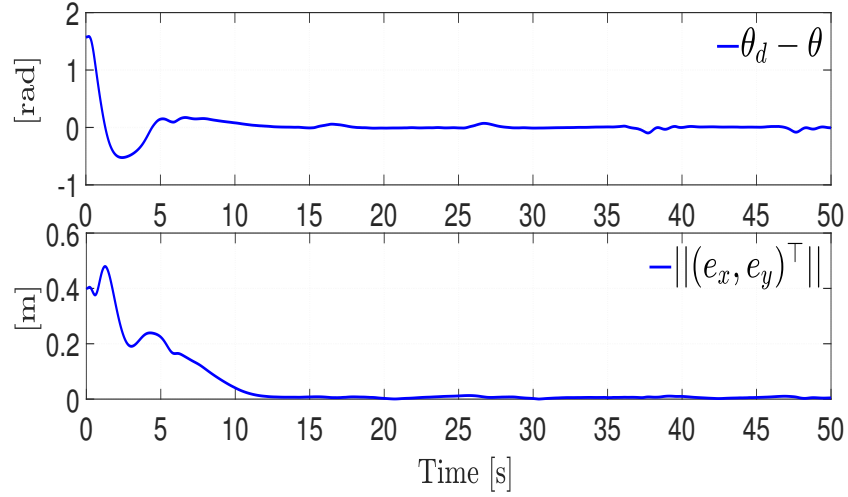


Figure 37: Tracking Error Norm, where $e_x = x_d - x$ and $e_y = y_d - y$ (Lemniscate Curve)

Table 2: Performance indexes (Lemniscate Curve)

	max	min	mean
$e_{\theta_{RMS}}$ [deg]	91.6962	8.6574×10^{-4}	3.7128
$e_{xy_{RMS}}$ [m]	0.4000	3.0932×10^{-6}	0.0263

7.5.2 Sine Curve Tracking

The desired trajectory is given by

$$\begin{aligned}\omega_d(t) &= \frac{\dot{x}_d \ddot{y}_d - \dot{y}_d \ddot{x}_d}{\dot{x}_d^2 + \dot{y}_d^2}, \\ v_d(t) &= \sqrt{\dot{x}_d^2 + \dot{y}_d^2}, \\ x_d(t) &= \omega_0 t, \\ y_d(t) &= \sin(2\omega_0 t), \\ \theta_d(t) &= \int_0^t \omega_d(\tau) d\tau,\end{aligned}$$

and $\omega_0 = 0.15$. Be aware that, in this experiment, no restrictions are considered for the state x . Note that this type of task can simulate the mobile robot moving along a hallway. The initial conditions for the kinematics are $x_0 = 0.5$ [m], $y_0 = 0.75$ [m] and $\theta_0 = 0$ [rad], and the state and input constraints sets are given as $\mathcal{Y} = [-1, 1]$, $\mathcal{V} = [-0.7, 0.7]$, and $\mathcal{W} = [-3, 3]$. To compute the control gains, let us apply the statements of Theorem 4. Considering $\delta_1 = 0.8679$, $\delta_2 = 0.6184$, $\gamma = 0.3$, $\bar{x}\bar{y} = 3$, $\kappa = 0.5$, $\tau_{1\max} = 3.4000$,

$\tau_{2\max} = 0.9236$, and fixing $u_{I_1\max} = 2.64$, $u_{0_1\max} = 0.76$, $u_{I_2\max} = 0.831$, and $u_{0_2\max} = 0.0926$, the following feasible solution is obtained:

$$R = \begin{pmatrix} 0.54 & 0.00 & 0.21 \\ 0.00 & 0.70 & 0.00 \\ 0.21 & 0.00 & 0.51 \end{pmatrix}, P = \begin{pmatrix} 0.80 & 0.00 & 0.33 \\ 0.00 & 0.80 & 0.00 \\ 0.33 & 0.00 & 0.70 \end{pmatrix},$$

$$K = \begin{pmatrix} -1.0128 & -0.0026 & -1.1459 \\ 0.0074 & -0.6554 & 0.0101 \end{pmatrix}.$$

The system trajectories are depicted in Fig. 38, which show that the state trajectories converge to the desired reference despite the presence of external perturbations. Note that the state trajectories y never transgress the state constraints. On the other hand, the control signals ω and v are depicted in Fig. 39. Observe that ω remains inside the linear region, while the control signal v gets saturated for some instance of time, and then, remains in the linear region. In Fig. 40, it can be seen that the trajectories of the tracking error are always inside $\mathcal{E}(P)$, which is completely contained in $\mathcal{E}(R)$. Finally, in Fig. 41, it is observed that the norm of the errors converges to a region close to the origin. Table 3 presents the RMS of the tracking errors to better illustrate the performance of the controller. It can be observed that the mean value is close to zero, thus, the controller performs well despite the presence of perturbations.

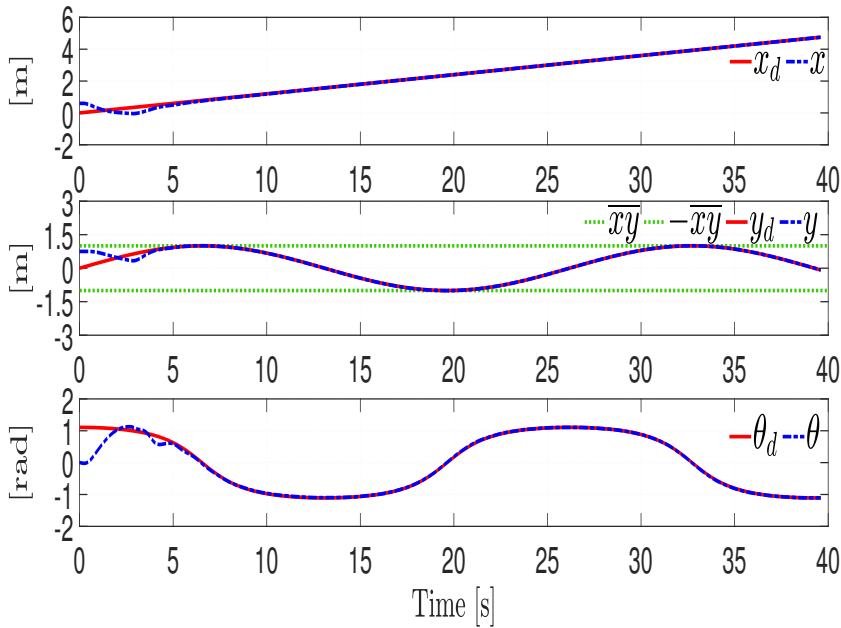


Figure 38: System Trajectories (Sine Curve)

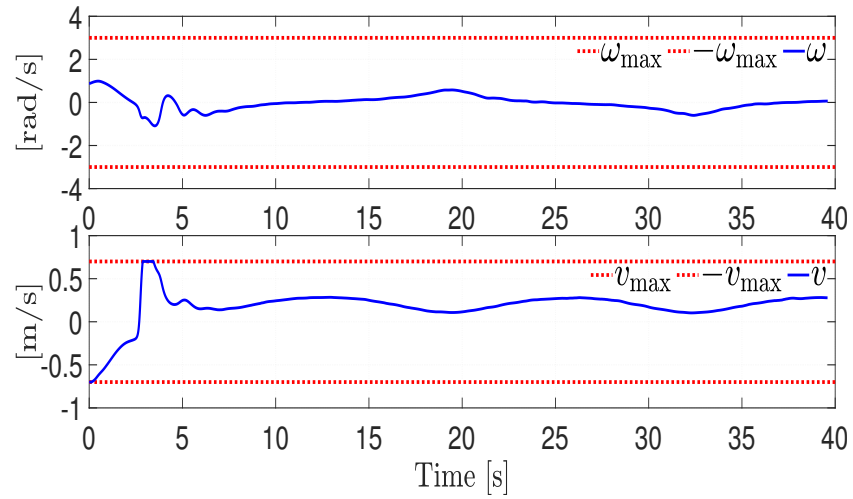


Figure 39: Control Signals (Sine Curve)

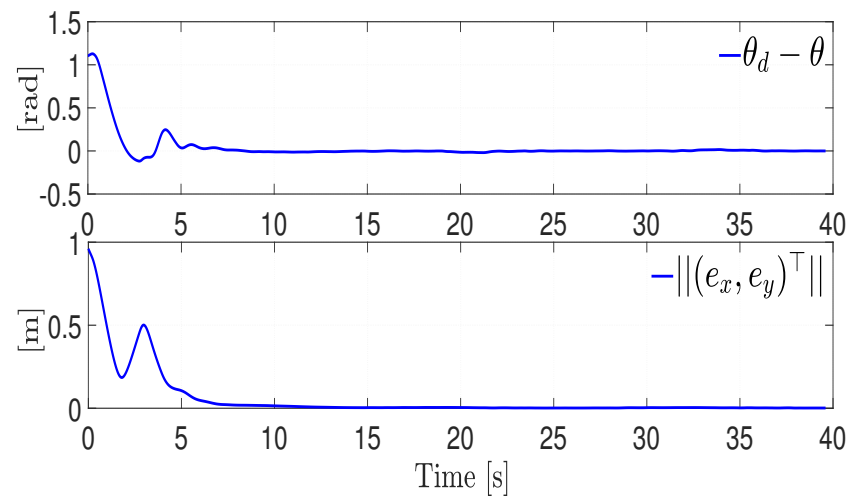


Figure 40: Tracking Error and Ellipsoids (Sine Curve)

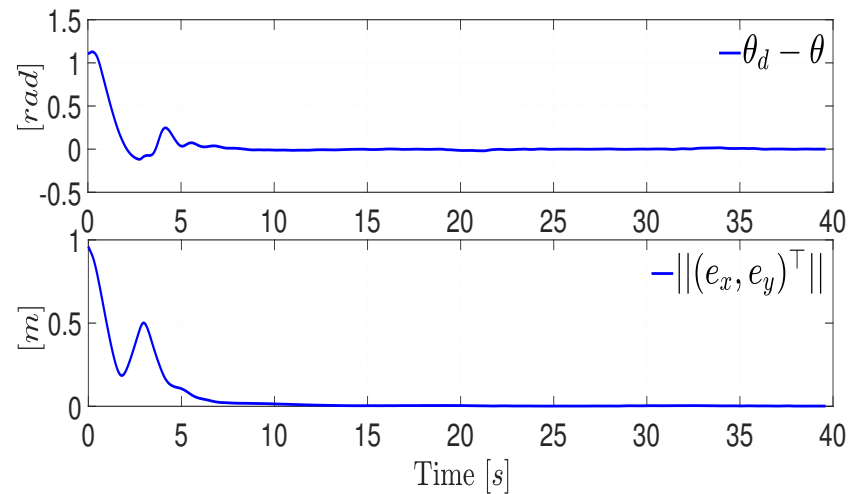
Figure 41: Tracking Error Norm, where $e_x = x_d - x$ and $e_y = y_d - y$ (Sine Curve)

Table 3: Performance indexes (Sine Curve)

	max	min	mean
$e_{\theta_{RMS}}$ [deg]	63.4322	2.1622×10^{-5}	2.7158
$e_{xy_{RMS}}$ [m]	0.5000	$7.4721e \times 10^{-8}$	0.0245

7.6 REMARKS

This chapter presents the results obtained from applying the algorithm presented in Chapter 3 to solve the trajectory tracking problem in the UMR with state and input constraints, affected by external perturbations. Note that due to the use of the tracking error dynamic is possible to apply the proposed algorithm to the trajectory tracking problem in the UMR. It can be seen in the experimental results that the asymptotic convergence to zero of the tracking error is ensured coping with the system constraints and perturbations.

TRAJECTORY TRACKING PROBLEM IN A UMR WITH COMMUNICATION CONSTRAINTS

This chapter presents a sampled robust controller for the trajectory tracking problem in UMRs with state, input, and communication constraints affected by external perturbations, e.g., the wheel slipping. The proposed controller, designed as in Chapter 5, comprises the design of an aperiodic control law based on an event-triggered controller and a periodic control law based on a constant sampled state-feedback controller. The proposed strategy ensures the ISS of the tracking error dynamics with respect to the multiplicative external perturbations.

8.1 INTRODUCTION

UMRs have been widely studied due to their capability of moving freely in the workspace and the wide variety of possible real-world applications. However, as real systems, it is well-known that UMRs have to operate in confined spaces and have energy limitations, *i.e.*, they must deal with state and input constraints. Moreover, in most cases, the UMRs are managed through a digital platform, and then there is limited bandwidth, so it is necessary to restrict the frequency of control input updates to save communication resources. A well-known technique to deal with this problem is the event-triggered control. Its main characteristic is that the control actions are updated only when certain well-defined events occur, resulting in an aperiodic sampling time [58]. Motivated by this, the algorithm presented in Chapter 5 is applied to an UMR to solve the trajectory tracking problem. Some experimental results, using the QBot2 by Quanser, validate the effectiveness of the proposed robust control strategy.

8.2 PROBLEM STATEMENT

Consider the perturbed kinematic model of a UMR given as in (96), *i.e.*,

$$\begin{aligned}\dot{\theta}(t) &= [1 + d_1(t)]\omega(t), \\ \dot{x}(t) &= [1 + d_2(t)]c(\theta(t))v(t), \\ \dot{y}(t) &= [1 + d_2(t)]s(\theta(t))v(t), \\ \mathbf{u}(t) &= (\omega(t), v(t))^\top = \mathbf{u}(t_k), \quad \forall t \in [t_k, t_{k+1}),\end{aligned}$$

where $\mathbf{u}(t)$ represents the sampled control inputs, which are applied at each time t_k , for all $k \in \mathbb{N}$; the terms $v(t)$ and $\omega(t)$ contain the linear and angular velocities of the UMR. The sampling instants t_k are monotonously increasing, so that $\lim_{k \rightarrow \infty} t_k = +\infty$, and $h(t) := t_{k+1} - t_k > h_{\min}$, where

$h_{\min} > 0$ is the minimum sampling interval; and $t_0 = 0$. It is assumed that the time-varying perturbations $d_i(t)$ are unknown but bounded, *i.e.*, $-d_{\max} < d_i(t) \leq d_{\max} < 1$, for $i = 1, 2$, with a known $d_{\max} > 0$. The constraint $d_i(t) > -1$ ensures that the perturbations do not cause a change of sign in the control inputs.

The aim of this chapter is to solve the trajectory-tracking problem for the UMR affected by multiplicative perturbations and taking into account communication constraints, *i.e.*, a minimum sampling time h_{\min} in which the control signal can be sent to the UMR; state and input constraints, *i.e.*, $x(t) \in \mathcal{X} := [x_{\min}, x_{\max}] \subset \mathbb{R}$, $y(t) \in \mathcal{Y} := [y_{\min}, y_{\max}] \subset \mathbb{R}$, $v(t) \in \mathcal{V} := [-v_{\max}, v_{\max}] \subset \mathbb{R}$, and $\omega(t) \in \mathcal{W} := [-\omega_{\max}, \omega_{\max}] \subset \mathbb{R}$, for all $t \geq t_0$, for some given sets \mathcal{X} , \mathcal{Y} , \mathcal{V} , and \mathcal{W} .

Following the same procedure as in subsection 7.3, and considering that $F_j \in \mathbb{R}^{2 \times 2}$, for $j = \overline{1, 4}$, are such that

$$F(\rho_2) = \sum_{j=1}^4 \alpha_j(\rho_2) F_j, \quad j = \overline{1, 4} \quad (118a)$$

$$\sum_{j=1}^4 \alpha_j(\rho_2) = 1, \quad \alpha_j(\rho_2) \in [0, 1], \quad (118b)$$

the following tracking error dynamics is obtained

$$\dot{e}(t) = \left[A_0 + \sum_{j=1}^4 \alpha_j(\rho_1) A_j \right] e(t) + B \left[\tau(t) + \sum_{j=1}^4 \alpha_j(\rho_2) F_j d(t) \right]. \quad (119)$$

Therefore, the problem now is to design a robust sampled control law τ such that the trajectories of the system (119) converge to zero, despite the perturbations d , taking into account the communication constraint, *i.e.*, $h(t) > h_{\min}$, and the state and input constraints, *i.e.*, $e(t) \in \mathcal{E}$ and $\tau(t) \in \mathcal{U}$, for all $t \geq 0$.

8.3 ROBUST CONTROL DESIGN

The proposed controller takes the following form:

$$\tau(t) = \begin{cases} \tilde{\tau}(t), & \text{if } e(t) \notin \mathcal{E}(P), \\ \hat{\tau}(t), & \text{if } e(t) \in \mathcal{E}(P), \end{cases} \quad (120)$$

where $\tilde{\tau}$ is an event-triggered controller designed according to Lemma 8, *i.e.*, $\tilde{\tau} = \sigma(\tau_0(t))$. On the other hand, $\hat{\tau}$ is a constant sampled state-feedback controller designed according to Lemma 9, *i.e.*, $\hat{\tau} = K_2 e(t_k)$, $\forall t \in [t_k, t_{k+1})$, $k \in \mathbb{N}$, and the ellipsoid $\mathcal{E}(P)$ is the switching and invariant set for system (119).

In order to apply the statements given in Lemmas 8 and 9, it is necessary to take into account that $\|F(\rho_2)\| \leq F_{\max}$ with $F_{\max} = d_{\max} \max(v_{\max}, \omega_{\max})$. Then, it is consider that $D = B F_{\max}$, $\bar{b}_1 = (0, \overline{xy}^{-1}, 0)^T$, $\bar{b}_2 = -\bar{b}_1$, $\bar{b}_3 = (0, 0, \overline{xy}^{-1})^T$, and $\bar{b}_4 = -\bar{b}_3$, with $\overline{xy} = (x_{\max} - x_{\min}) + (y_{\max} - y_{\min})$, and

$A_{\max} = \sum_{j=1}^4 \alpha^* \|A_j\|$, where $\alpha^* = \arg \max_{\alpha \in \Gamma} \sum_{j=1}^4 \alpha_j \|A_j\|$, and $\Gamma \subset \mathbb{R}^4$ the set of all convex weight vectors $\alpha = (\alpha_1, \dots, \alpha_4)^\top \in \mathbb{R}^4$ such that (104) and (118) holds.

8.4 EXPERIMENTAL RESULTS

The proposed robust strategy is applied to the QBot2 manufactured by Quanser (see Fig. 32). The desired trajectory is given by

$$\begin{aligned}\omega_d(t) &= \frac{\dot{x}_d(t)\ddot{y}_d(t) - \dot{y}_d(t)\ddot{x}_d(t)}{\dot{x}_d^2(t) + \dot{y}_d^2(t)}, \\ v_d &= \sqrt{\dot{x}_d^2(t) + \dot{y}_d^2(t)}, \\ x_d(t) &= \cos(\omega_0 t), \\ y_d(t) &= \sin(2\omega_0 t), \\ \theta_d(t) &= \int_0^t \omega_d(\tau) d\tau,\end{aligned}$$

with $\omega_0 = 0.15$, thus, $\bar{\omega}_d = 1.1663$, $\underline{v}_d = 0.1392$, and $\bar{v}_d = 0.4472$. The initial conditions are $x_0 = 0.5[\text{m}]$, $y_0 = -1.4[\text{m}]$, and $\theta_0 = 0[\text{rad}]$, thus, $e_1(0) = 1.5708$, $e_2(0) = 0.2$, and $e_3(0) = 1.4$. The state and input constraints sets are given as $\mathcal{X} = [-1.5, 1.5]$, $\mathcal{Y} = [-1.5, 1.5]$, $\mathcal{V} = [-0.7, 0.7]$, $\mathcal{W} = [-3, 3]$, and thus, $\bar{x}\bar{y} = 6$, $\bar{\tau}_1 = 4.1663$, and $\bar{\tau}_2 = 1.4472$. Note that $e(0) \in \mathcal{E}$ and $\tau(0) \in \mathcal{U}$. The perturbations are taken as $d_1(t) = 0.01 \cos(t) + 0.01$ and $d_2(t) = 0.02 \sin(t) + 0.01$, thus $d_{\max} = 0.03$. These perturbations are added by means of software. Note that the UMR platform has intrinsic perturbations such as noise in the measurements. The matrices A_0 and A_j can be obtained as in (117). Therefore, it is obtained that $F_{\max} = 1.65$ and $A_{\max} = 0.5261$.

To compute the control gains for the aperiodic control law, let us apply the statements of Lemma 7. Consider $\delta_1 = 1.5039$, $\delta_2 = 1.2501$, $\gamma = 0.2$, $\tau_{1\max} = 4.1663$, and $\tau_{2\max} = 1.1472$, then the following feasible solution is obtained:

$$\begin{aligned}R &= \begin{pmatrix} 0.33 & 0.00 & 0.14 \\ 0.00 & 0.37 & 0.00 \\ 0.14 & 0.00 & 0.32 \end{pmatrix}, \quad P = \begin{pmatrix} 0.62 & -0.01 & 0.27 \\ -0.01 & 0.66 & -0.01 \\ 0.27 & -0.01 & 0.56 \end{pmatrix}, \\ K &= \begin{pmatrix} -1.6165 & 0.0069 & -1.2105 \\ 0.0080 & -0.9458 & 0.0022 \end{pmatrix}.\end{aligned}$$

Therefore it can be verified that the LMI (72) is satisfied, hence, the event-triggered control can be applied.

To compute the control gains for the periodic control law, let us apply the statements of Lemma 9. Taking into account $h_{\min} = 0.001$ [s], $\gamma_2 = 0.2$, $\epsilon = 0.5$, then, the following feasible solution is obtained:

$$P_1 = \begin{pmatrix} 0.57 & -0.01 & -0.23 \\ -0.01 & 0.75 & -0.01 \\ -0.23 & -0.01 & 0.81 \end{pmatrix}, P_2 = \begin{pmatrix} 0.61 & 0.00 & -0.19 \\ 0.00 & 0.78 & -0.01 \\ -0.19 & -0.01 & 0.77 \end{pmatrix},$$

$$K_2 = \begin{pmatrix} -2.0962 & 0.0110 & -0.7544 \\ 0.0211 & -1.9829 & 0.0094 \end{pmatrix}, \bar{h} = 0.2.$$

Additionally, it is given that $\epsilon = 0.1401$ and thus $R_s = 7.1352I_3$. The system trajectories are depicted in Figs. 42–43, which shows that they converge to a close region of the desired reference despite the external perturbations. Note that the trajectories x and y never transgress the state constraints. The control signals ω and v are depicted in Fig. 44. Observe that both control signals, ω and v , get saturated in some instants and then remain inside the linear region. The projection of the ellipsoids $\mathcal{E}(R)$, $\mathcal{E}(P)$, $\mathcal{E}(P_c)$, and $(\mathcal{E}(R) - \mathcal{E}(R_s))$, in the plane e_2 – e_3 are depicted in Fig. 45. It can be seen that the trajectories of the tracking error start in $(\mathcal{E}(R) - \mathcal{E}(R_s))$, remain inside $\mathcal{E}(R)$, then converge to $\mathcal{E}(P)$, and finally remain inside $\mathcal{E}(P_c)$. The projection at the coordinate e_1 is not shown since e_1 does not have constraints. Finally, in Fig. 46, it is observed that the norm of the errors converges to a region close to the origin. Table 4 presents the RMS of the tracking errors to better illustrate the performance of the controller. It can be observed that the mean value is close to zero, thus, that the controller performs well despite the presence of perturbations. Also, it is evident that in the case when communication constraints are considered, aiming to minimize bandwidth usage results in a larger tracking error, as can be seen in table 4 compared to the results presented in table 2. Nevertheless, this is expected since in this case the sampling interval is 200 times greater than when the full bandwidth is used, *i.e.*, the sampling time used is 0.2 [s], compared to 0.001 [s] when the full bandwidth is employed.

8.5 REMARKS

This chapter presents the results obtained from applying the algorithm presented in Chapter 5 to solve the trajectory tracking problem in the UMR with state, input, and communication constraints, affected by external perturbations. The proposed approach ensures the ISS properties of the trajectory tracking error dynamics with respect to external perturbations. Some experimental results, using the QBot2 by Quanser, validate the effectiveness of the proposed robust control strategy, considering the sampling time given by the platform.

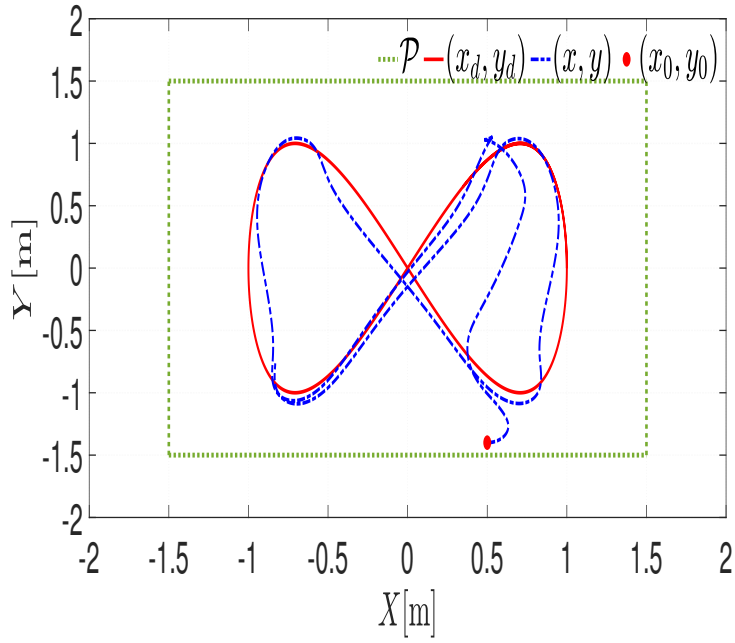


Figure 42: System Trajectories

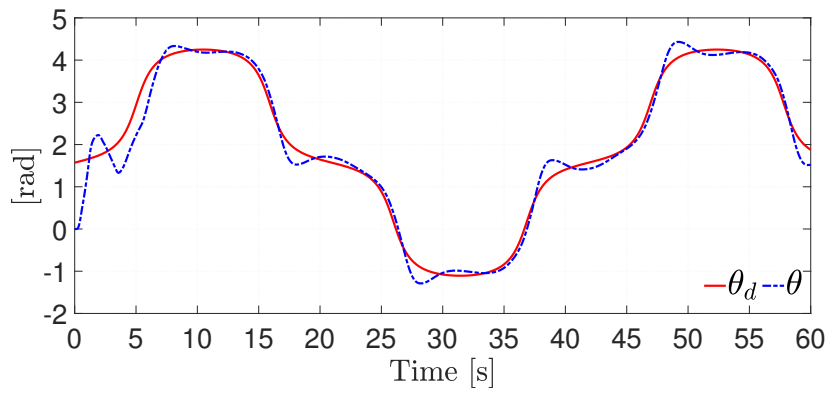


Figure 43: System Trajectories

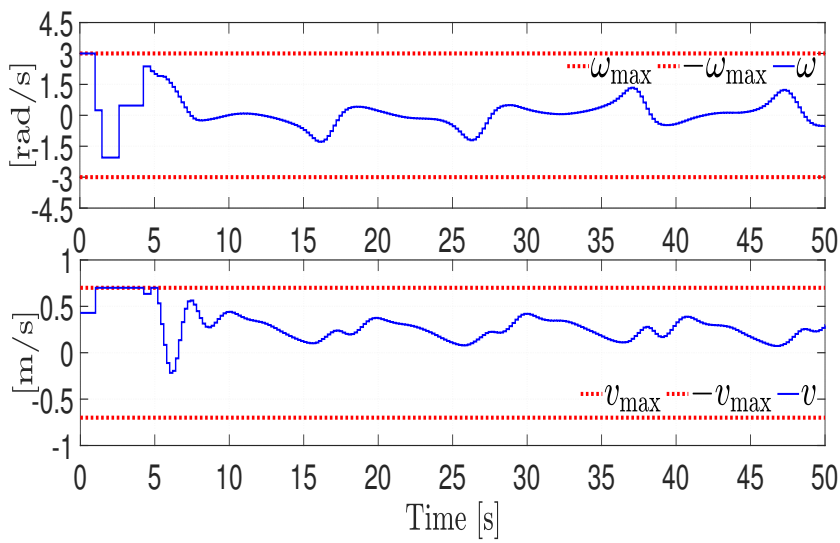


Figure 44: Control Signals

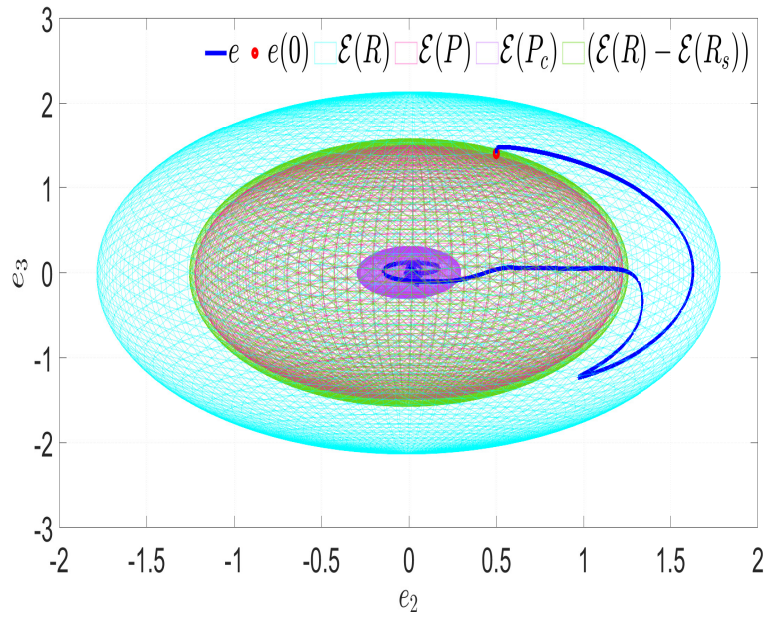


Figure 45: Tracking Error and Ellipsoids

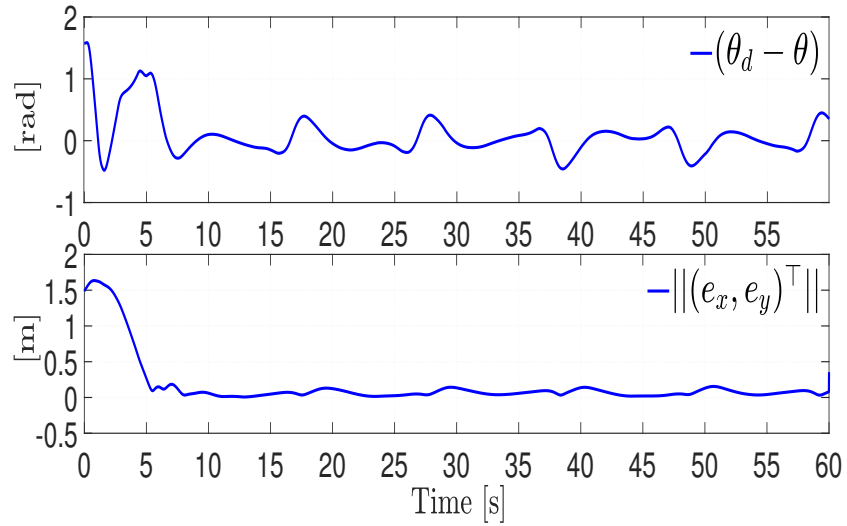
Figure 46: Tracking Error Norm, where $e_x = x_d - x$ and $e_y = y_d - y$

Table 4: Performance indexes

	max	min	mean
$e_{\theta_{RMS}}$ [deg]	90.8425	0.0061	11.7743
$e_{xy_{RMS}}$ [m]	1.5900	$6.0274e \times 10^{-6}$	0.1272

CONCLUSIONS

In this thesis, new robust control strategies were developed for stabilizing some classes of disturbed dynamical systems, taking into account state, input, and communication constraints, using a wide variety of tools, *e.g.*, the use of the AEM, BLF, ISMC, IP, MPC, and event-triggered control.

The particular contributions of this thesis can be summarized as follows:

- 1) The design of a robust control strategy to regulate the output of a particular class of uncertain linear systems, with input saturation and state constraints.

Proposed Solution:

- A robust output-regulation control composed of a linear and nonlinear part. The linear control part deals with the input saturation, the state constraints and the parameter uncertainties, while the nonlinear part deal with the external perturbations.
- The proposed scheme guarantees asymptotic convergence to zero of the output regulation error coping with the system constraints and perturbations.
- Simulation and experimental results are presented.

Academic results: [4], [5], [6], [7], [8], and [9].

- 2) The design of a robust control strategy to stabilize a particular class of uncertain nonlinear systems, taking into account state and input constraints, and external perturbations.

Proposed Solution:

- A discrete-time interval predictor-based state-feedback controller and an MPC approach.
- The proposed scheme guarantees local ISpS of the constrained nonlinear systems with respect to external perturbations.
- Simulation results are presented.

Academic results: [10], [11], [12], and [13].

- 3) The design of a sampled robust control strategy to stabilize a particular class of uncertain nonlinear systems, taking into account state, input, and communication constraints, and external perturbations.

Proposed Solution:

- A sampled control strategy composed of an aperiodic and a periodic sampled controller. The aperiodic control part takes into account the state and input constraints, while the periodic control part takes into account the minimum sampling time.

- The proposed approach ensures the ISS properties of the trajectory tracking error dynamics with respect to external perturbations.
- Simulation and experimental results are presented.

Academic results: [14], [15], and [16].

SCIENTIFIC PRODUCTION

Published Journal Papers

- 1a) **A. Gutiérrez, H. Ríos and M. Mera.** “Robust output–regulation for uncertain linear systems with input saturation”. *IET Control Theory & Applications* 14(16), 2020, pp. 2372–2384. [4]
- 2a) **A. Gutiérrez, M. Mera and H. Ríos.** “Integral Sliding–Mode–based Robust Output–Regulation for Constrained and Uncertain Linear Systems”. *International Journal of Robust and Nonlinear Control* 33(3), 2023, pp. 2205–2218. [5]
- 3a) **A. Gutiérrez, H. Ríos and M. Mera,** “A Discontinuous Integral Action for Robust Output Tracking in Uncertain Linear Systems”, *International Journal of Robust and Nonlinear Control* 2023, pp. 5819–5833. [71]

Journal Papers Under Review

- 1b) **A. Gutiérrez, H. Ríos and M. Mera.** “A Robust Trajectory Tracking Controller for Constrained and Perturbed Unicycle Mobile Robots”, Submitted to *Asian Journal of Control*. [9]
- 2b) **A. Gutiérrez, H. Ríos, M. Mera, D. Efimov, and R. Ushirobira.** “An Interval Predictor–based Robust Control for a Class of Constrained Nonlinear Systems”, Submitted to *European Journal of Control*. [10]
- 3b) **A. Gutiérrez, H. Ríos, M. Mera, D. Efimov, and R. Ushirobira.** “Constrained and Perturbed Unicycle Mobile Robots: A Sampled Robust Trajectory Control Approach”, Submitted to *IEEE Transactions on Industrial Electronics*. [14]

Book Chapter

- 1c) **A. Gutiérrez, H. Ríos, M. Mera, and D. Efimov.** “Robust Control for Constrained Nonlinear Systems: An Interval–Predictor Approach”. *Nonlinear and Constrained Control–Applications, Synergies, Challenges and Opportunities*, Springer Nature. [11]

Published International Conference Papers

- 1d) **A. Gutiérrez, M. Mera and H. Ríos.** “An Integral Sliding–Mode Robust Regulation for Constrained and Uncertain Three–Wheeled Omnidirectional Mobile Robots”. In the 61st IEEE Conference on Decision and Control, Cancún, Mexico, 2022, pp. 3637–3642. [7]
- 2d) **A. Gutiérrez, H. Ríos, M. Mera, D. Efimov, and R. Ushirobira.** “An Interval Predictor–based Robust Control for a Class of Constrained Nonlinear Systems”, In the 62nd IEEE Conference on Decision and Control, Marina Bay Sands, Singapore, 2023, pp. 1736–1741. [12]
- 3d) **A. Gutiérrez, H. Ríos, M. Mera, D. Efimov, and R. Ushirobira.** “An Event–Triggered Robust Control for Unicycle Mobile Robots with Communication, State, and Input Constraints”, In the 63rd IEEE Conference on Decision and Control 2024. [15]

Published National Conference Papers

- 1f) **A. Gutiérrez, H. Ríos and M. Mera.** “Control Robusto por Salida para Sistemas Lineales Perturbados con Entrada Saturada”. In the 27 Congreso Argentino de Control Automático AADECA’20 Virtual, 2020, pp. 87–92. [72]
- 2f) **A. Gutiérrez, M. Mera and H. Ríos.** “Robust Output–Regulation for Constrained and Uncertain Linear Systems: An Attractive Ellipsoid Approach”. In the 2021 Congreso Nacional de Control Automático, Guanajuato, México, pp. 243–248. [6]
- 3f) **A. Gutiérrez, M. Mera and H. Ríos.** “Robust Output Regulation for a Constrained Omnidirectional Mobile Robot”. In the 2022 Congreso Nacional de Control Automático, Chiapas, México, pp. 94–99. [8]
- 4f) **A. Gutiérrez, H. Ríos, M. Mera, D. Efimov, A. Polyakov and R. Ushirobira,** “A Sampled–time Controller for a Class of Constrained Nonlinear Systems via Interval Prediction”, In the 2023 Congreso Nacional de Control Automático, Acapulco, Guerrero, pp. 1–6. [13]

National Conference Paper Under Review

- 1g) **A. Gutiérrez, H. Ríos, M. Mera, D. Efimov, A. Polyakov and R. Ushirobira,** “Sampled Robust Control for Trajectory Tracking in Constrained Unicycle Mobile Robots”, In the 2024 Congreso Nacional de Control Automático. [16]

Academic Stays

- 1) Academic stay from May 5 to June 29, 2022 at Inria Lille–Nord Europe Center by the project 315597 “*Artificial Intelligence-based Control Approaches for Multiple Mobile Robots*”, ECOS NORD 2020.
- 2) Academic stay from September 1 to October 21, 2023 at Inria Lille–Nord Europe Center as part of the project 315597 “*Artificial Intelligence-based Control Approaches for Multiple Mobile Robots*”, ECOS NORD 2020.

BIBLIOGRAPHY

- [1] T. Kiefer, K. Graichen, and A. Kugi, "Trajectory tracking of a 3dof laboratory helicopter under input and state constraints," *IEEE Transactions on Control Systems Technology*, vol. 18, no. 4, pp. 944–952, 2009.
- [2] N. Cao and A. F. Lynch, "Inner–outer loop control for quadrotor uavs with input and state constraints," *IEEE Transactions on Control Systems Technology*, vol. 24, no. 5, pp. 1797–1804, 2015.
- [3] Y. Huang and Y. Jia, "Adaptive finite-time 6-dof tracking control for spacecraft fly around with input saturation and state constraints," *IEEE Transactions on Aerospace and Electronic Systems*, vol. 55, no. 6, pp. 3259–3272, 2019.
- [4] A. Gutiérrez, H. Ríos, and M. Mera, "Robust output–regulation for uncertain linear systems with input saturation," *IET Control Theory & Applications*, vol. 14, no. 16, pp. 2372–2384, 2020.
- [5] A. Gutierrez, M. Mera, and H. Ríos, "Integral sliding–mode–based robust output–regulation for constrained and uncertain linear systems," *International Journal of Robust and Nonlinear Control*, vol. 33, no. 3, pp. 2205–2218, 2023.
- [6] A. Gutiérrez, M. Mera, and H. Ríos, "Robust output–regulation for constrained and uncertain linear systems: An attractive ellipsoid approach," *Congreso Nacional de Control Automático, Guanajuato, México*, pp. 243–248, 2021.
- [7] A. Gutiérrez, M. Mera, and H. Ríos, "An integral sliding–mode robust regulation for constrained three–wheeled omnidirectional mobile robots," in *61st IEEE Conference on Decision and Control (CDC)*, pp. 3637–3642, 2022.
- [8] A. Gutiérrez, M. Mera, and H. Ríos, "Robust output regulation for a constrained omnidirectional mobile robot," *Congreso Nacional de Control Automático, Chiapas, México*, pp. 94–99, 2022.
- [9] A. Gutiérrez, H. Ríos, and M. Mera, "A robust trajectory tracking controller for constrained and perturbed unicycle mobile robots," *Submitted to Asian Journal of Control*, pp. 1–17, 2024.
- [10] A. Gutiérrez, H. Ríos, M. Mera, D. Efimov, and R. Ushirobira, "A robust trajectory tracking controller for constrained and perturbed unicycle mobile robots," *Submitted to European Journal of Control*, pp. 1–16, 2024.

- [11] A. Gutiérrez, H. Ríos, M. Mera, D. Efimov, and R. Ushirobira, "Robust control for constrained nonlinear systems: An interval–predictor approach," in *Nonlinear and Constrained Control–Applications, Synergies, Challenges and Opportunities*, Springer Nature, 2024.
- [12] A. Gutiérrez, H. Ríos, M. Mera, D. Efimov, and R. Ushirobira, "An interval predictor–based robust control for a class of constrained nonlinear systems," in *62nd IEEE Conference on Decision and Control (CDC)*, pp. 1736–1741, 2023.
- [13] A. Gutiérrez, H. Ríos, M. Mera, D. Efimov, and R. Ushirobira, "A sampled–time controller for a class of constrained nonlinear systems via interval prediction," *Congreso Nacional de Control Automático, Aca-pulco, Guerrero*, pp. 1–6, 2023.
- [14] A. Gutiérrez, H. Ríos, M. Mera, D. Efimov, and R. Ushirobira, "Constrained and perturbed unicycle mobile robots: A sampled robust trajectory control approach," *Submitted to IEEE Transactions on Industrial Electronics*, pp. 1–8, 2024.
- [15] A. Gutiérrez, H. Ríos, M. Mera, D. Efimov, and R. Ushirobira, "An event–triggered robust control for unicycle mobile robots with communication, state, and input constraints," in *Submitted to 63st IEEE Conference on Decision and Control (CDC)*, pp. 1–6, 2024.
- [16] A. Gutiérrez, H. Ríos, M. Mera, D. Efimov, and R. Ushirobira, "Sampled robust control for trajectory tracking in constrained unicycle mobile robots," *Submitted to Congreso Nacional de Control Automático*, pp. 1–6, 2024.
- [17] E. Bernuau, A. Polyakov, D. Efimov, and W. Perruquetti, "Verification of iss, iiss and ioss properties applying weighted homogeneity," *Systems & Control Letters*, vol. 62, no. 12, pp. 1159–1167, 2013.
- [18] D. Efimov, L. Fridman, T. Raissi, A. Zolghadri, and R. Seydou, "Interval estimation for LPV systems applying high order sliding mode techniques," *Automatica*, vol. 48, no. 9, pp. 2365–2371, 2012.
- [19] H. K. Khalil, *Nonlinear Systems*, ch. Lyapunov Stability, pp. 111–181. Prentice Hall, third ed., 2002.
- [20] K. P. Tee, S. S. Ge, and E. H. Tay, "Barrier lyapunov functions for the control of output-constrained nonlinear systems," *Automatica*, vol. 45, no. 4, pp. 918–927, 2009.
- [21] S. Tarbouriech, G. Garcia, J. M. da Silva Jr, and I. Queinnec, *Stability and stabilization of linear systems with saturating actuators*. Springer Science & Business Media, 2011.
- [22] A. Poznyak, A. Polyakov, and V. Azhmyakov, *Attractive ellipsoids in robust control*. Springer, 2014.

- [23] V. Utkin and J. Shi, "Integral sliding mode in systems operating under uncertainty conditions," in *Proceedings of 35th IEEE conference on decision and control*, vol. 4, pp. 4591–4596, IEEE, 1996.
- [24] B. Niu and J. Zhao, "Barrier lyapunov functions for the output tracking control of constrained nonlinear switched systems," *Systems & Control Letters*, vol. 62, no. 10, pp. 963–971, 2013.
- [25] D. Llorente-Vidrio, M. Mera, I. Salgado, and I. Chairez, "Robust control for state constrained systems based on composite barrier lyapunov functions," *International Journal of Robust and Nonlinear Control*, vol. 30, no. 17, pp. 7238–7254, 2020.
- [26] Y. Song and S. Zhou, "Tracking control of uncertain nonlinear systems with deferred asymmetric time-varying full state constraints," *Automatica*, vol. 98, pp. 314–322, 2018.
- [27] X. Niu, W. Lin, and X. Gao, "Static output feedback control of a chain of integrators with input constraints using multiple saturations and delays," *Automatica*, vol. 125, p. 109457, 2021.
- [28] T. A. De Almeida and C. E. Dorea, "Output feedback constrained regulation of linear systems via controlled-invariant sets," *IEEE Transactions on Automatic Control*, 2020.
- [29] Y. Wu and X.-J. Xie, "Stabilisation of high-order nonlinear systems with full-state constraints and input saturation," *International Journal of Control*, pp. 1–11, 2019.
- [30] L. Lu and B. Yao, "Online constrained optimization based adaptive robust control of a class of mimo nonlinear systems with matched uncertainties and input/state constraints," *Automatica*, vol. 50, no. 3, pp. 864–873, 2014.
- [31] S. Boyd and Vandenberghe, *Convex optimization*. Los Angeles: Cambridge University Press, 2009.
- [32] V. Utkin, J. Guldner, and J. Shi, *Sliding mode control in electro-mechanical systems*. CRC press, 2017.
- [33] F. Castaños and L. Fridman, "Analysis and design of integral sliding manifolds for systems with unmatched perturbations," *IEEE Transactions on Automatic Control*, vol. 51, no. 5, pp. 853–858, 2006.
- [34] M. Allenspach and G. J. Ducard, "Nonlinear model predictive control and guidance for a propeller-tilting hybrid unmanned air vehicle," *Automatica*, vol. 132, p. 109790, 2021.
- [35] Z. Sun, L. Dai, K. Liu, Y. Xia, and K. H. Johansson, "Robust MPC for tracking constrained unicycle robots with additive disturbances," *Automatica*, vol. 90, pp. 172–184, 2018.

- [36] A. Weiss, M. Baldwin, R. S. Erwin, and I. Kolmanovsky, "Model predictive control for spacecraft rendezvous and docking: Strategies for handling constraints and case studies," *IEEE Transactions on Control Systems Technology*, vol. 23, no. 4, pp. 1638–1647, 2015.
- [37] D. Q. Mayne, J. B. Rawlings, C. V. Rao, and P. O. Scokaert, "Constrained model predictive control: Stability and optimality," *Automatica*, vol. 36, no. 6, pp. 789–814, 2000.
- [38] M. Bujarbaruah, U. Rosolia, Y. R. Stürz, X. Zhang, and F. Borrelli, "Robust MPC for LPV systems via a novel optimization-based constraint tightening," *Automatica*, vol. 143, p. 110459, 2022.
- [39] B. Ding and H. Pan, "Output feedback robust MPC for LPV system with polytopic model parametric uncertainty and bounded disturbance," *International Journal of Control*, vol. 89, no. 8, pp. 1554–1571, 2016.
- [40] X. Ping, Z. Li, and A. Al-Ahmari, "Dynamic output feedback robust MPC for LPV systems subject to input saturation and bounded disturbance," *International Journal of Control, Automation and Systems*, vol. 15, no. 3, pp. 976–985, 2017.
- [41] D. Q. Mayne, S. Raković, R. Findeisen, and F. Allgöwer, "Robust output feedback model predictive control of constrained linear systems: Time varying case," *Automatica*, vol. 45, no. 9, pp. 2082–2087, 2009.
- [42] M. Farina, L. Giulioni, L. Magni, and R. Scattolini, "An approach to output-feedback MPC of stochastic linear discrete-time systems," *Automatica*, vol. 55, pp. 140–149, 2015.
- [43] J. M. Manzano, D. Limón, D. Muñoz de la Peña, and J. P. Calliess, "Robust learning-based MPC for nonlinear constrained systems," *Automatica*, vol. 117, p. 108948, 2020.
- [44] H. Xie, L. Dai, Y. Luo, and Y. Xia, "Robust MPC for disturbed nonlinear discrete-time systems via a composite self-triggered scheme," *Automatica*, vol. 127, p. 109499, 2021.
- [45] E. Leurent, O. Maillard, and D. Efimov, "Robust-adaptive control of linear systems: beyond quadratic costs," *Advances in Neural Information Processing Systems*, vol. 33, pp. 3220–3231, 2020.
- [46] A. Dhar and S. Bhasin, "Indirect adaptive MPC for discrete-time LTI systems with parametric uncertainties," *IEEE Transactions on Automatic Control*, vol. 66, no. 11, pp. 5498–5505, 2021.
- [47] D. Ji, J. Ren, C. Liu, and Y. Shi, "Stabilizing terminal constraint-free nonlinear MPC via sliding mode-based terminal cost," *Automatica*, vol. 134, p. 109898, 2021.

- [48] A. Reis de Souza, D. Efimov, T. Raïssi, and X. Ping, "Robust output feedback model predictive control for constrained linear systems via interval observers," *Automatica*, vol. 135, p. 109951, 2022.
- [49] A. Reis de Souza, D. Efimov, and T. Raïssi, "Robust output feedback MPC for LPV systems using interval observers," *IEEE Transactions on Automatic Control*, vol. 67, no. 6, pp. 3188–3195, 2021.
- [50] E. Leurent, D. Efimov, and O.-A. Maillard, "Robust-adaptive interval predictive control for linear uncertain systems," *2020 59th IEEE Conference on Decision and Control (CDC), Jeju, Korea (South)*, vol. pp. 1429–1434, 2020.
- [51] A. M. Nagy, G. Mourot, B. Marx, J. Ragot, and G. Schutz, "Systematic multimodeling methodology applied to an activated sludge reactor model," *Industrial & Engineering Chemistry Research*, vol. 49, no. 6, pp. 2790–2799, 2010.
- [52] X. Chen, Y. Jia, and F. Matsuno, "Tracking control for differential-drive mobile robots with diamond-shaped input constraints," *IEEE Transactions on Control Systems Technology*, vol. 22, no. 5, pp. 1999–2006, 2014.
- [53] D. Limon, A. Ferramosca, I. Alvarado, and T. Alamo, "Nonlinear MPC for tracking piece-wise constant reference signals," *IEEE Transactions on Automatic Control*, vol. 63, no. 11, pp. 3735–3750, 2018.
- [54] S.-L. Dai, K. Lu, and X. Jin, "Fixed-time formation control of unicycle-type mobile robots with visibility and performance constraints," *IEEE Transactions on Industrial Electronics*, vol. 68, no. 12, pp. 12615–12625, 2021.
- [55] J. Huang, W. Wang, C. Wen, and G. Li, "Adaptive event-triggered control of nonlinear systems with controller and parameter estimator triggering," *IEEE Transactions on Automatic Control*, vol. 65, no. 1, pp. 318–324, 2019.
- [56] T. Liu and Z.-P. Jiang, "A small-gain approach to robust event-triggered control of nonlinear systems," *IEEE Transactions on Automatic Control*, vol. 60, no. 8, pp. 2072–2085, 2015.
- [57] Q. Zhu, "Stabilization of stochastic nonlinear delay systems with exogenous disturbances and the event-triggered feedback control," *IEEE Transactions on Automatic Control*, vol. 64, no. 9, pp. 3764–3771, 2018.
- [58] P. Tabuada, "Event-triggered real-time scheduling of stabilizing control tasks," *IEEE Transactions on Automatic Control*, vol. 52, no. 9, pp. 1680–1685, 2007.
- [59] A. Ferramosca, D. Limon, I. Alvarado, T. Alamo, F. Castaño, and E. F. Camacho, "Optimal MPC for tracking of constrained linear systems,"

- International Journal of Systems Science*, vol. 42, no. 8, pp. 1265–1276, 2011.
- [60] L. Xing, C. Wen, Z. Liu, H. Su, and J. Cai, “Event-triggered adaptive control for a class of uncertain nonlinear systems,” *IEEE transactions on automatic control*, vol. 62, no. 4, pp. 2071–2076, 2016.
- [61] K. Hashimoto, S. Adachi, and D. V. Dimarogonas, “Event-triggered intermittent sampling for nonlinear model predictive control,” *Automatica*, vol. 81, pp. 148–155, 2017.
- [62] H. Li and Y. Shi, “Robust distributed model predictive control of constrained continuous-time nonlinear systems: A robustness constraint approach,” *IEEE Transactions on Automatic Control*, vol. 59, no. 6, pp. 1673–1678, 2013.
- [63] Z. Sun, L. Dai, K. Liu, D. V. Dimarogonas, and Y. Xia, “Robust self-triggered mpc with adaptive prediction horizon for perturbed nonlinear systems,” *IEEE Transactions on Automatic Control*, vol. 64, no. 11, pp. 4780–4787, 2019.
- [64] E. Fridman, *Introduction to time-delay systems: Analysis and control*. Springer, 2014.
- [65] M. Tanaka, M. Nakajima, Y. Suzuki, and K. Tanaka, “Development and control of articulated mobile robot for climbing steep stairs,” *IEEE/ASME Transactions on Mechatronics*, vol. 23, no. 2, pp. 531–541, 2018.
- [66] X. Zhang, Y. Fang, and N. Sun, “Visual servoing of mobile robots for posture stabilization: from theory to experiments,” *International journal of robust and nonlinear control*, vol. 25, no. 1, pp. 1–15, 2015.
- [67] L. Ovalle, H. Ríos, M. Llama, V. Santibáñez, and A. Dzul, “Omni-directional mobile robot robust tracking: Sliding-mode output-based control approaches,” *Control Engineering Practice*, vol. 85, pp. 50–58, 2019.
- [68] K. D. Do, “Bounded controllers for global path tracking control of unicycle-type mobile robots,” *Robotics and Autonomous Systems*, vol. 61, no. 8, pp. 775–784, 2013.
- [69] S. L. Dai, K. Lu, and X. Jin, “Fixed-time formation control of unicycle-type mobile robots with visibility and performance constraints,” *IEEE Transactions on Industrial Electronics*, vol. 68, no. 12, pp. 12615–12625, 2020.
- [70] H. Ríos, M. Mera, T. Raïssi, and D. Efimov, “Robust interval predictive tracking control for constrained and perturbed unicycle mobile robots,” *International Journal of Robust and Nonlinear Control*, vol. 34, no. 9, pp. 6303–6320, 2024.

- [71] A. Gutiérrez, H. Ríos, and M. Mera, "A discontinuous integral action for robust output tracking in uncertain linear systems," *International Journal of Robust and Nonlinear Control*, vol. 33, no. 10, pp. 5819–5833, 2023.
- [72] A. Gutiérrez, H. Ríos, and M. Mera, "Control robusto por salida para sistemas lineales perturbados con entrada saturada," in *the 27 Congreso Argentino de Control Automático AADECA'20 Virtual*, pp. 87–92, 2020.